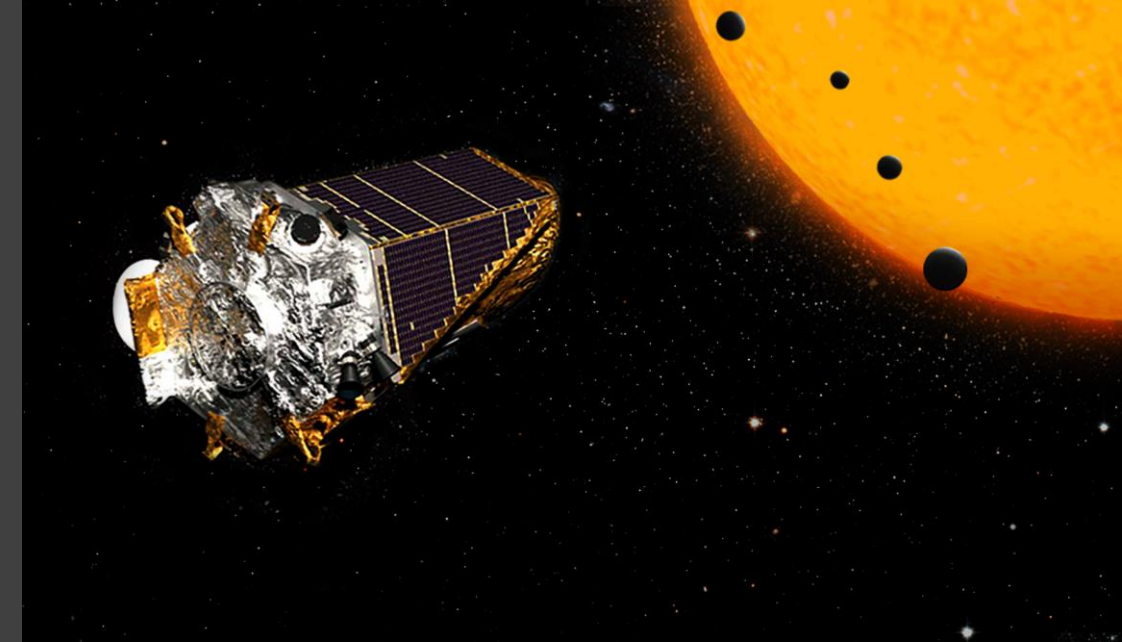
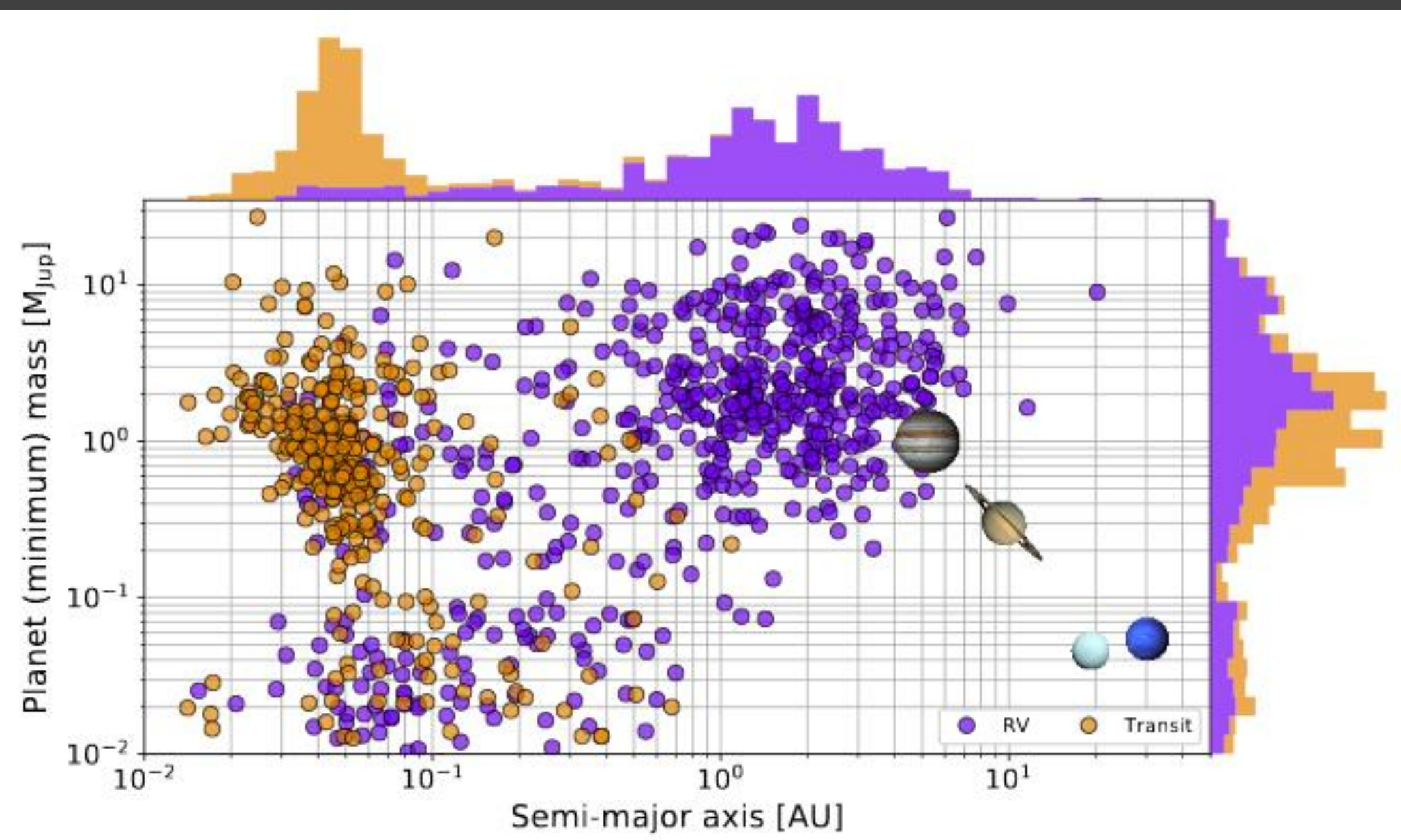


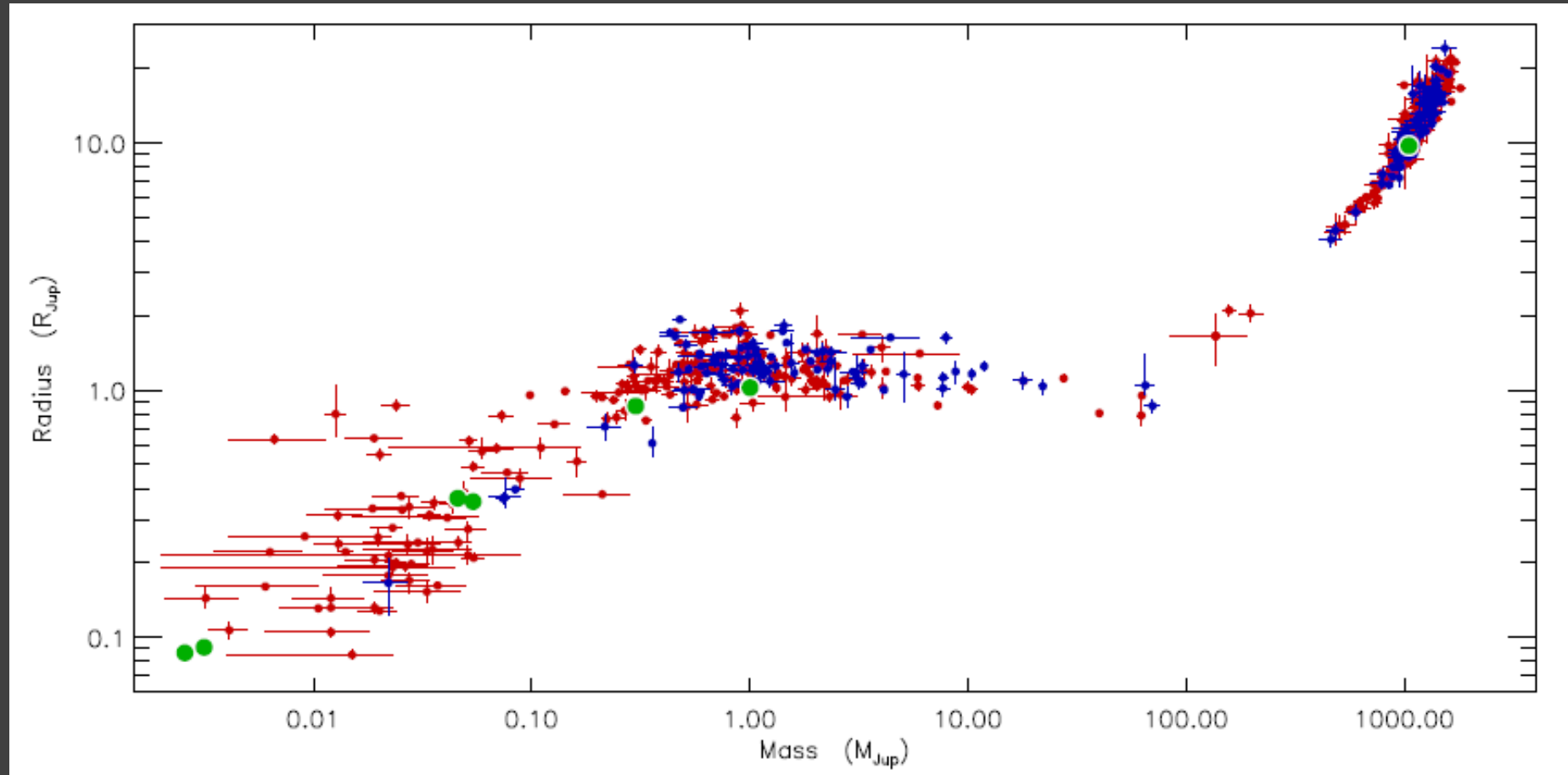
Planet detection methods

SERGEI POPOV





Planets, brown dwarfs stars



Exoplanet catalogues

Catalog	Mass criteria	Confidence criteria	Number of planets [†]
Exoplanet Encyclopaedia	$M_p - 1\sigma < 60M_{Jup}$	Submitted paper, conference talk	3741
NASA Exoplanet Archive	$M_p < 30M_{Jup}$	Accepted, refereed paper	3704
Open Exoplanet Catalog	None listed	Open-source	3504

[†]: as of February 27th, 2018.

<http://exoplanet.eu/catalog>

<http://exoplanetarchive.ipac.caltech.edu/index.html>

<http://www.openexoplanetcatalogue.com>

The screenshot shows the homepage of exoplanets.org. At the top right, there are links for "Exoplanets Data Explorer", "Methodology and FAQ", "Exoplanets Links", and "California Planet Survey". Below this, there is a large image of a green and blue exoplanet. To the right of the image are three buttons: "Table" (with a grid icon), "Plots" (with a scatter plot icon), and "Search" (with a magnifying glass icon). To the right of these buttons, there are four statistics: "2925 Planets with good orbits listed in the Exoplanet Orbit Database", "25 Other Planets including microlensing and imaged planets", "2950 Total Confirmed Planets", and "2337 Unconfirmed Kepler Candidates". Below these, there is a "Total Planets" section with "5287" and a note about including Kepler Candidates. A detailed description of the Exoplanet Orbit Database and Explorers is provided, along with a link to a detailed description and a download link for the entire database in CSV format.

NASA Exoplanet Archive

All Exoplanets	4201
Confirmed Planets with Kepler Light Curves for Stellar Host	2362
Confirmed Planets Discovered by Kepler	2342
Kepler Project Candidates Yet To Be Confirmed	2418
Confirmed Planets with K2 Light Curves for Stellar Host	431
Confirmed Planets Discovered by K2	410
K2 Candidates Yet To Be Confirmed	889
Confirmed Planets Discovered by TESS ¹	67
TESS Project Candidates Integrated into Archive (2020-08-20 13:00:02) ²	2174
Current date TESS Project Candidates at ExoFOP	2174
TESS Project Candidates Yet To Be Confirmed ³	1317

Counts by Mass

$M \leq 3 M_{\text{Earth}}$	38
$3 < M \leq 10 M_{\text{Earth}}$	140
$10 < M \leq 30 M_{\text{Earth}}$	97
$30 < M \leq 100 M_{\text{Earth}}$	94
$100 < M \leq 300 M_{\text{Earth}}$	222
$300 M_{\text{Earth}} < M$	379

Counts by Radius

$R \leq 1.25 R_{\text{Earth}}$	408
$1.25 < R \leq 2 R_{\text{Earth}}$	851
$2 < R \leq 6 R_{\text{Earth}}$	1329
$6 < R \leq 15 R_{\text{Earth}}$	460
$15 R_{\text{Earth}} < R$	166

Confirmed Exoplanet Statistics

Discovery Method	Number of Planets
Astrometry	1
Imaging	50
Radial Velocity	810
Transit	3191
Transit timing variations	21
Eclipse timing variations	16
Microlensing	96
Pulsar timing variations	7
Pulsation timing variations	2
Orbital brightness modulations	6
Disk Kinematics	1
Transiting Exoplanets	3214
All Exoplanets	4201

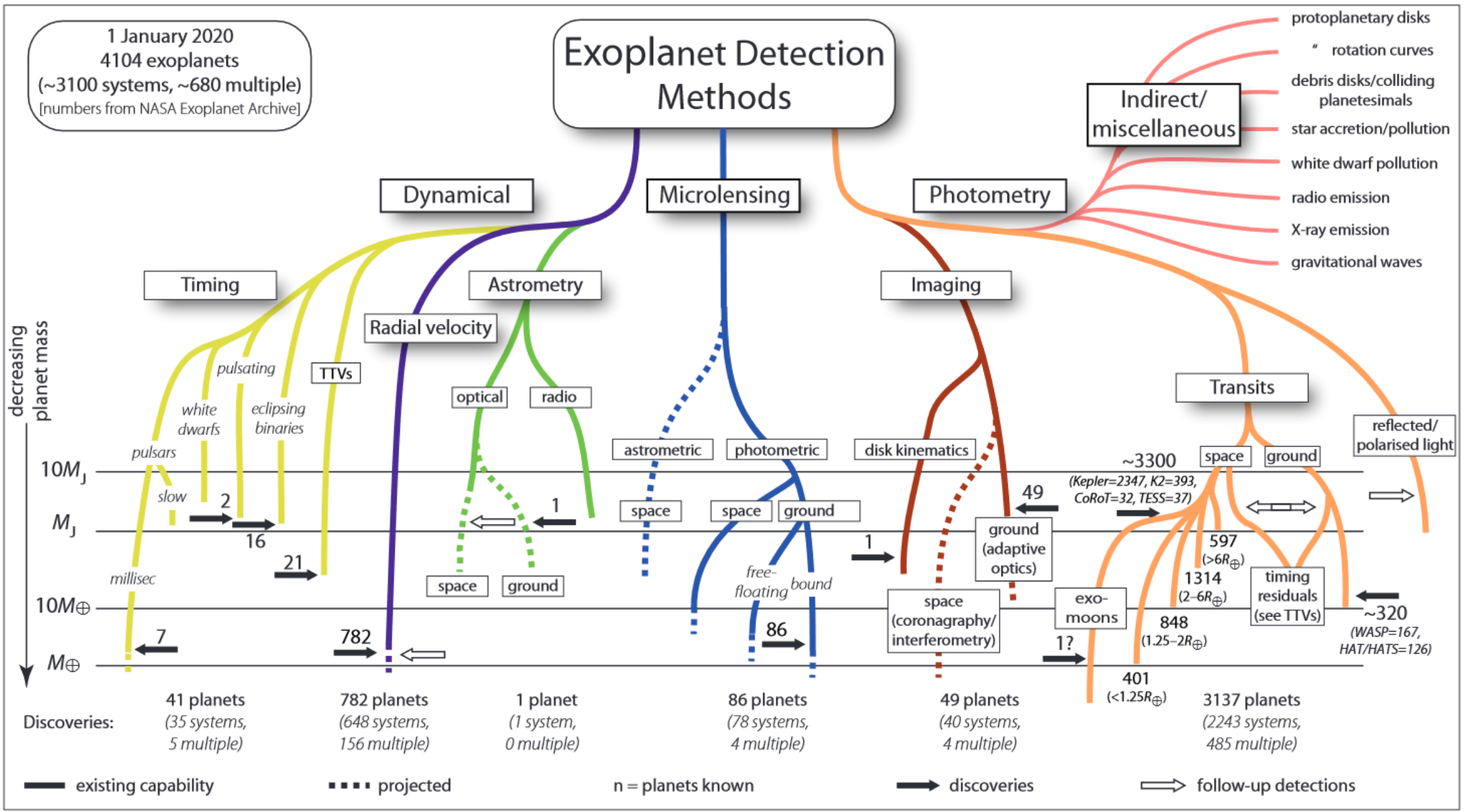
Exoplanet Mass and Radius

Confirmed Planets with mass	970
Confirmed Planets with $m \sin i$	818
Confirmed Planets with radius	3214

Confirmed Planets Discovered by TESS ¹

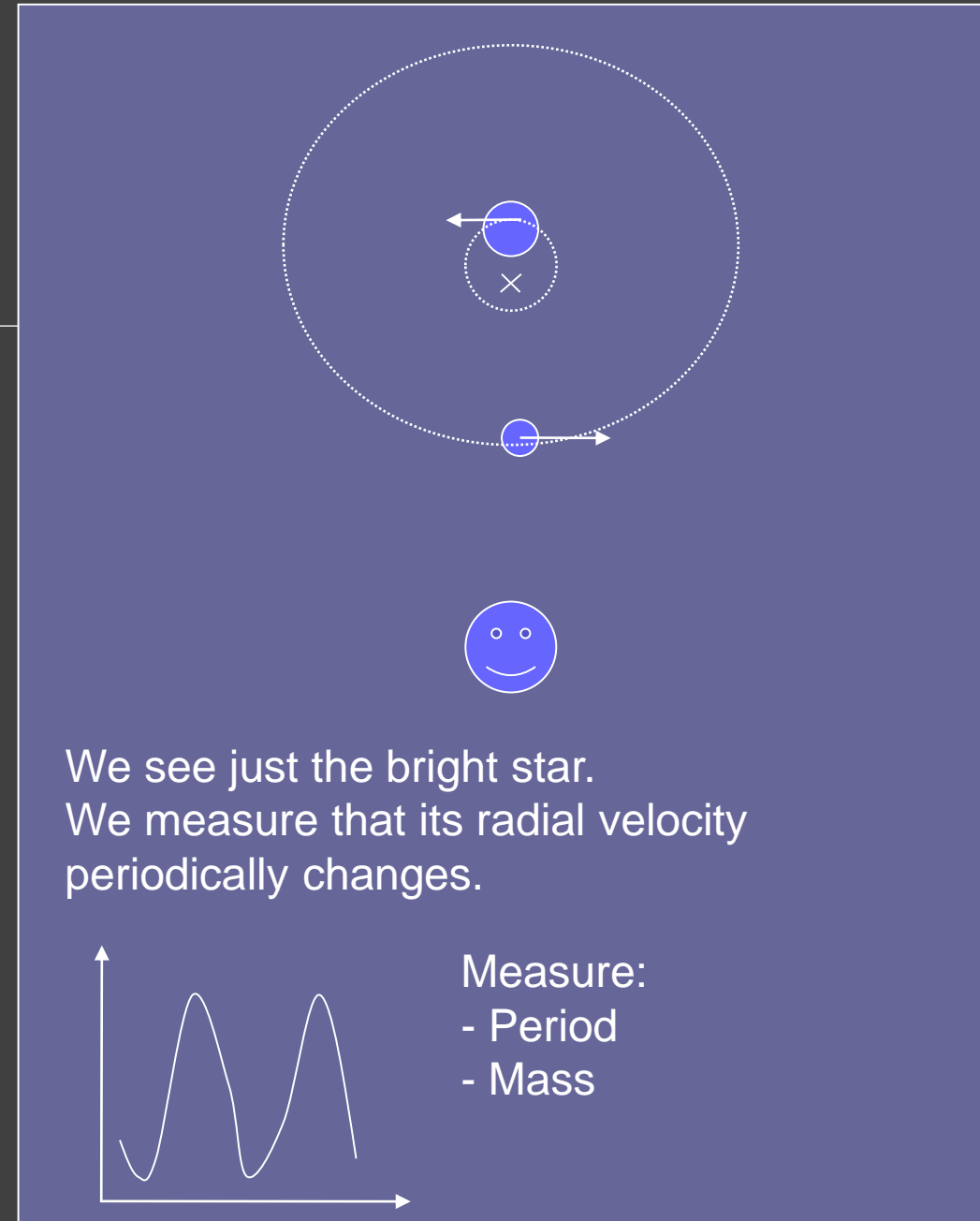
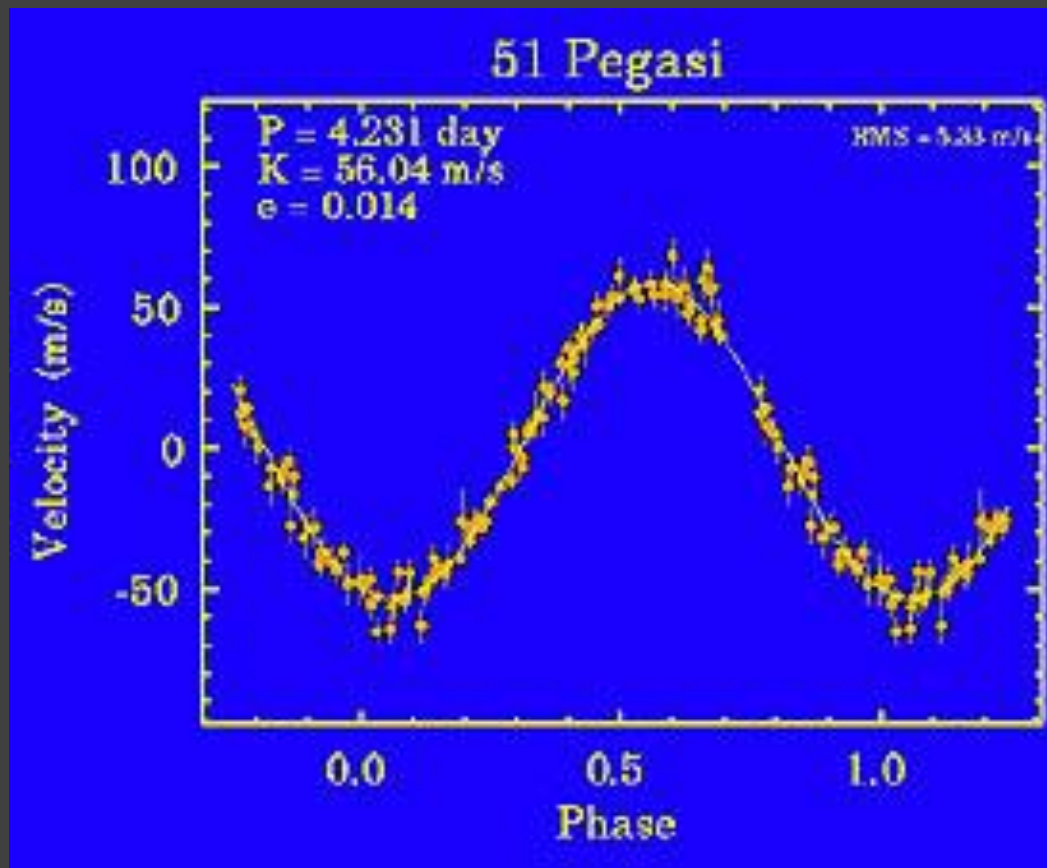
Confirmed Planets Discovered by TESS ¹	148
TESS Project Candidates Integrated into Archive (2021-08-14 13:00:03) ²	4436
Current date TESS Project Candidates at ExoFOP	4436
TESS Project Candidates Yet To Be Confirmed ³	3051

TESS data – 15/08/2021

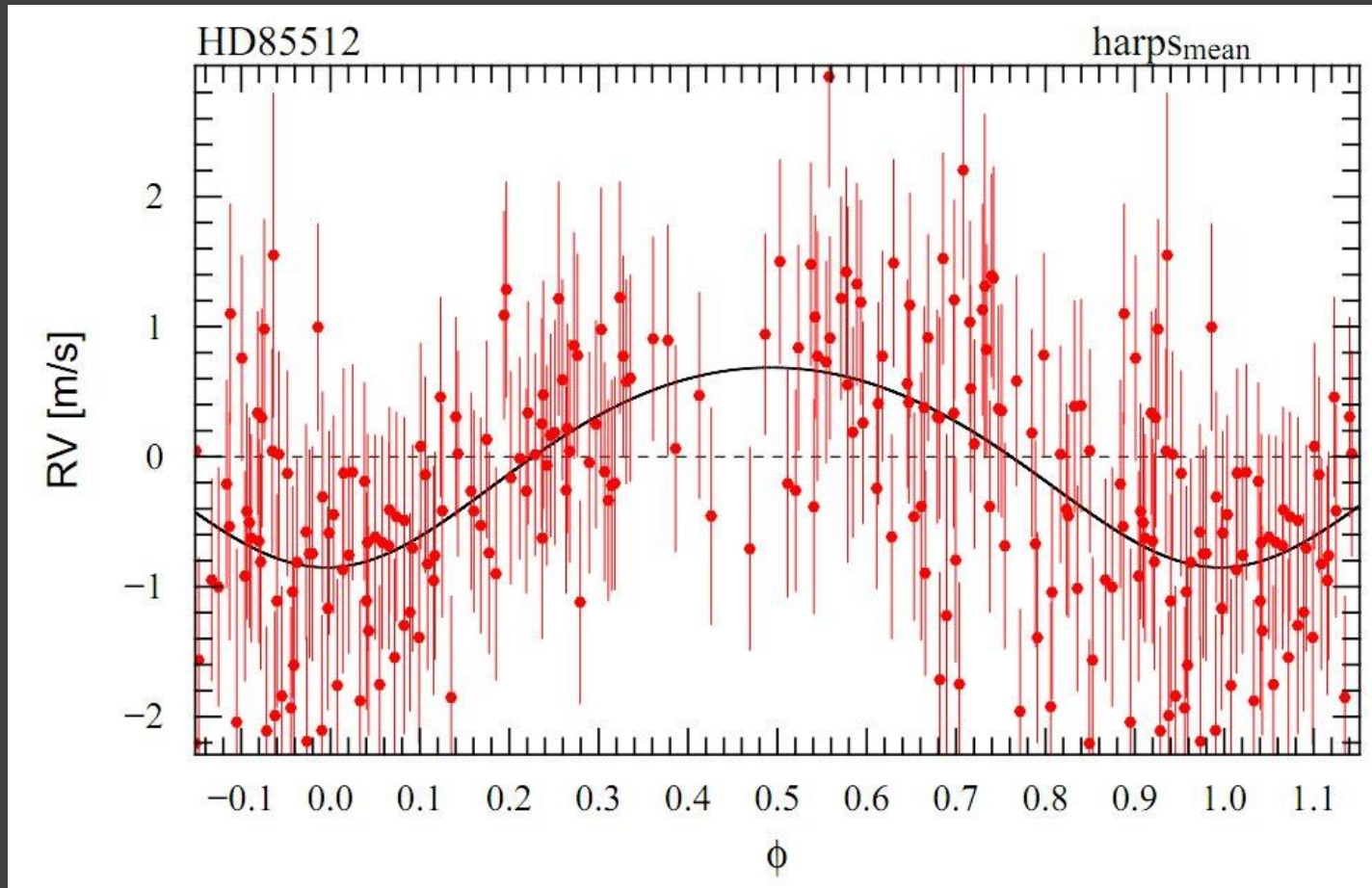


Radial velocities

Michel Mayor and Didier Queloz 1995



First light planets

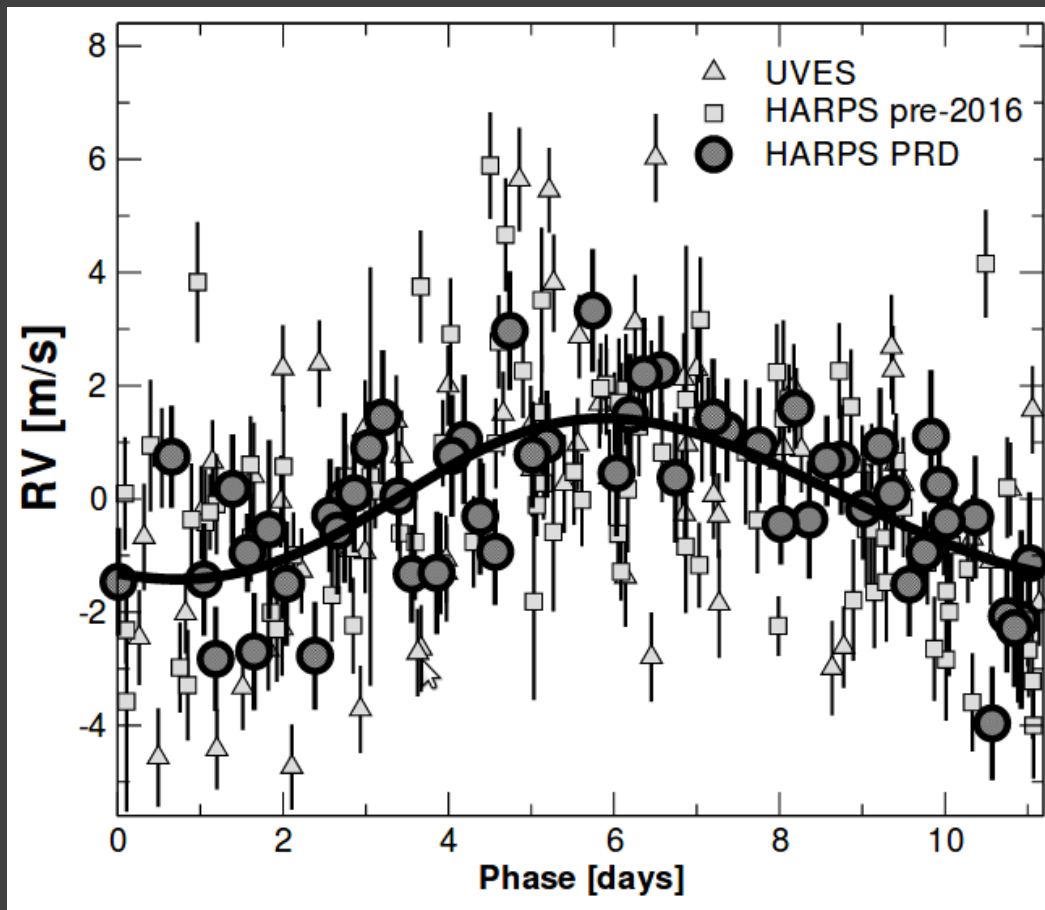


The problem is to measure small velocity variations for relatively long time.

Quality and stability of the spectrograph is more important than the telescope size.

This planet discovered by HARPS.
Situated just near the zone of habitability.

Proxima Centauri b



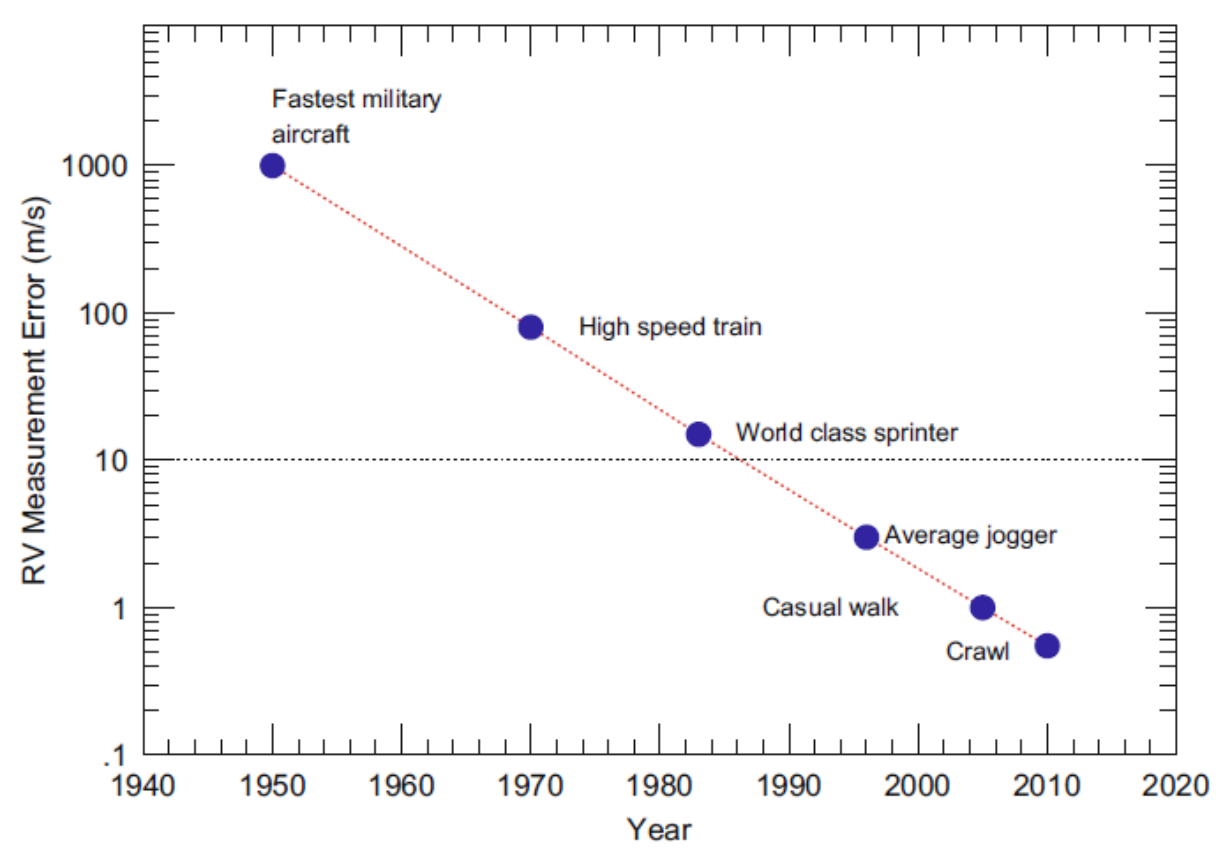
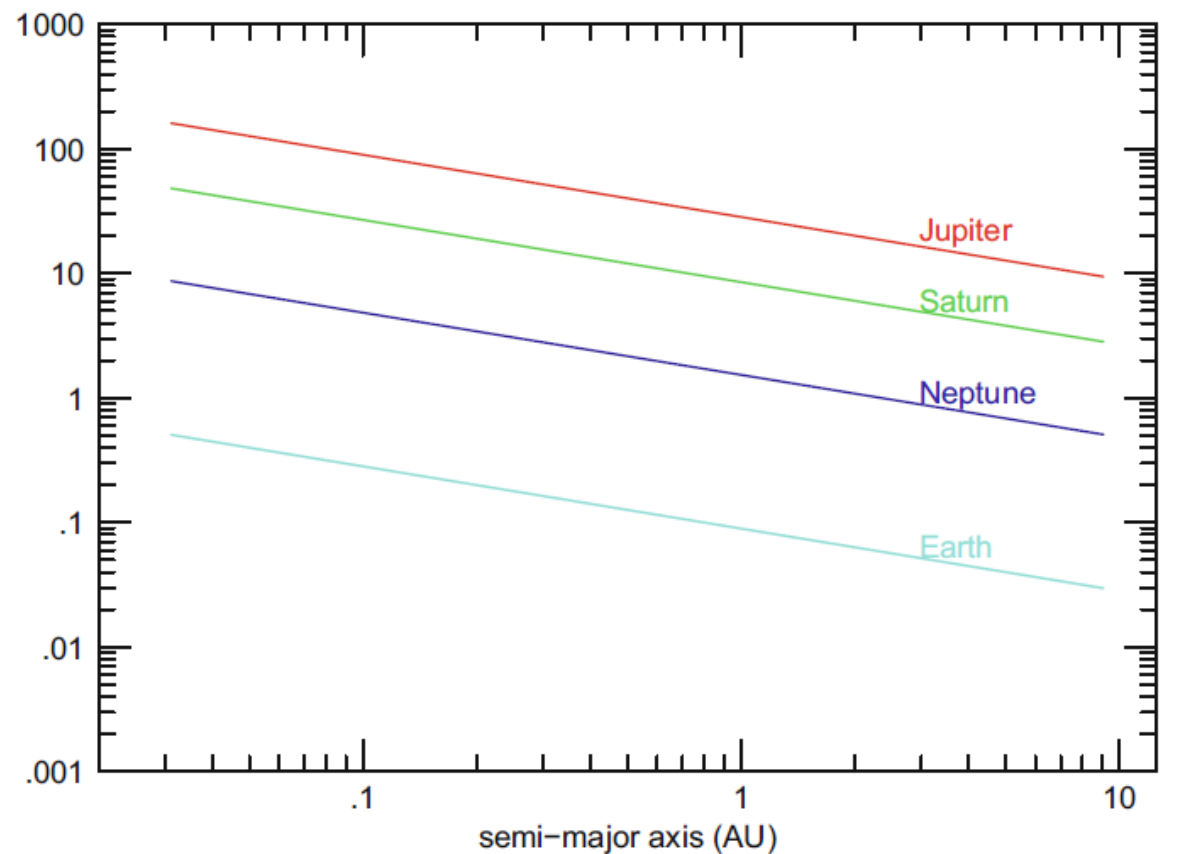
1.3 Earth masses

0.05 AU

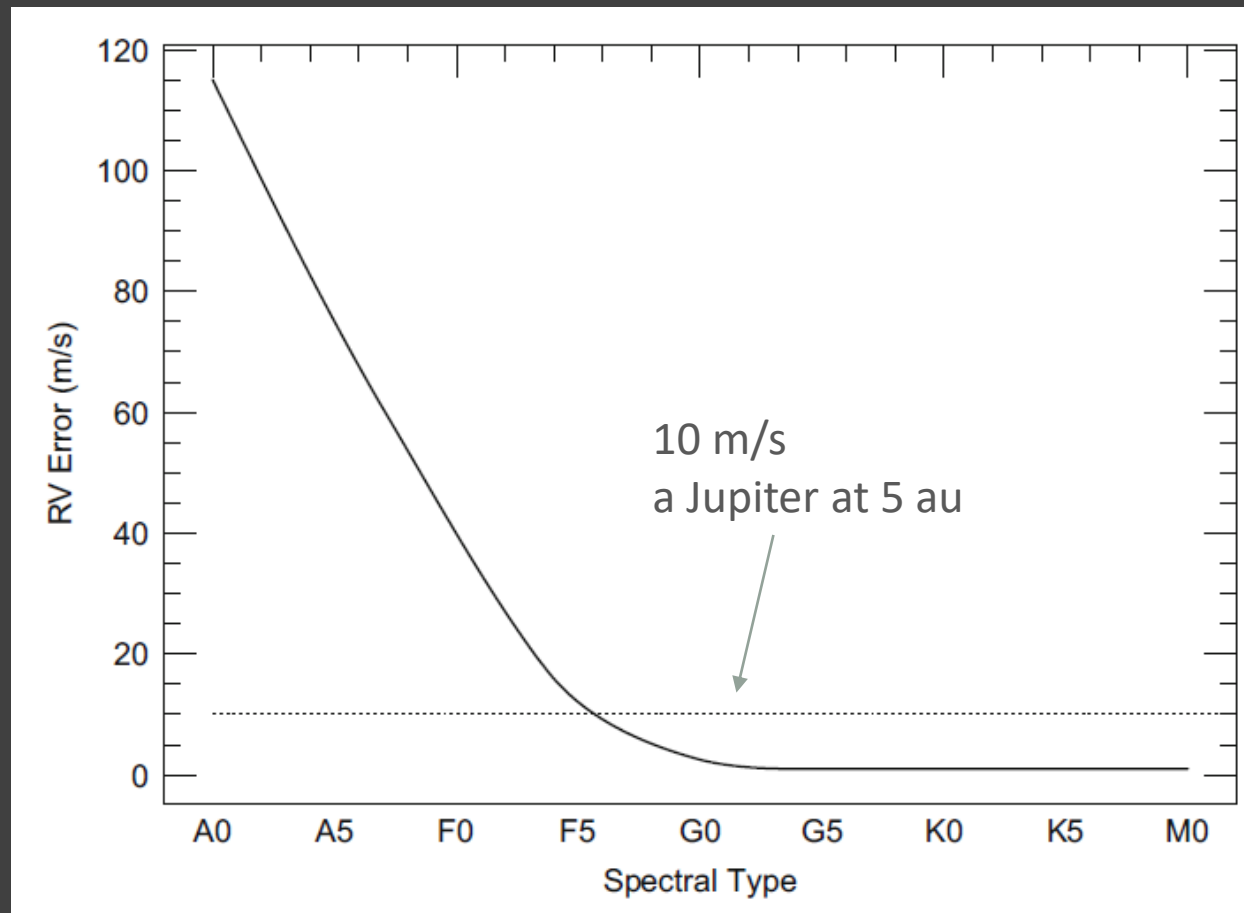
11 days

Habitability zone

Radial velocities: data and measurements



Role of a star



Difference is mainly due to

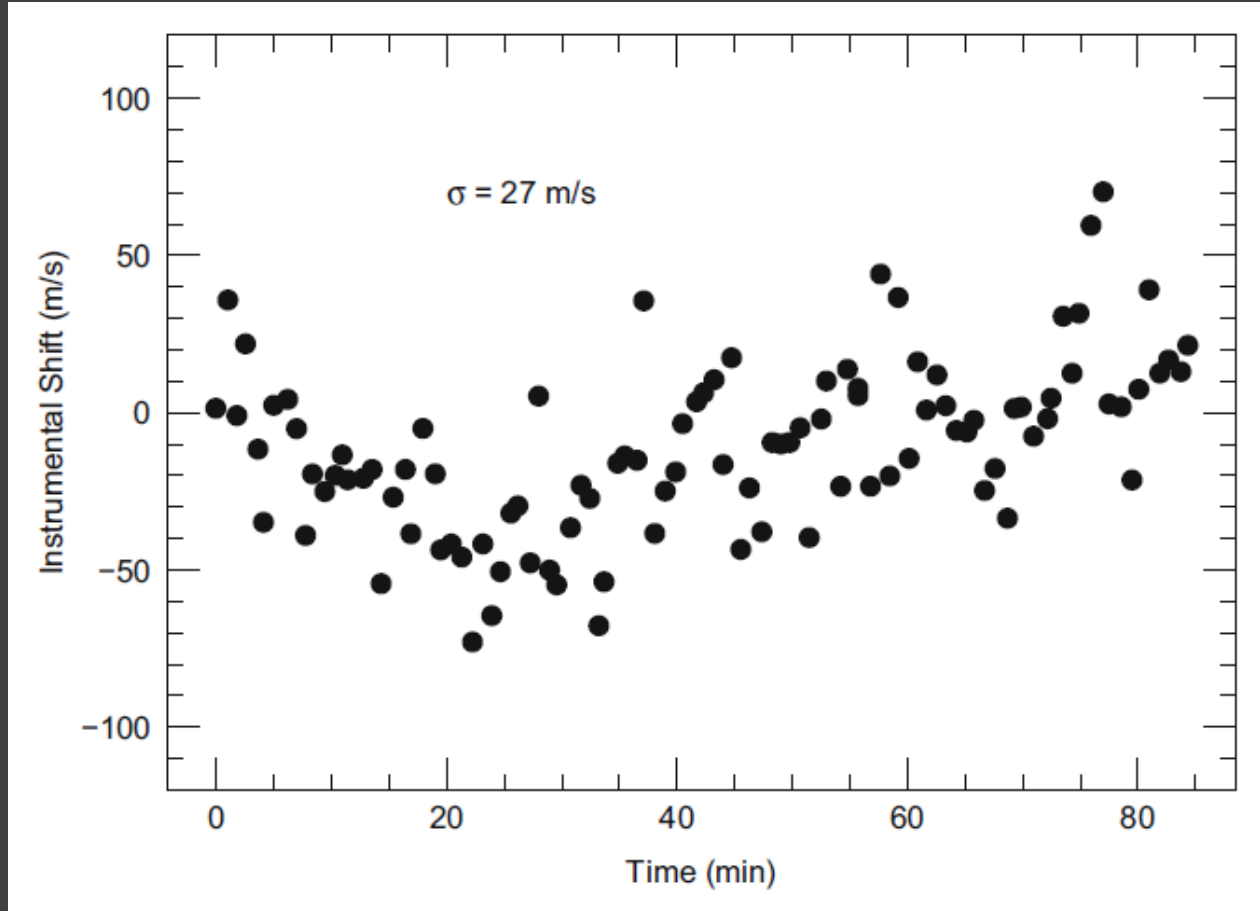
- Rapid rotation
- Smaller number of spectral lines

Without additional errors due to the instrument:

$$\sigma[\text{m/s}] = C(\text{S/N})^{-1} R^{-3/2} B^{-1/2} (v \sin i / 2) f(\text{SpT})$$

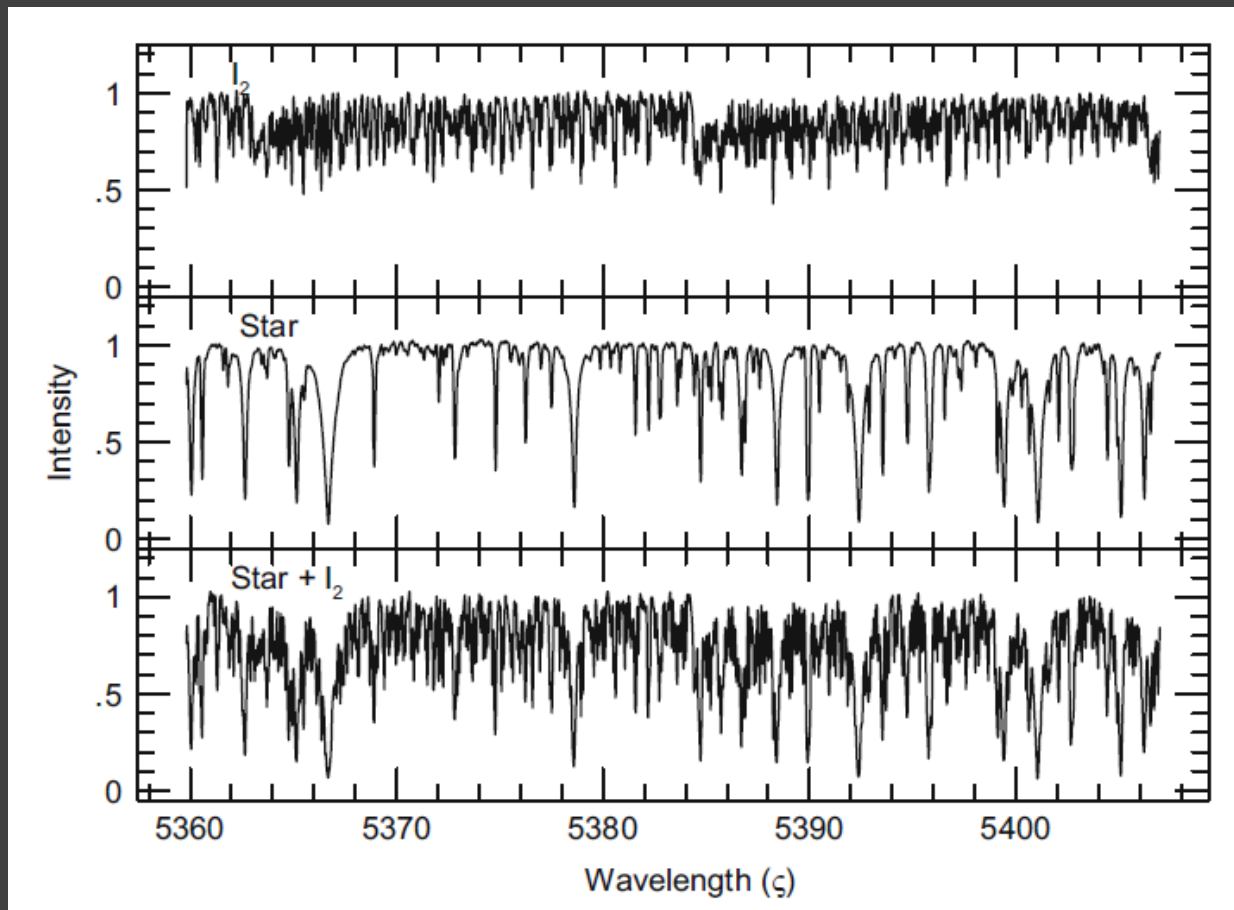
B - band width, R - resolution ($\lambda / \Delta\lambda$)

Necessity for simultaneous record of the stellar and calibration spectra



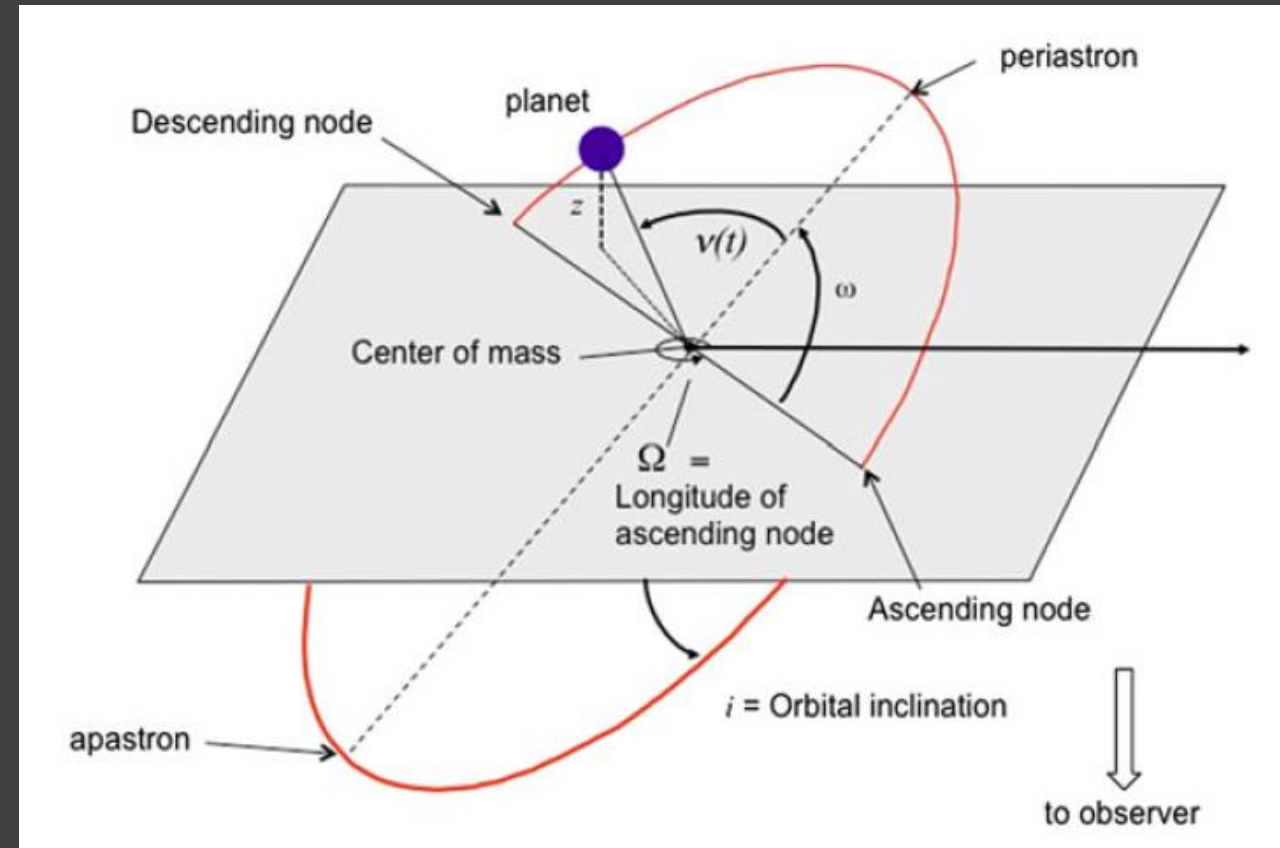
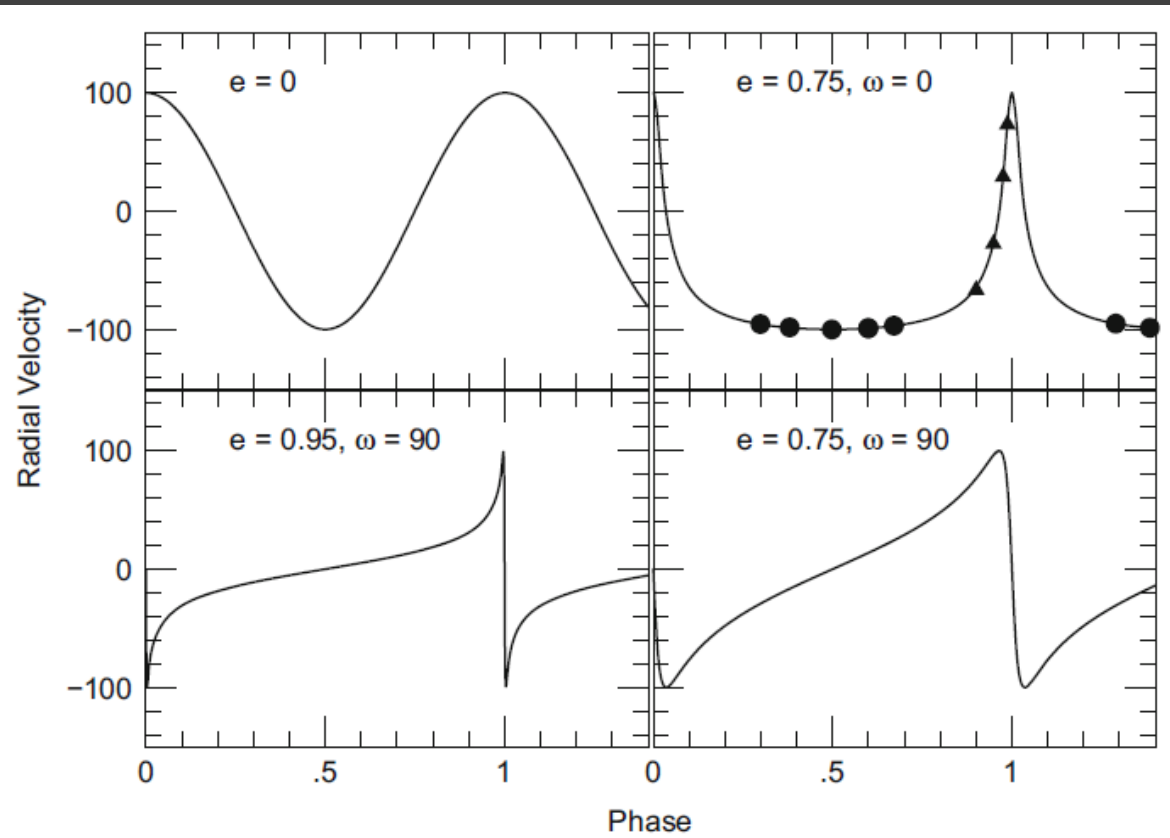
It is necessary to take the stellar and the laboratory spectra simultaneously, as the shift due to stellar velocity is very small and so the device cannot be stabilized to such level. Any external mechanical influence can shift the detector so that the position of the line cannot be determined with precision high enough to detect the signal from the planet presence.

Molecular iodine cell



I₂ cell became the first effective tool to provide lines for RV measurements.

Velocity vs. phase for different orbits



Planet mass

$$f(m) = \frac{M_2^3 \sin^3 i}{(M_1 + M_2)^2} = \frac{K_1^3 P (1 - e^2)^{3/2}}{2\pi G} \approx \frac{M_2^3 \sin^3 i}{M_1^2}$$

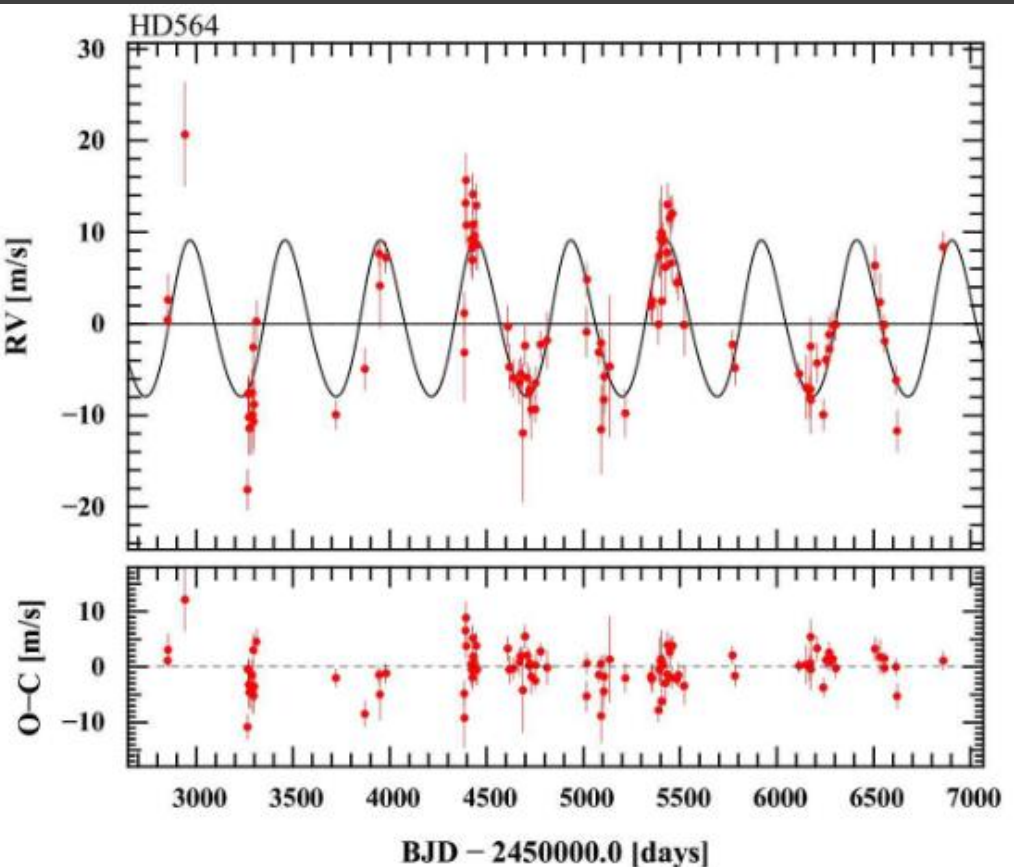
Thus, it is necessary to know the stellar mass (M_1)

$$\langle \sin i \rangle = \frac{\int_0^\pi p(i) \sin i \, di}{\int_0^\pi p(i) \, di} = \frac{\pi}{4} = 0.79$$

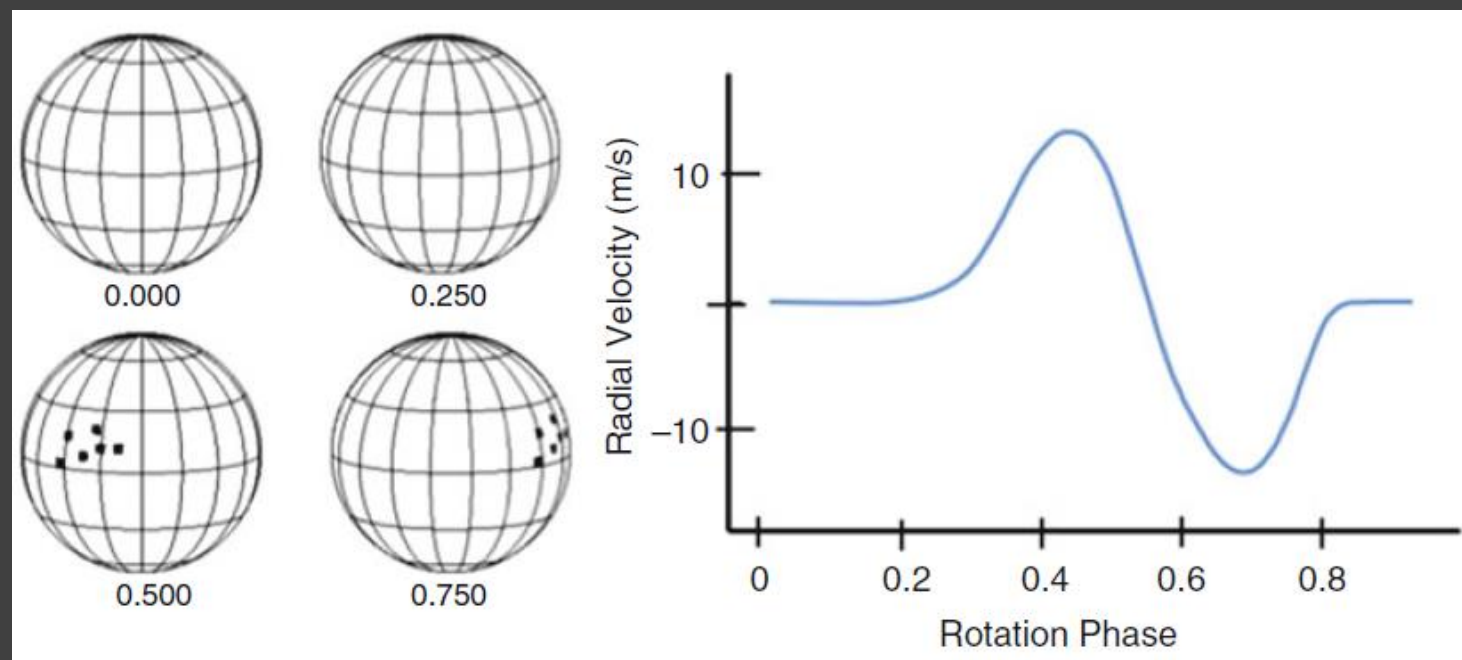
For the mass function
 $\langle \sin^3 i \rangle$ is important:

$$\frac{\int_0^\pi p(i) \sin^3 i \, di}{\int_0^\pi p(i) \, di} = 0.5 \int_0^\pi \sin^4 i \, di = \frac{3\pi}{16} = 0.59$$

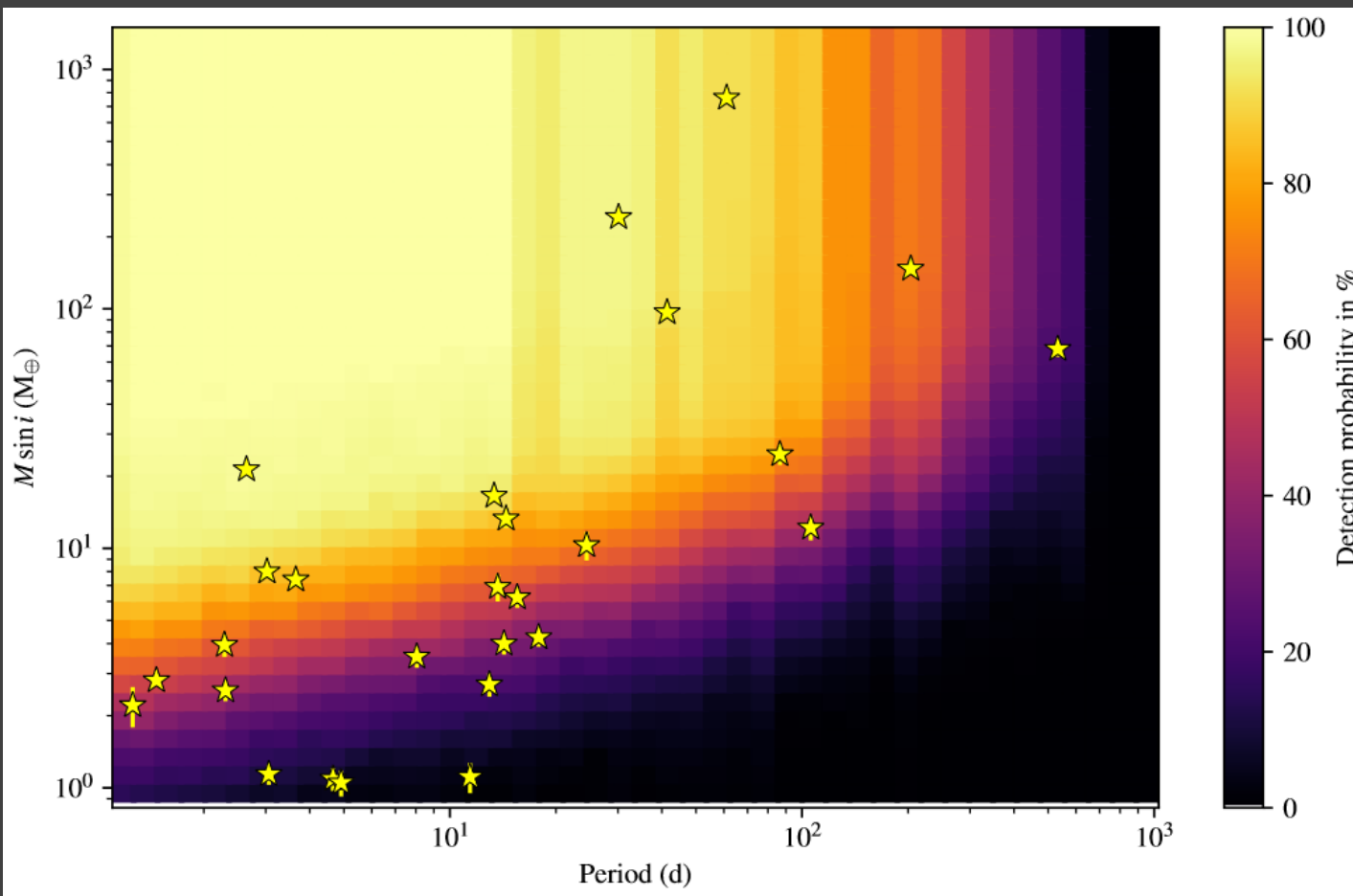
Stellar noise



Phenomenon	RV amplitude (m s^{-1})	Time scales
Solar-like oscillations	0.2–0.5	$\sim 5\text{--}15 \text{ min}$
Stellar activity (e.g., spots)	1–200	$\sim 2\text{--}50 \text{ days}$
Granulation/Convection pattern	$\sim \text{few}$	$\sim 3\text{--}30 \text{ years}$

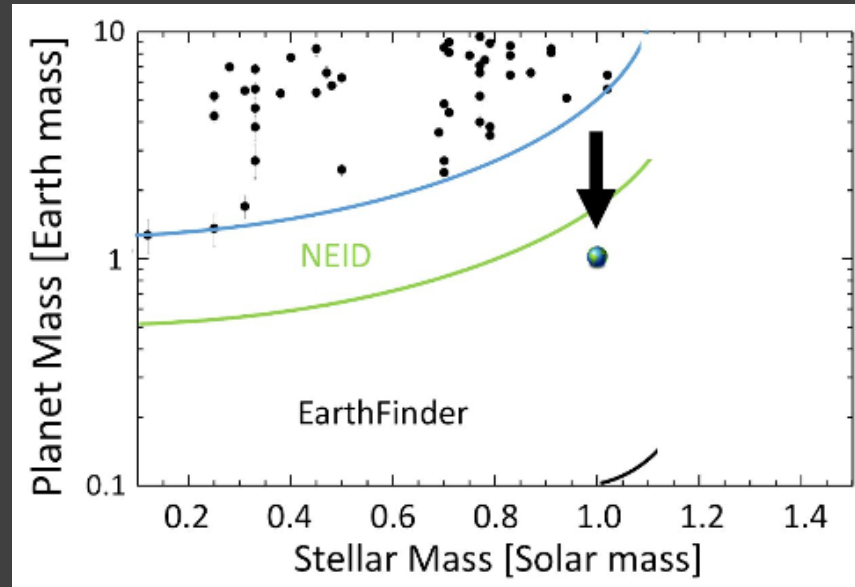
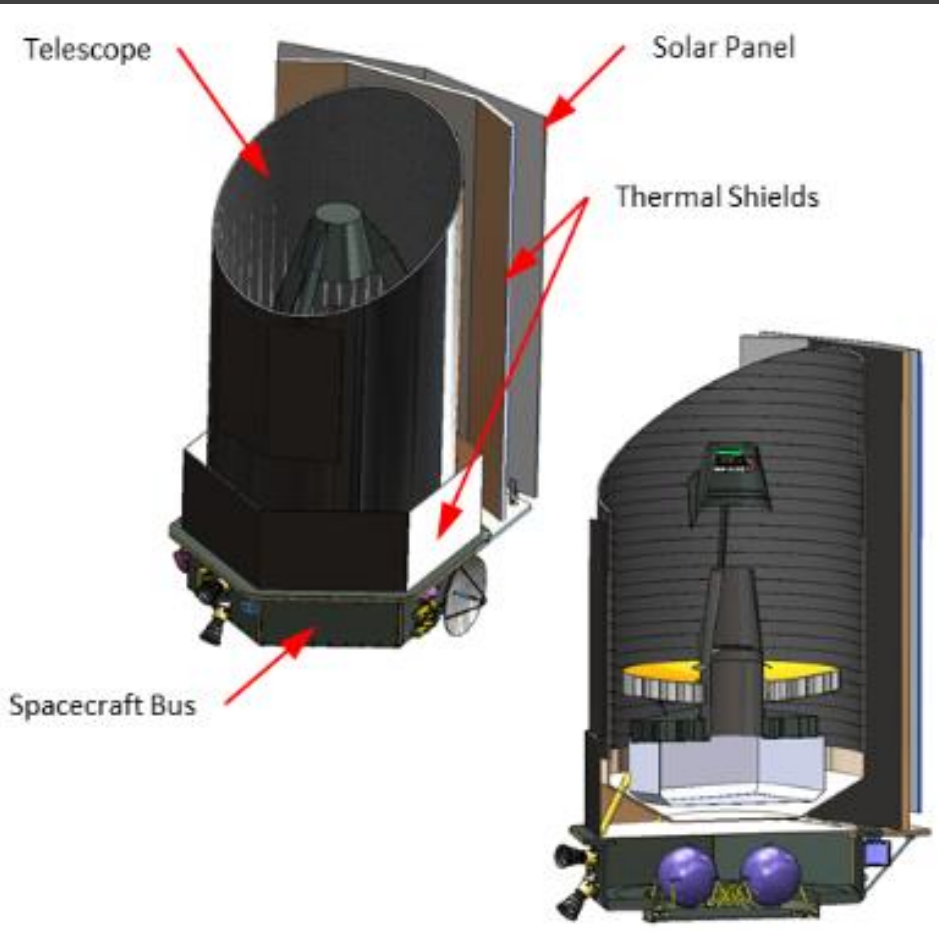


Selection effects for M-dwarf hosts



(a) All M stars of the sample (71 stars)		
P (d)		
1–10	10–100	100–1000
$N_{\text{pl,det}} = 0$	$N_{\text{pl,det}} = 2$	$N_{\text{pl,det}} = 1$
$\bar{n}_{\text{pl}} < 0.03$	$\bar{n}_{\text{pl}} = 0.04^{+0.03}_{-0.02}$	$\bar{n}_{\text{pl}} = 0.05^{+0.04}_{-0.03}$
(b) M stars with $M_{\star} > 0.34 M_{\odot}$ (48 stars)		
P (d)		
1–10	10–100	100–1000
$N_{\text{pl,det}} = 0$	$N_{\text{pl,det}} = 2$	$N_{\text{pl,det}} = 0$
$\bar{n}_{\text{pl}} < 0.04$	$\bar{n}_{\text{pl}} = 0.06^{+0.04}_{-0.03}$	$\bar{n}_{\text{pl}} < 0.07$
(c) M stars with $M_{\star} < 0.34 M_{\odot}$ (23 stars)		
P (d)		
1–10	10–100	100–1000
$N_{\text{pl,det}} = 0$	$N_{\text{pl,det}} = 0$	$N_{\text{pl,det}} = 1$
$\bar{n}_{\text{pl}} < 0.08$	$\bar{n}_{\text{pl}} < 0.08$	$\bar{n}_{\text{pl}} = 0.16^{+0.15}_{-0.09}$

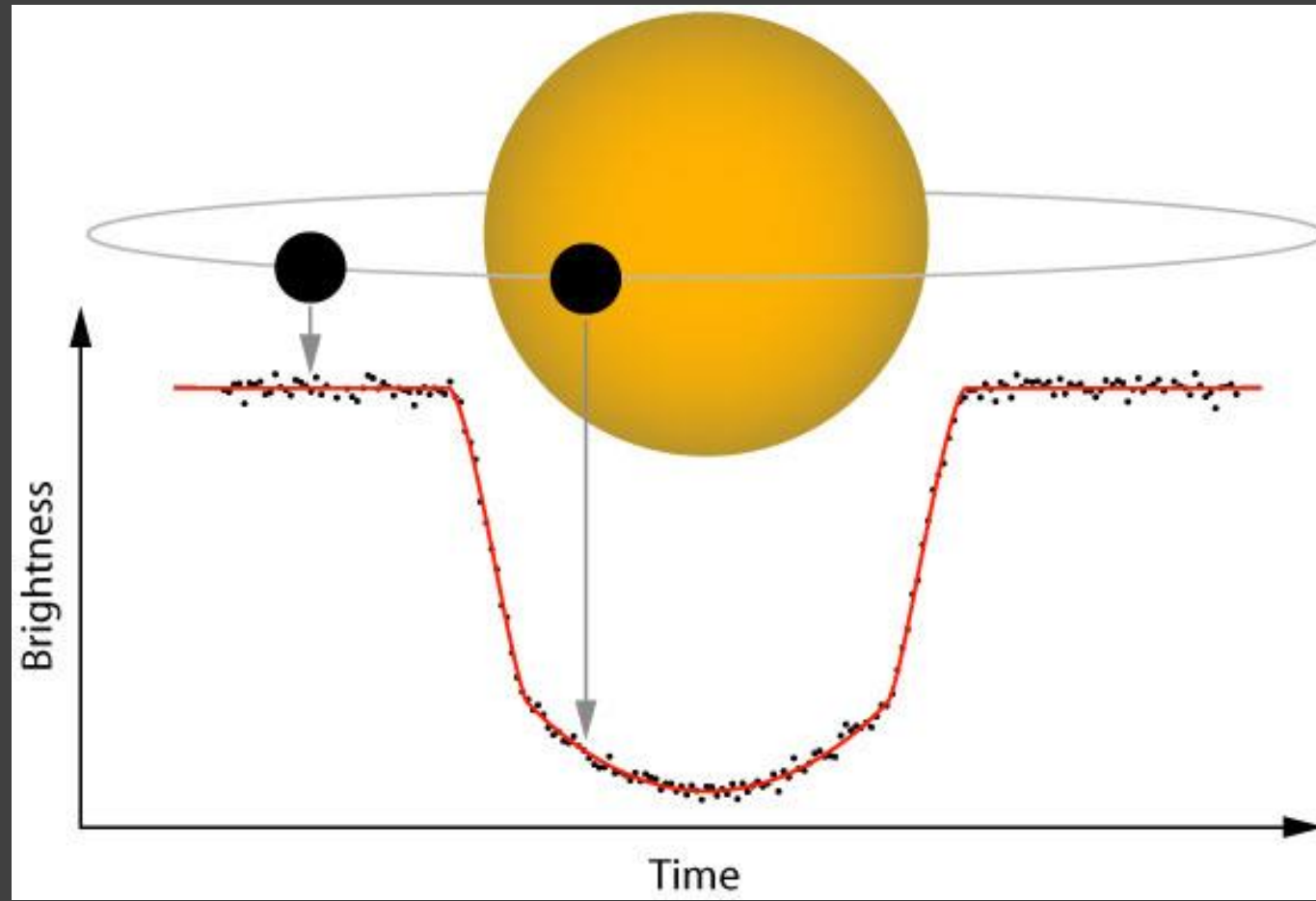
EarthFinder: Proposals of special space mission



The nominal spacecraft design is based upon the Kepler spacecraft by Ball Aerospace, with a 1.4-m primary, with the starlight coupled into single-mode fibers illuminating three high-resolution, compact and diffraction-limited spectrometer “arms”, one covering the near-UV (200-380nm), visible(380-900 nm) and near-infrared (NIR; 900-2500 nm) respectively with a spectral resolution of greater than 150,000 in the visible and near-infrared arms.

Planet transits

Proposed by
Otto Struve
in 1952

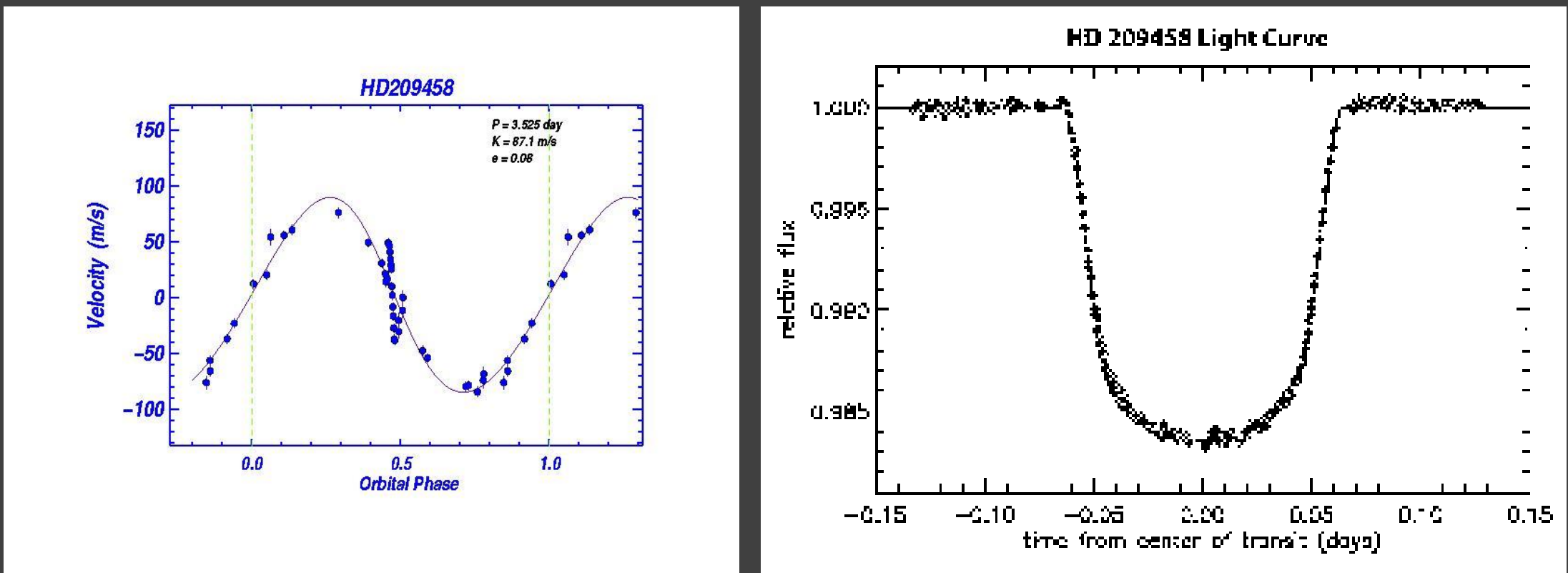


$$\frac{S_{\text{star}} - S_{\text{planet}}}{S_{\text{star}}}$$

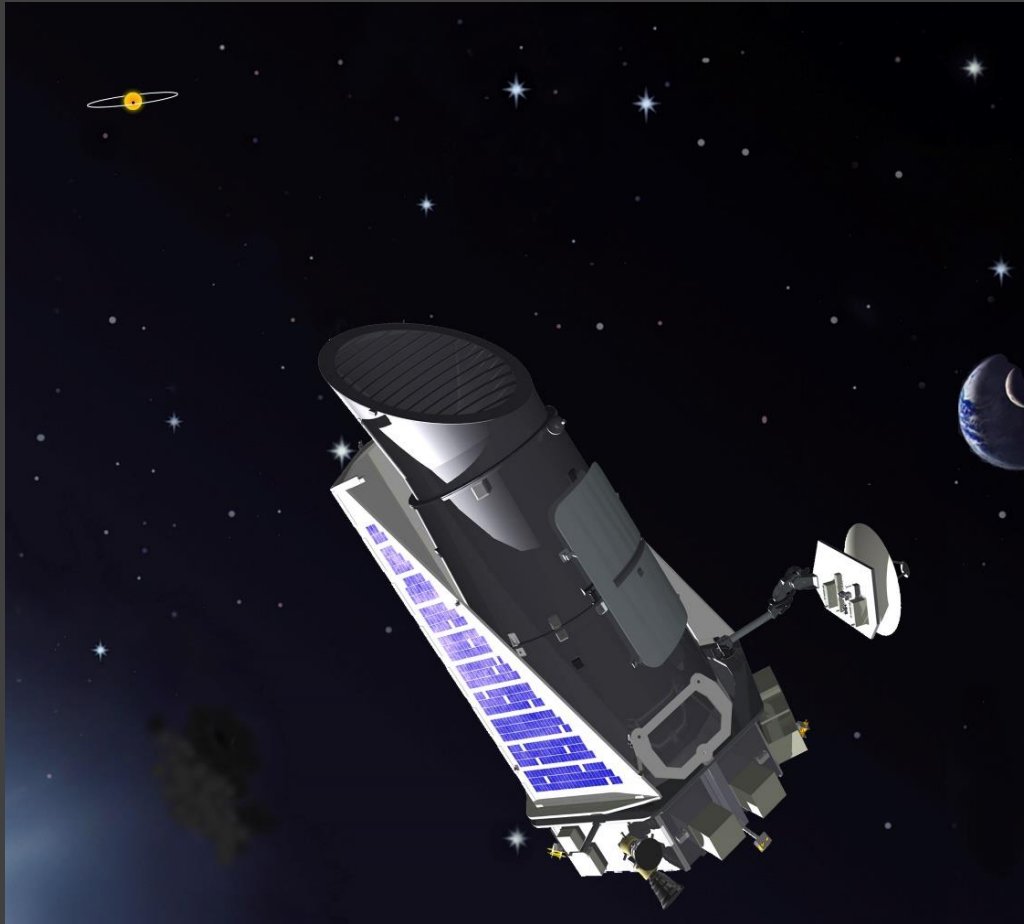
Limb darkening
is important!!!

The first transit measurement. HD 209458

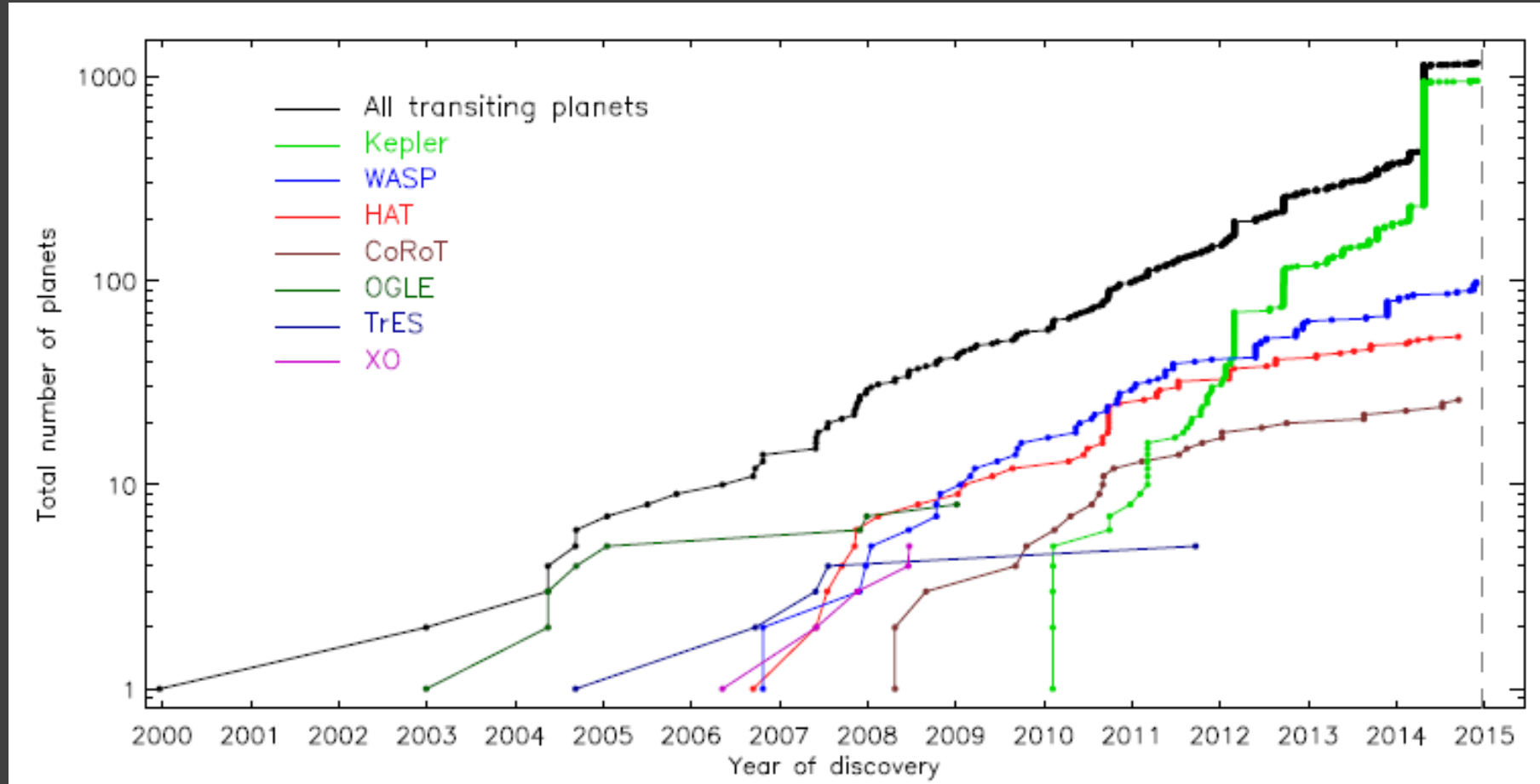
The first measurements of a transit was made from the ground for a planet discovered by RV, and so known orbital parameters.



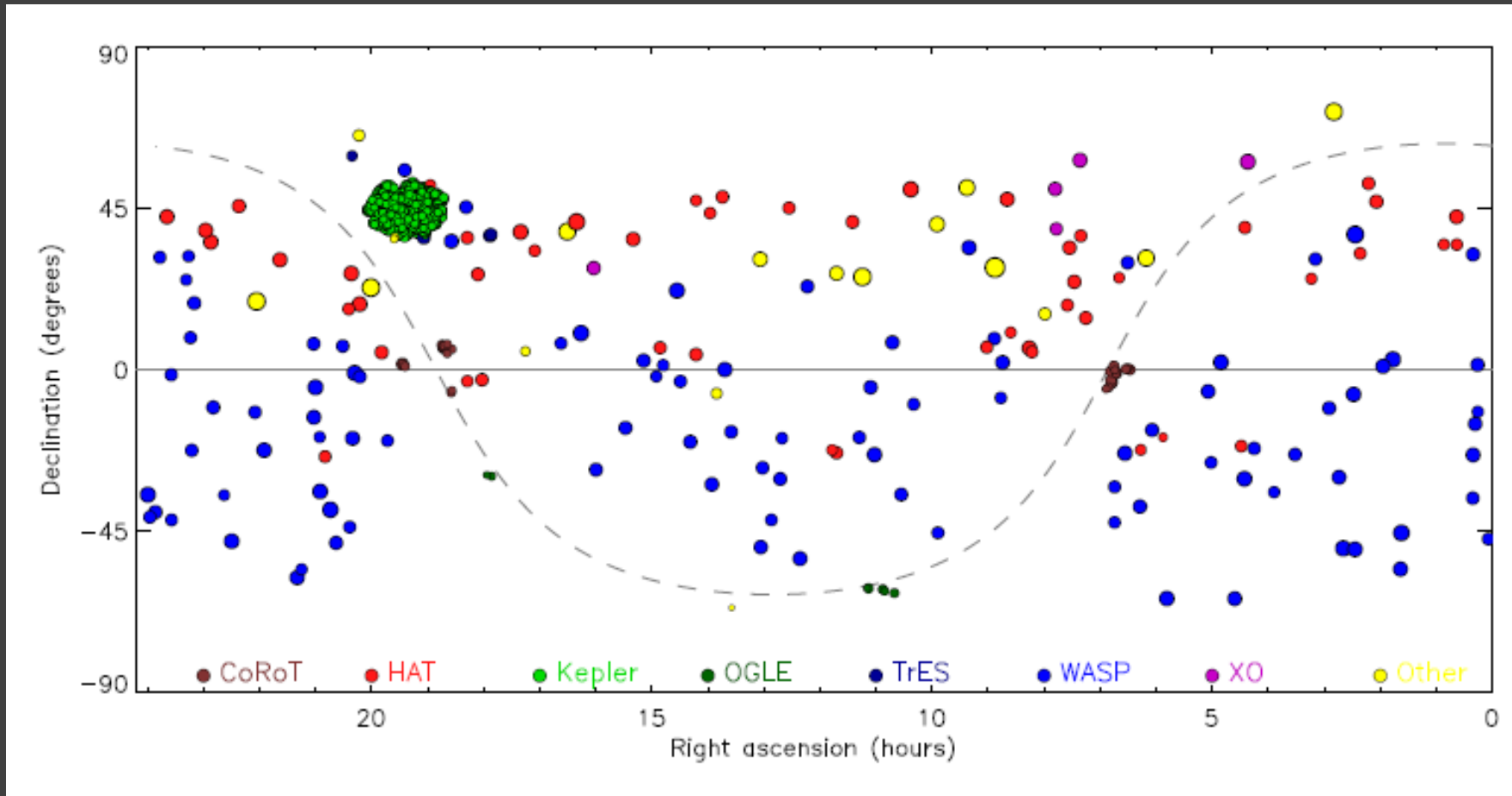
Kepler and CoRoT



Rate of discovery



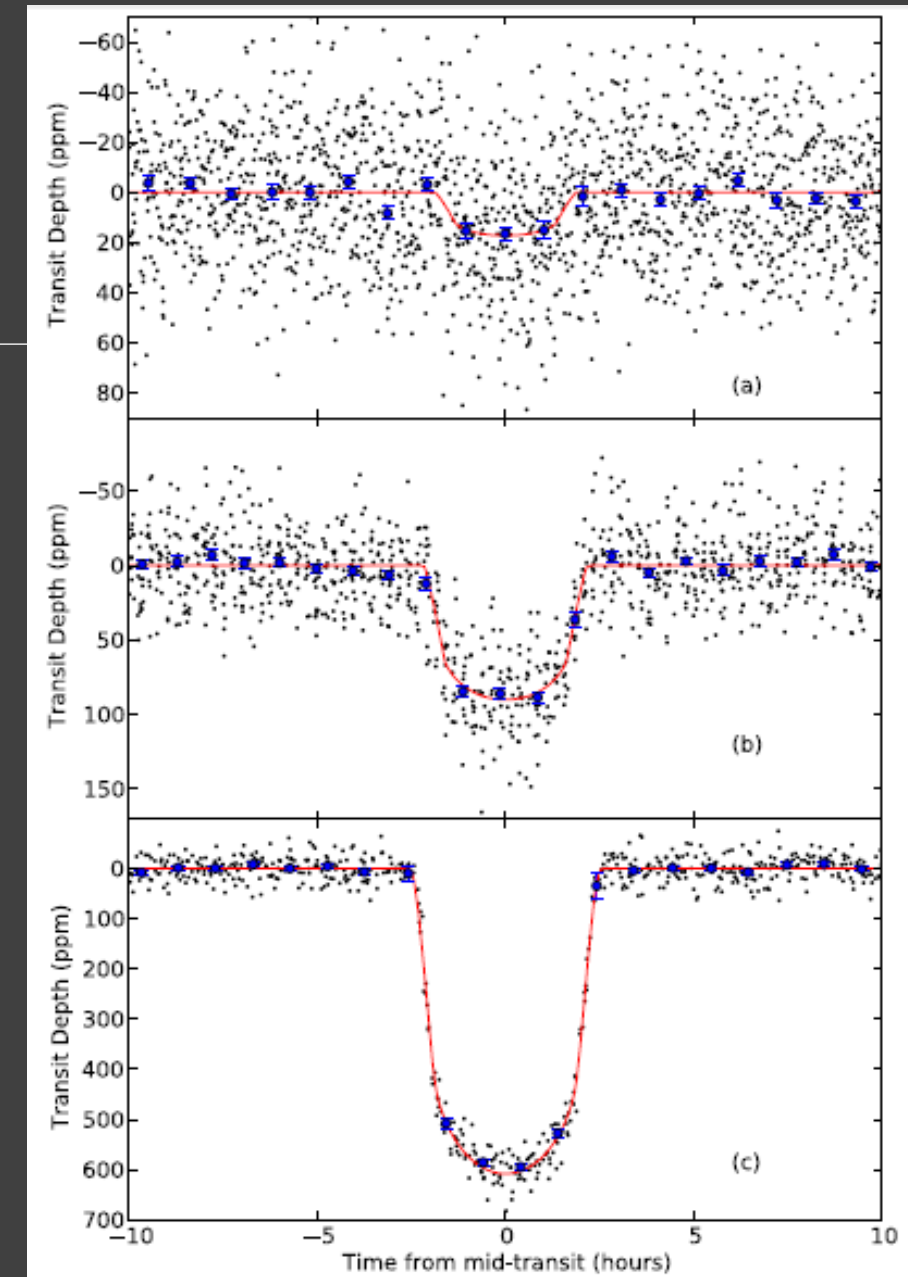
Transiting planets in the sky



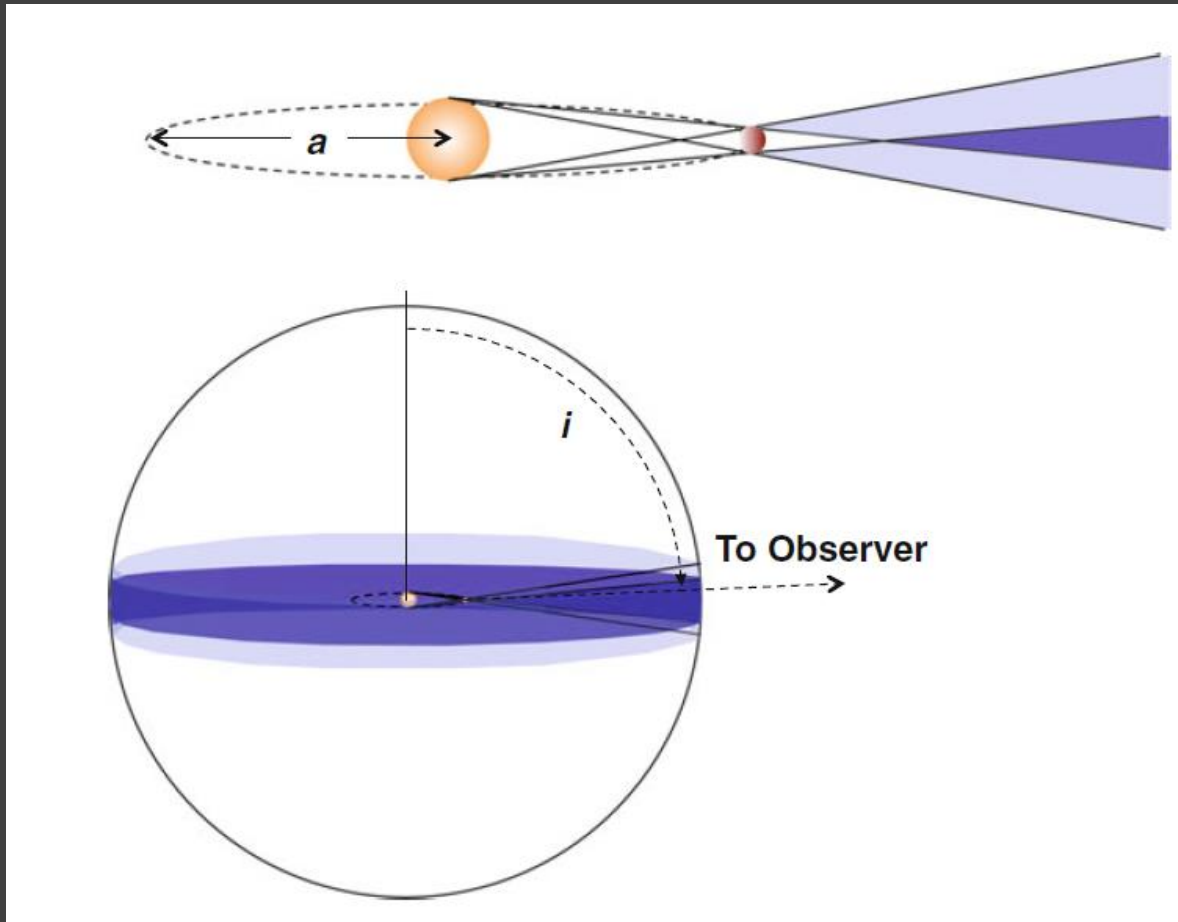
Very small planets

Kepler-37b

The first discovered exoplanet
with size smaller than Mercury

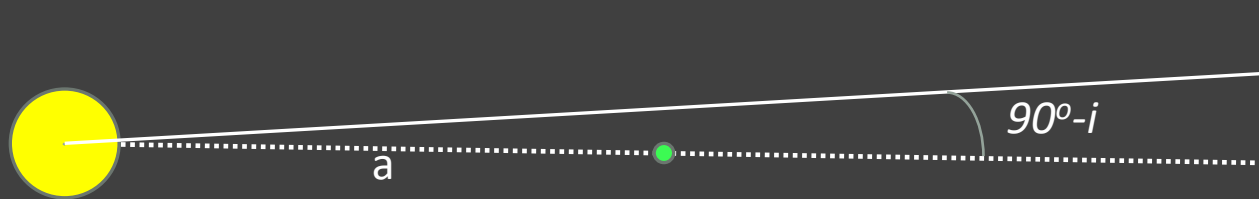


Transit probability



$$\Pr \left(\cos i < \frac{R_*}{a} \right) = \simeq 0.0046 \left(\frac{R_*}{R_\odot} \right) \left(\frac{1 \text{ au}}{a} \right).$$

Transit conditions



i is the angle between the angular-momentum vector of the planet's orbit and the line of sight

$$b = \frac{a \cos i}{R_*}.$$

$$\frac{d\Omega}{4\pi} = \frac{2\pi \sin i \, di}{4\pi} = \frac{d(\cos i)}{2}.$$

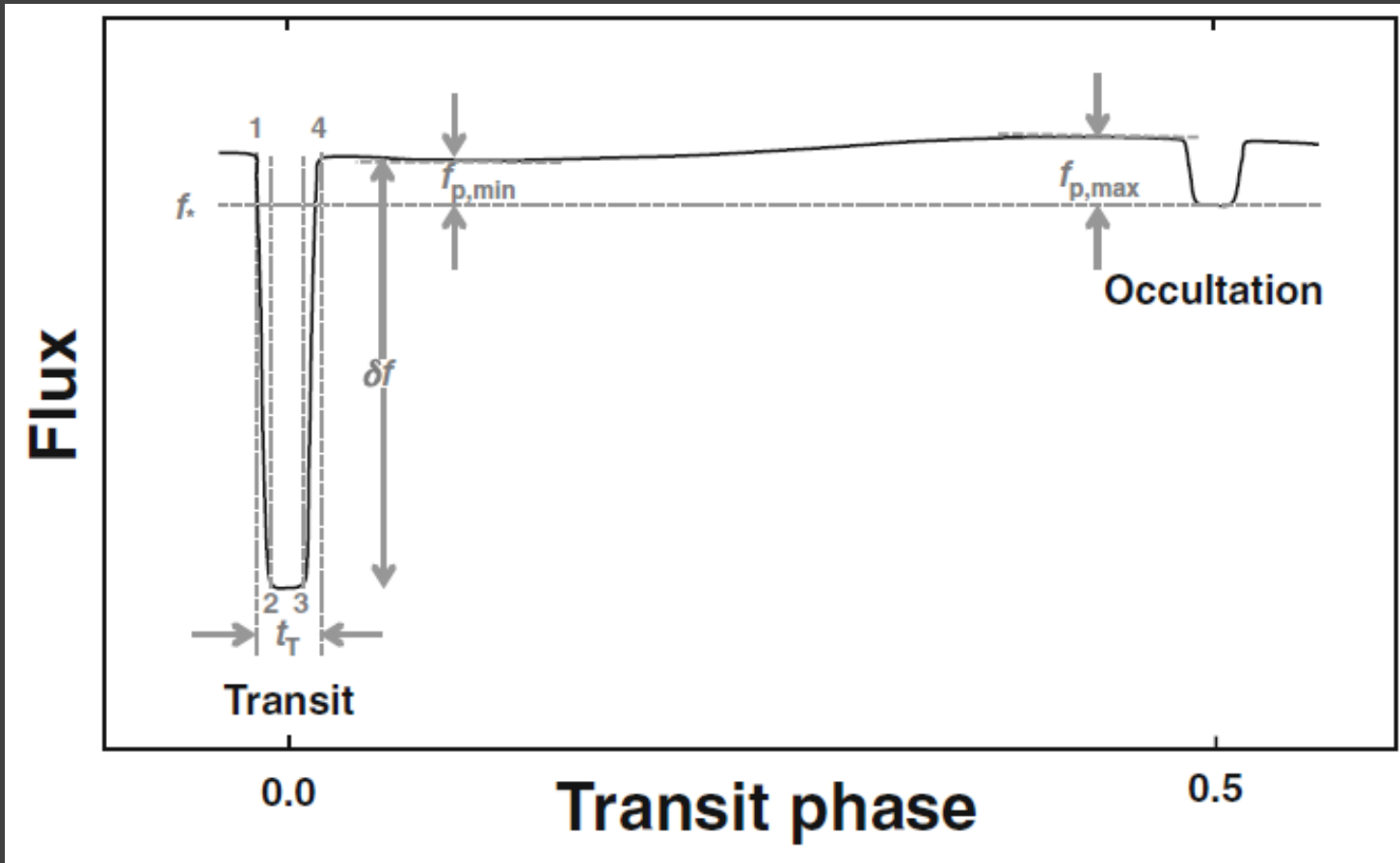
$$\Pr\left(\cos i < \frac{R_* + R_p}{a}\right) = \frac{1}{2} \int_{-(R_* + R_p)/a}^{(R_* + R_p)/a} = \frac{R_* + R_p}{a}.$$

$$R_p \ll R_*,$$

$$\Pr\left(\cos i < \frac{R_*}{a}\right) \simeq 0.0046 \left(\frac{R_*}{R_\odot}\right) \left(\frac{1\text{au}}{a}\right).$$

Selection in favour
of close-in planets.

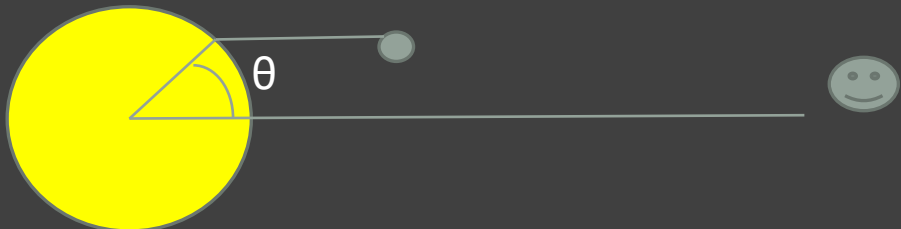
Transit depth



$$\frac{\Delta f}{f} \simeq \left(\frac{R_p}{R_*} \right)^2 = 0.0105 \left(\frac{R_p}{R_{\text{Jup}}} \right)^2 \left(\frac{R_*}{R_\odot} \right)^{-2}$$

Non-uniform brightness distribution (limb darkening) is important.

Limb darkening



$$\mu = \cos \theta = \sqrt{1 - b^2}.$$

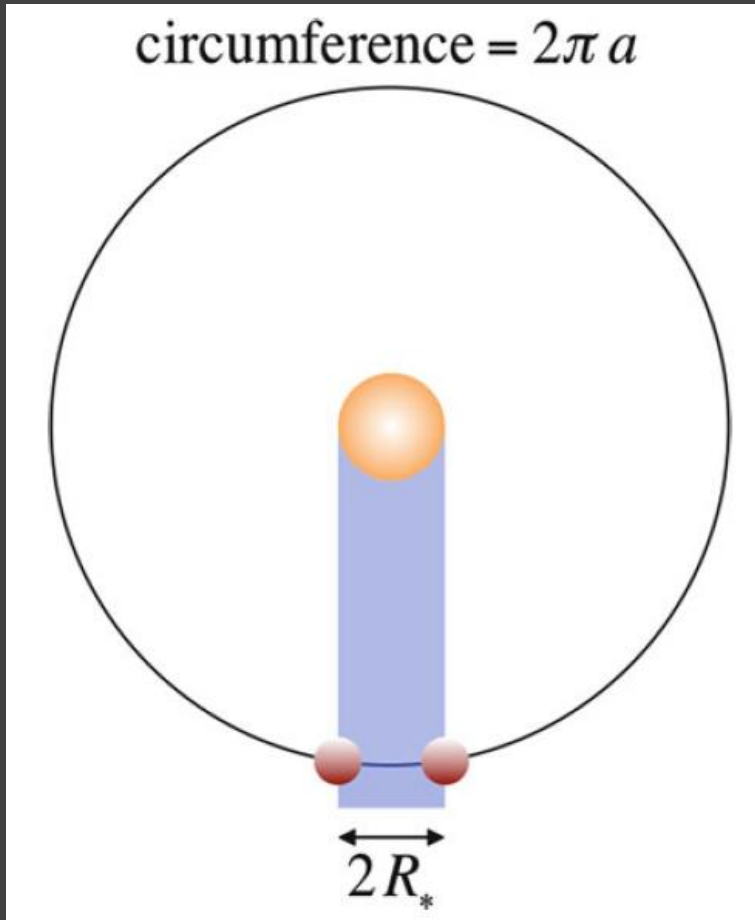
$$I = I_0(1 - u(1 - \mu))$$

Limb darkening can be taken into account in a more precise manner

$$\frac{I(\mu)}{I_0} = 1 - \sum_{n=1}^4 u_n (1 - \mu^{n/2}).$$

$$\begin{aligned}\frac{\Delta f}{f} &= \frac{\pi R_p^2 I_0 (1 - u + u \cos \theta)}{2\pi R_*^2 I_0 \int_0^{\pi/2} (1 - u + u \cos \theta) \sin \theta \cos \theta d\theta} \\ &= \frac{3(1 - u + u\sqrt{1 - b^2})}{3 - u} \left(\frac{R_p}{R_*}\right)^2.\end{aligned}$$

Transit duration



$$\frac{T}{P} = \frac{1}{\pi} \sin^{-1} \frac{R_*}{a}$$

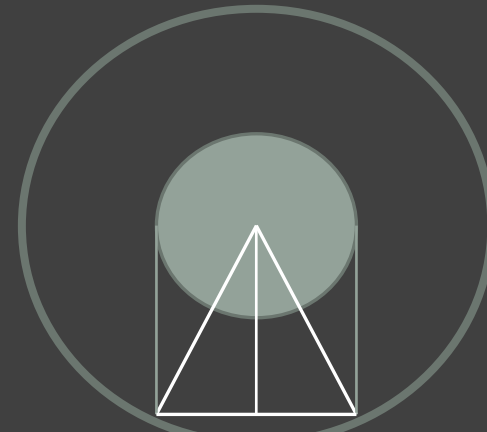
$$\frac{T}{P} = \frac{1}{\pi} \sin^{-1} R_* \left(\frac{4\pi^2}{GM_* P^2} \right)^{1/3}$$

$$\frac{t_T}{P} = \frac{1}{\pi} \sin^{-1} \left(\frac{R_*}{a} \left\{ \frac{[1 + (R_p/R_*)]^2 - [(a/R_*) \cos i]^2}{1 - \cos^2 i} \right\}^{1/2} \right)$$

t_T – from first to last contact

For $\cos i \ll 1$

$$\frac{t_{\text{tr}}}{P} \simeq \frac{R_*}{a} \frac{\sqrt{(1 + R_p/R_*)^2 - b^2}}{\pi} \frac{1 + e \sin \omega}{1 - e^2}.$$



$$\frac{t_T}{P} = \frac{R_*}{\pi a} \sqrt{\left(1 + \frac{R_p}{R_*}\right)^2 - b^2}.$$

System parameters

$$T \simeq 3h \left(\frac{P}{4d} \right)^{1/3} \left(\frac{\rho_*}{\rho_\odot} \right)^{-1/3}$$

Stellar density estimate

$$\frac{dv_r}{dt} = \frac{2\pi K}{P} = \frac{GM_p}{a^2} = g_p \frac{R_p^2}{a^2} = g_p \frac{R_p^2}{R_*^2} \frac{R_*^2}{a^2},$$

K – stellar velocity

$$g_p = \frac{2\pi K}{P} \left(\frac{R_*}{R_p} \right)^2 \left(\frac{a}{R_*} \right)^2$$

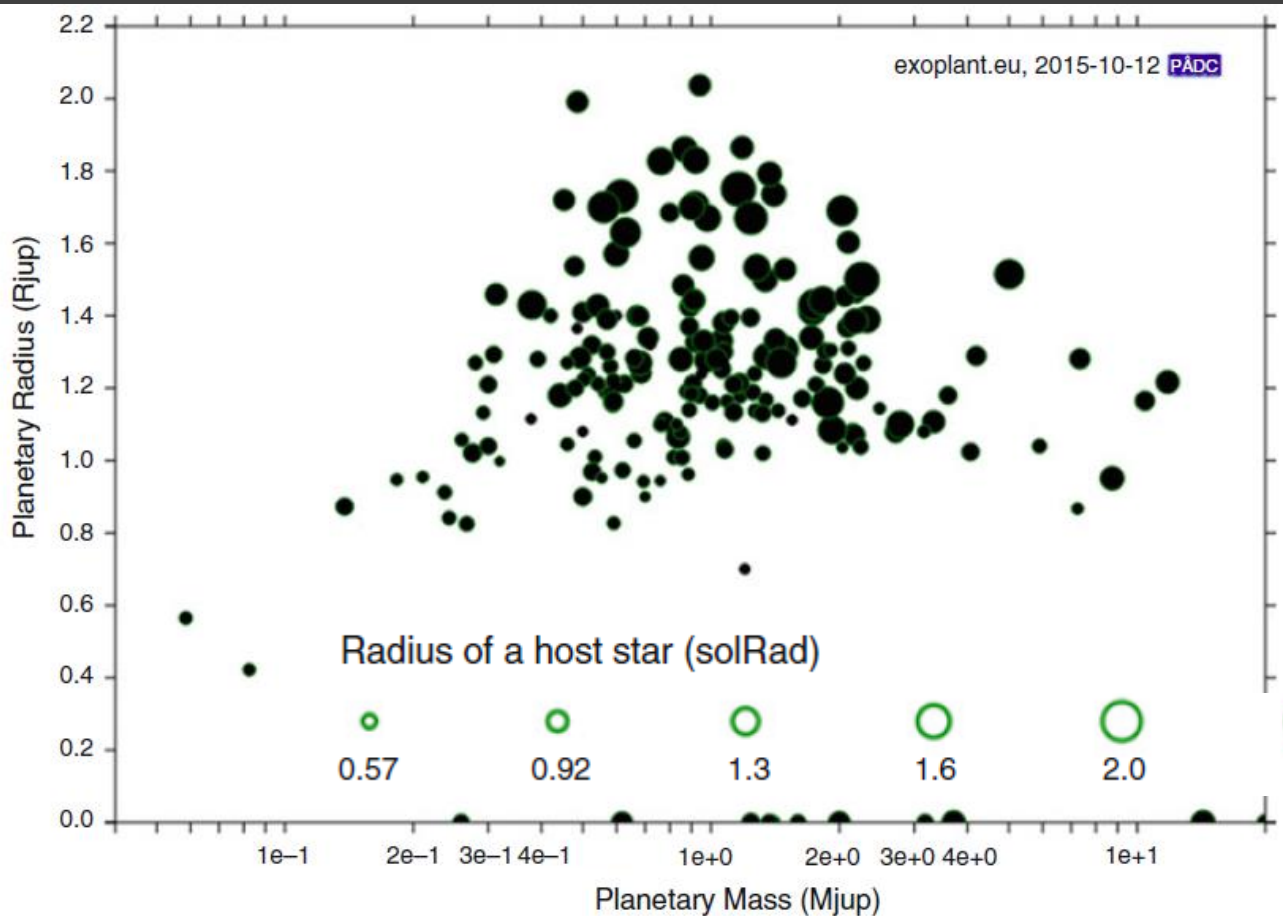
Planet density

$$\rho_p = \frac{3g_p}{4\pi G R_p} = \frac{3g_p}{4\pi G R_*} \left(\frac{R_*}{R_p} \right)$$

$$R_* = \theta d = \theta / \hat{\pi}:$$

$$\rho_p = \frac{3g_p \hat{\pi}}{4\pi G \theta} \left(\frac{R_*}{R_p} \right)$$

Ground based searches with small cameras



It is expected to have one hot Jupiter per 82 sq. degrees at V<12

$$3600 \times \frac{180}{\pi} \frac{1}{f} = \frac{206265}{f} \text{ arcsec/mm,}$$

For 200-mm camera we have:

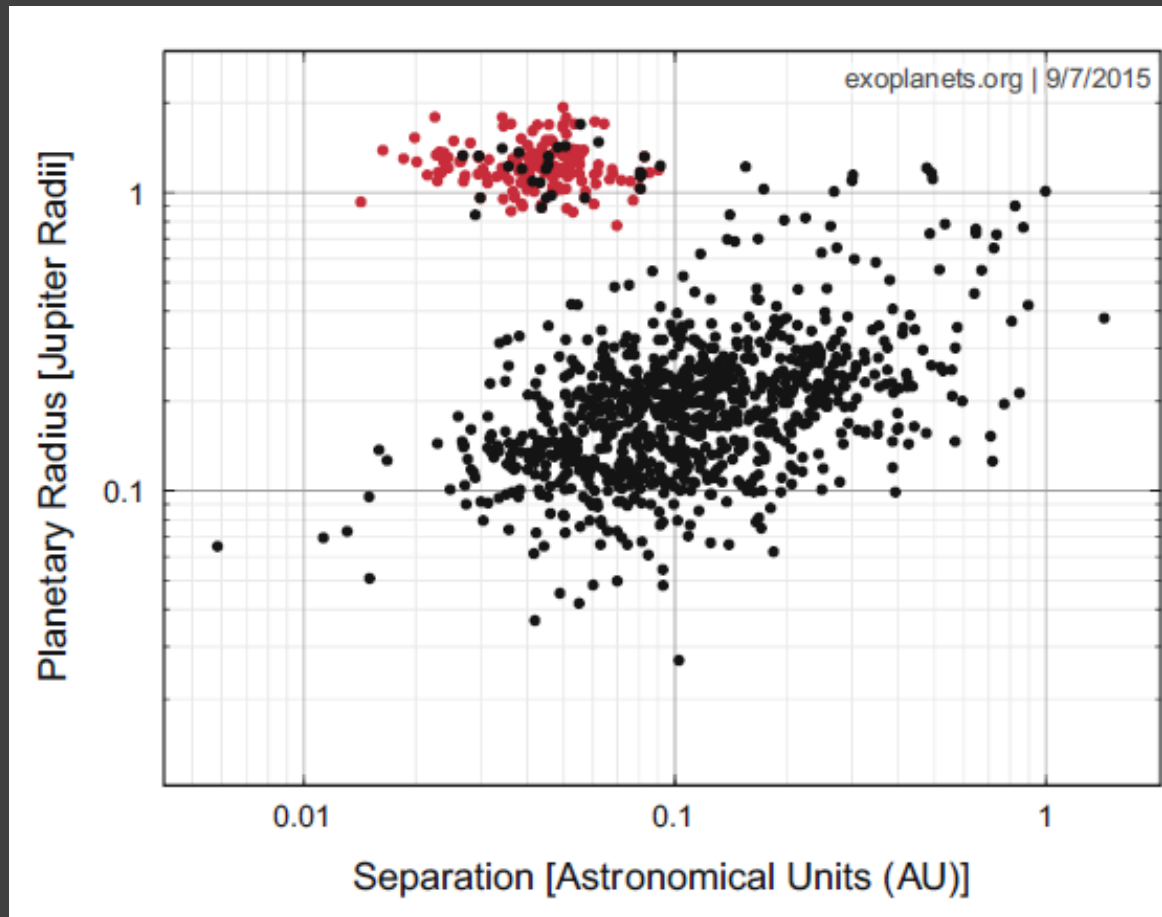
$$3600 \times \frac{180}{\pi} \frac{1}{f} = 1031 \text{ arcsec/mm,}$$

$$0.0135 \times 1031 = 13.9 \text{ arcsec/pixel}$$

FOV is:
which gives
52 sq. deg.

$$\frac{2048 \times 13.9}{3600} = 7.9 \text{ degrees,}$$

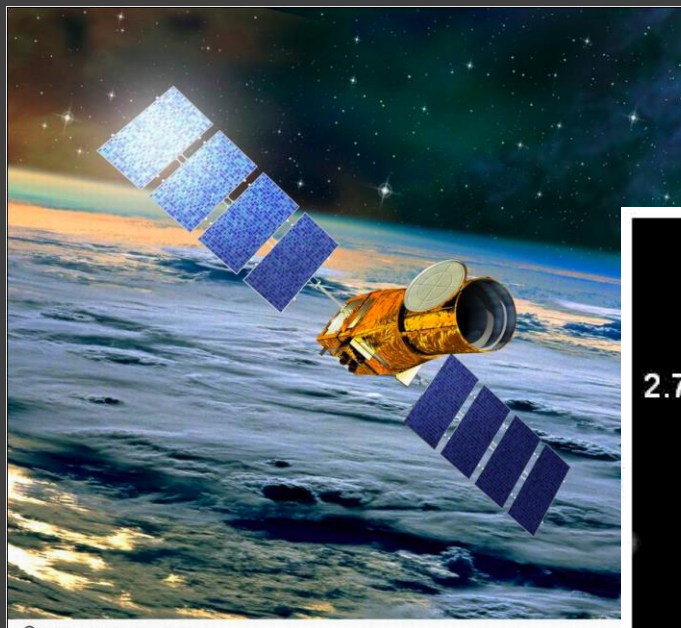
Space surveys vs. ground based



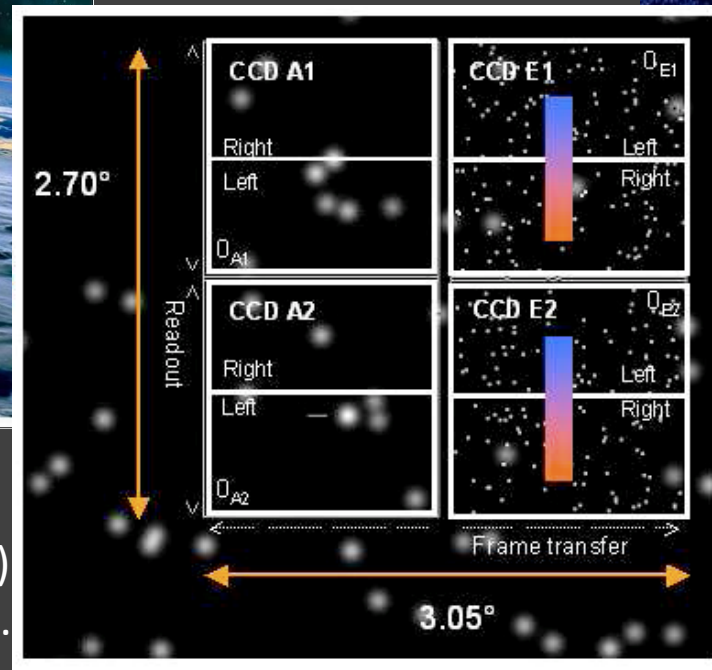
Hot jupiters are rare, but easy to detect from Earth.
Space surveys (here – Kepler) show mostly
different types of planets.

CoRoT

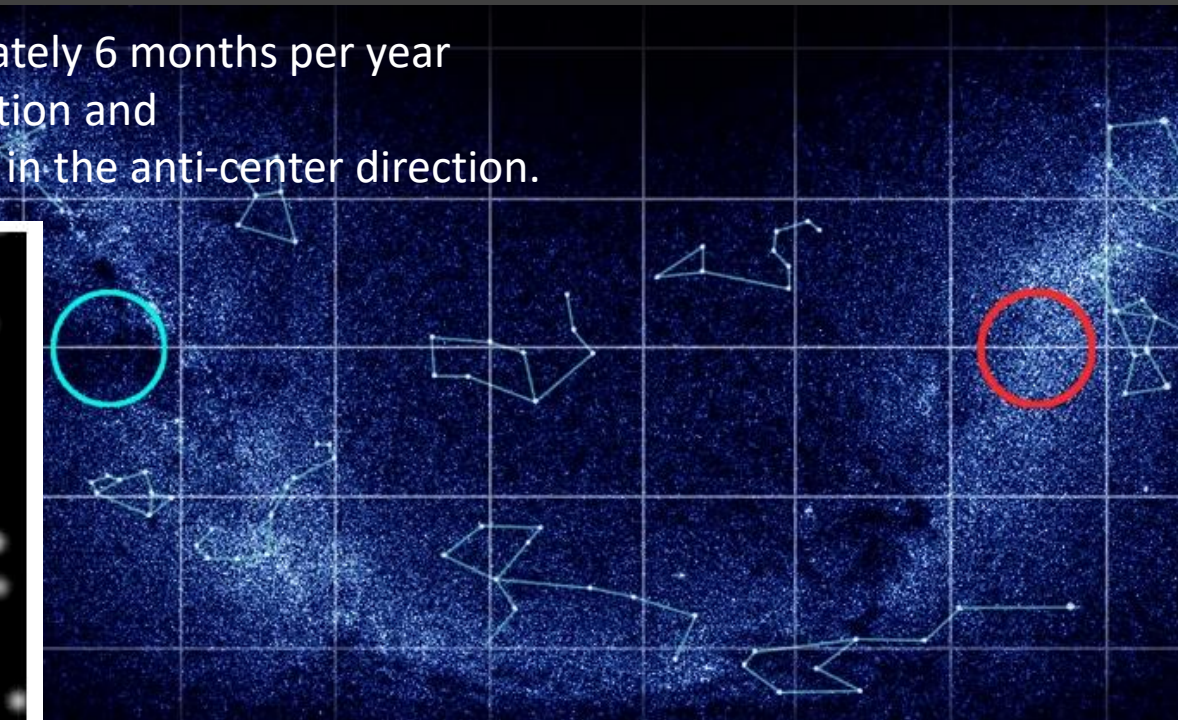
December 2006 – November 2012
27-cm telescope



Focal planet arrangement
of the asteroseismology (A1, A2)
and the exoplanet (E1, E2) CCDs.



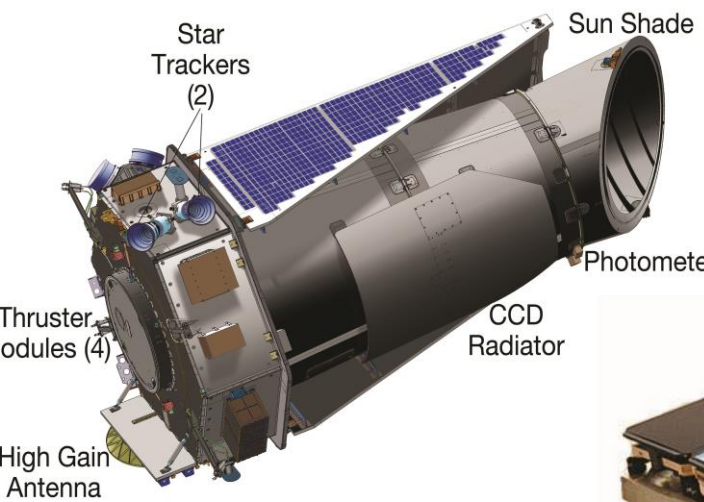
The satellite spent approximately 6 months per year
observing in the center direction and
6 months per year observing in the anti-center direction.



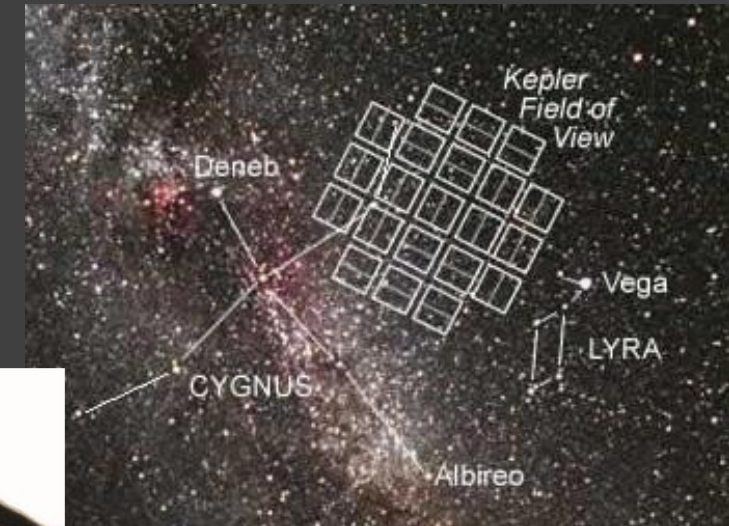
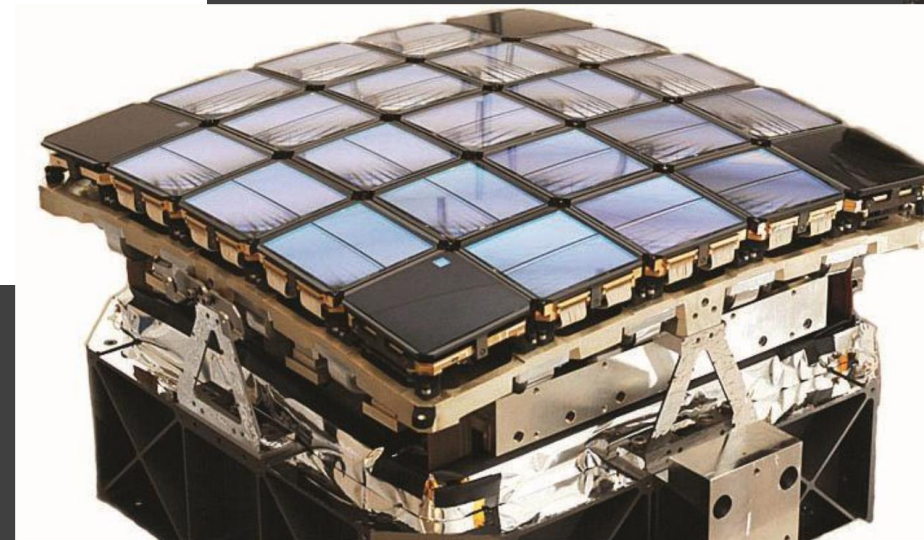
Position of the CoRoT eyes in the sky.
The blue and red circles represent the center
and anti-center.

Kepler

2009-2013 + K2-mission
0.95 m telescope

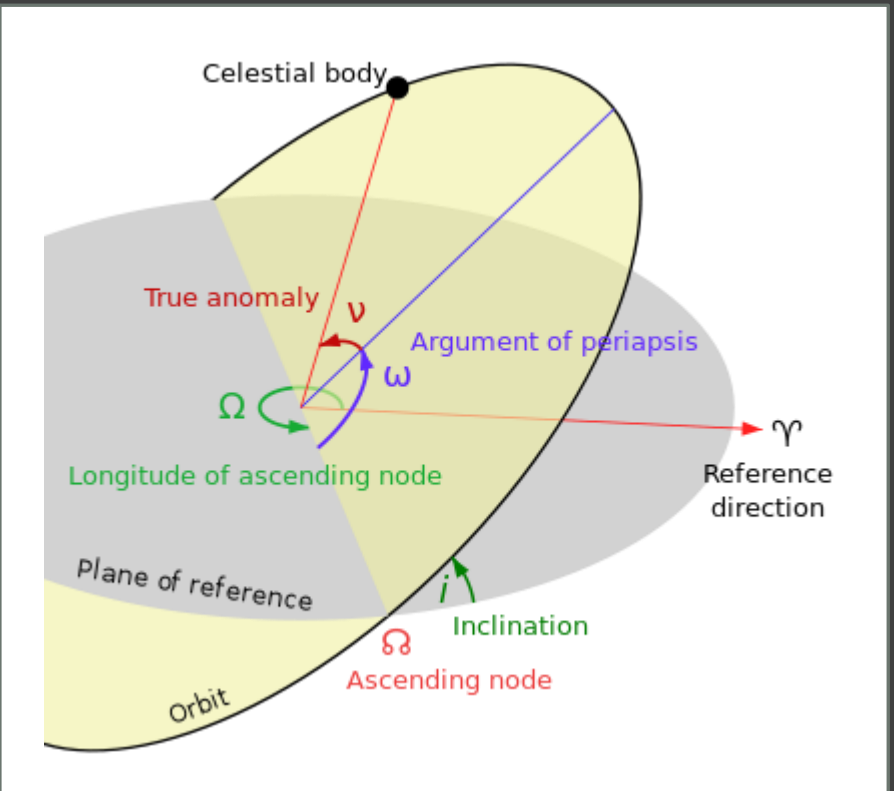


Monitoring of ~150 000 stars

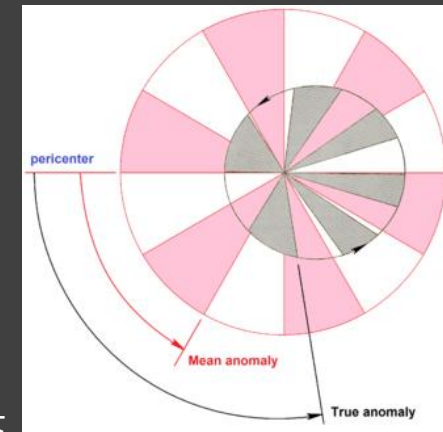
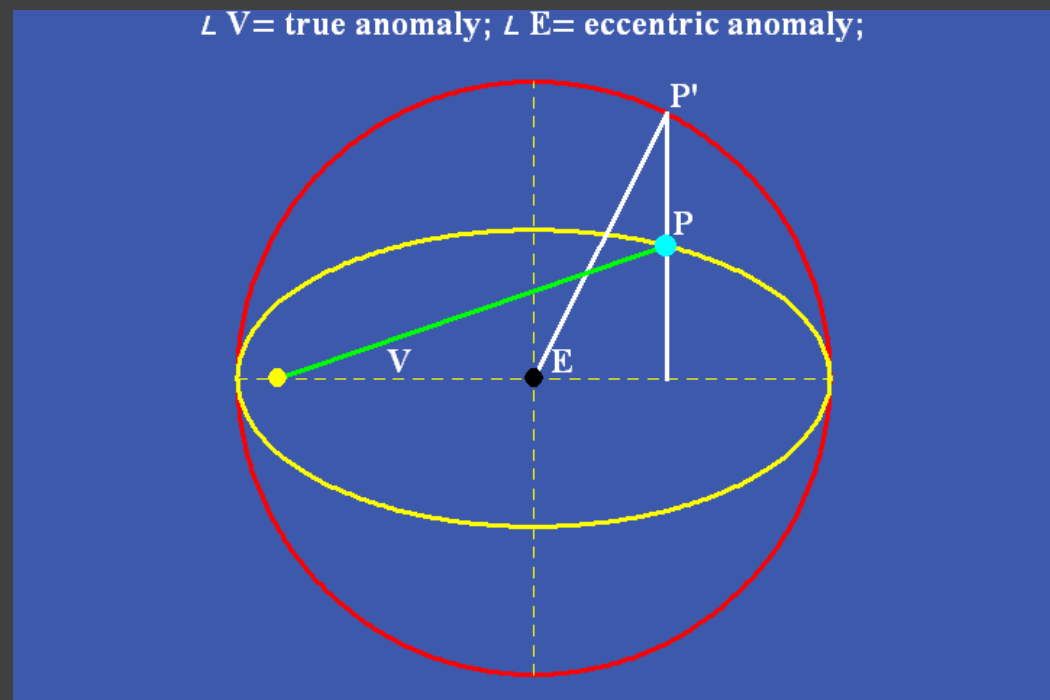


Field of view ~115 sq. degrees

Orbital elements

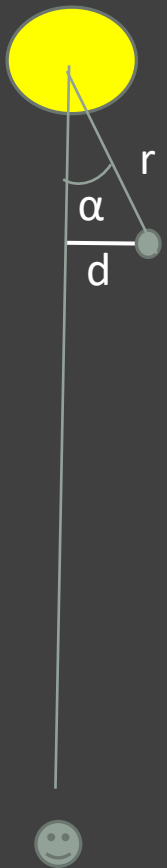


v – true anomaly
 ω – argument of periastron
E - eccentric anomaly
M – mean anomaly



<http://www.wlym.com/antidummies/part66.html>

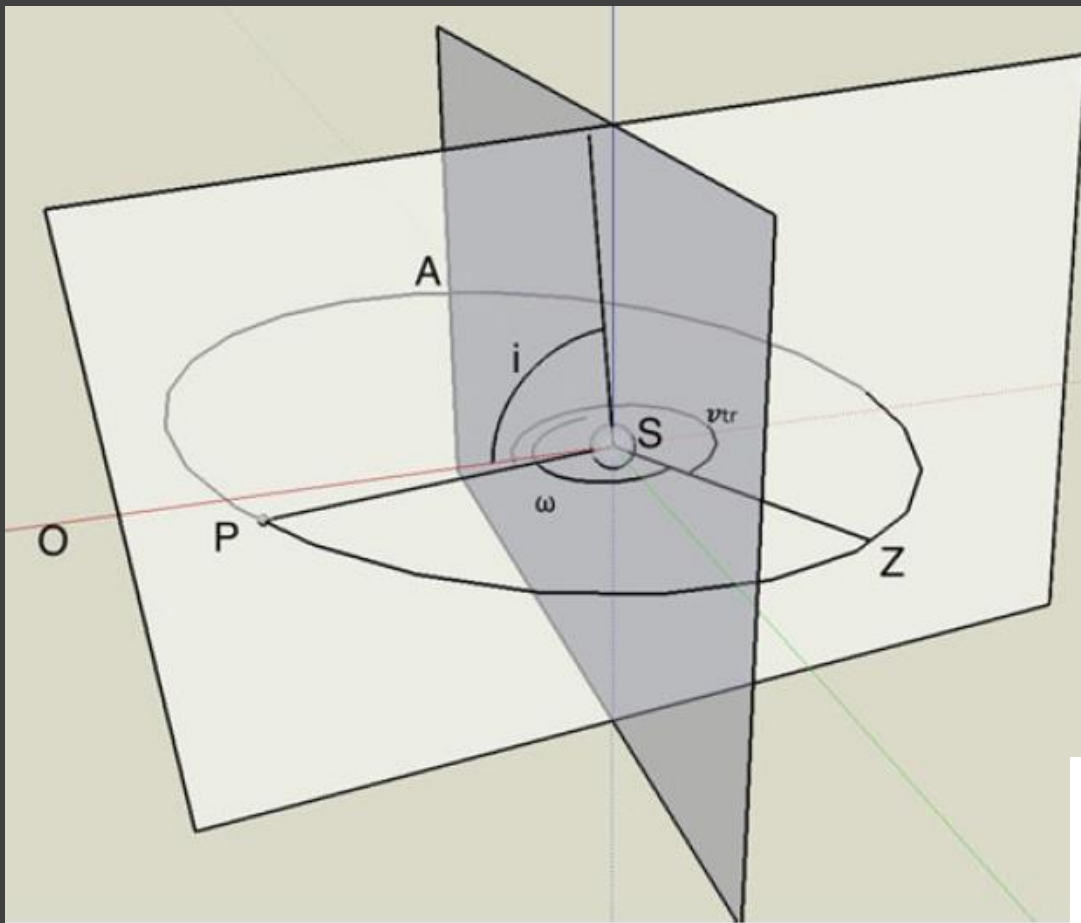
Orbital parameters



$$d = r \sin \alpha$$

$$z = d/R_{\text{star}}$$

$$p = R_p/R_{\text{star}}$$



$$\nu_{\text{tr}} = \frac{\pi}{2} - \omega$$

$$\nu_{\text{occ}} = \frac{3\pi}{2} - \omega,$$

$$E = 2 \tan^{-1} \left[\sqrt{\frac{1-e}{1+e}} \tan \frac{\nu}{2} \right]$$

$$t_{\text{tr}} - t_0 = \frac{P}{2\pi} M_{\text{tr}} = \frac{P}{2\pi} (E_{\text{tr}} - e \sin E_{\text{tr}}).$$

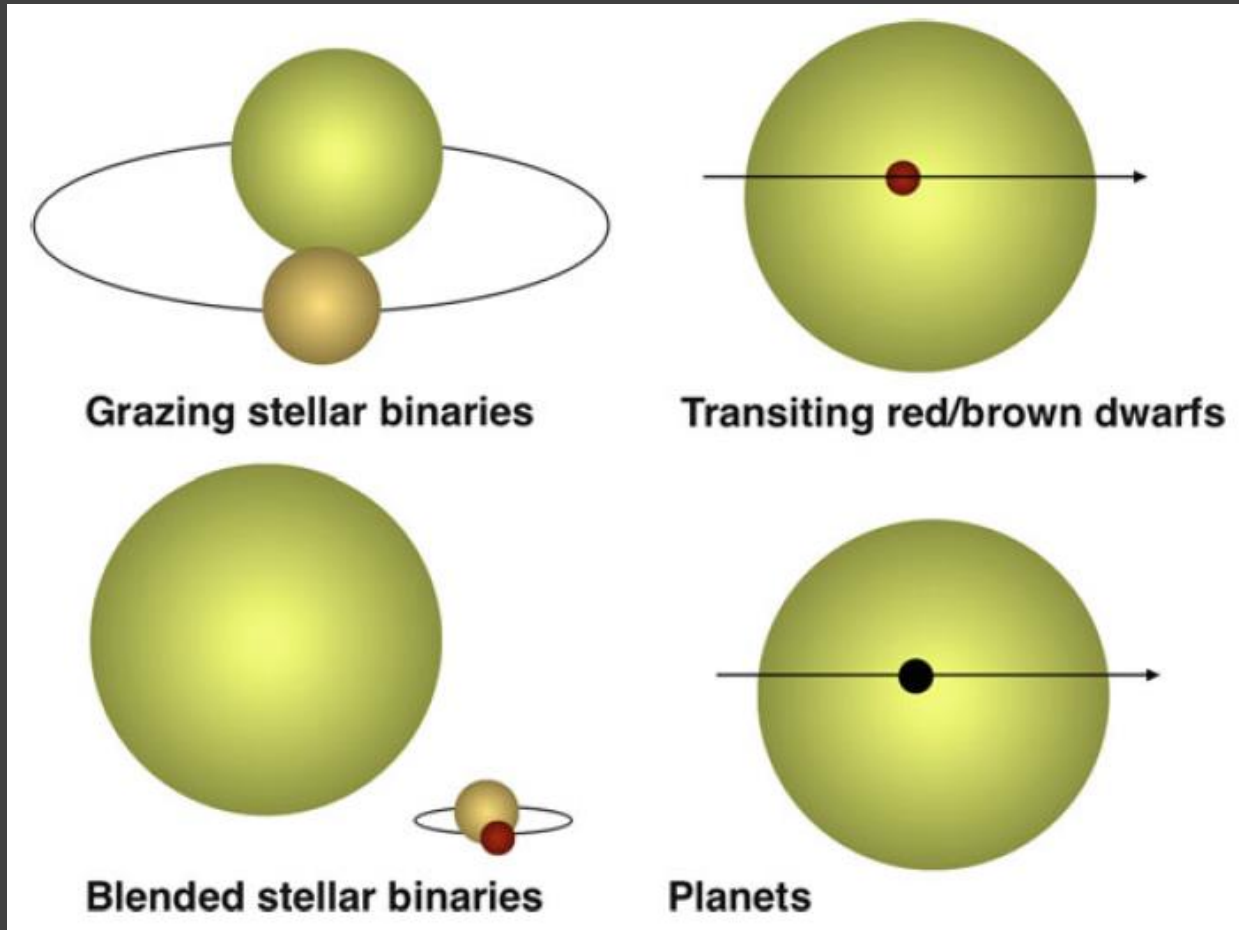
$$M = E - e \sin E.$$

$$E_{i+1} = M + e \sin E_i.$$

$$E_1 = M,$$

$$\frac{t_{\text{tr}}}{P} \simeq \frac{R_*}{a} \frac{\sqrt{(1+R_p/R_*)^2 - b^2}}{\pi} \frac{1+e \sin \omega}{1-e^2}.$$

Transits and transit-like events



Spectral lines and planet/star mass ratio

$$\dot{v}_r \simeq \frac{GM_*}{a^2} = \frac{2\pi K}{P} \frac{M_*}{M_p}.$$

Measurements of the radial acceleration (due to observations of spectral lines in the planet atmosphere) allow to measure stellar mass.

Observations of spectral line in the planet atmosphere can allow to measure important parameters of the system!

$$\frac{T}{P} = \frac{1}{\pi} \sin^{-1} \frac{R_*}{a}$$

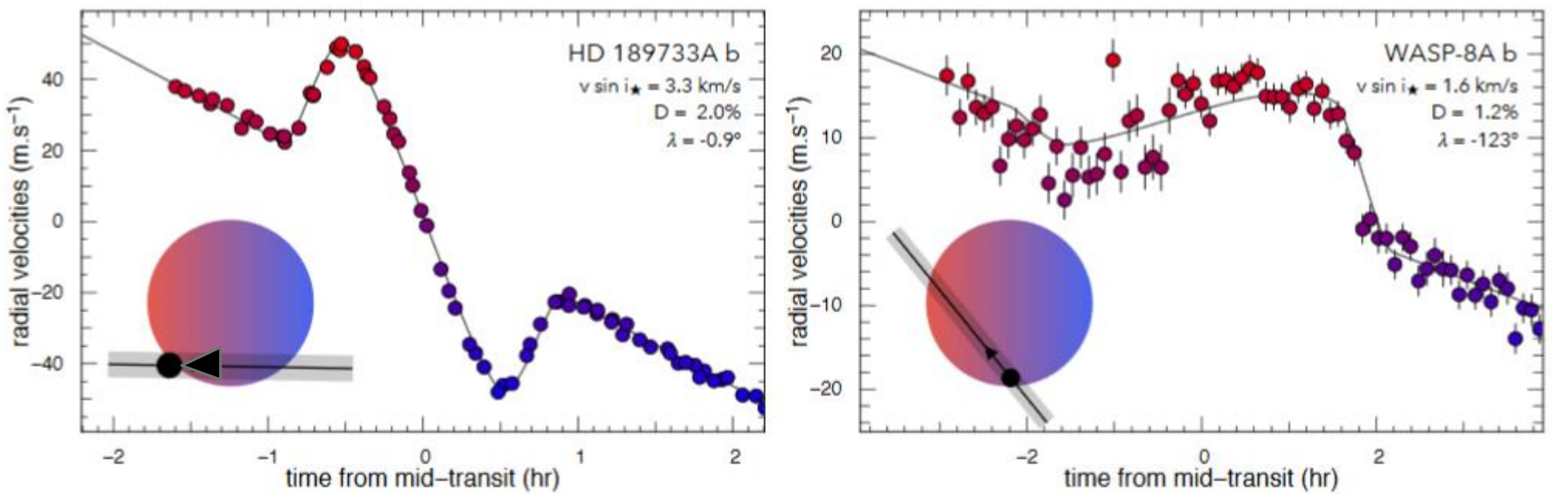
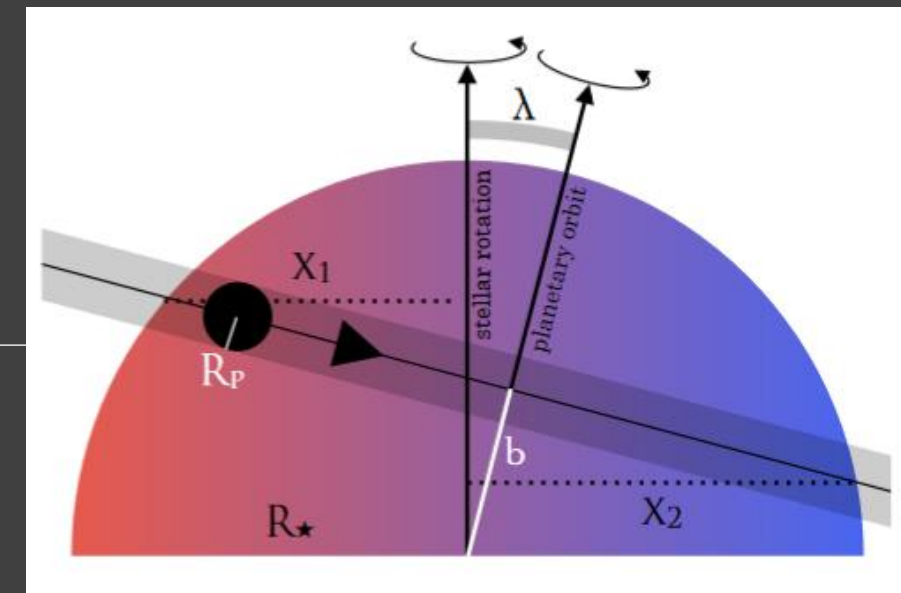
$$\delta v_r \simeq \frac{P}{\pi} \frac{R_*}{a} \frac{2\pi K}{P} \frac{M_*}{M_p}.$$

If narrow spectral lines in the planet atmosphere can be observed during transit then it is possible to derive $M_{\text{star}}/M_{\text{planet}}$

Rossiter–McLaughlin effect

$$A_{\text{RM}} \simeq \frac{2}{3} D v \sin i_\star \sqrt{1 - b^2}$$

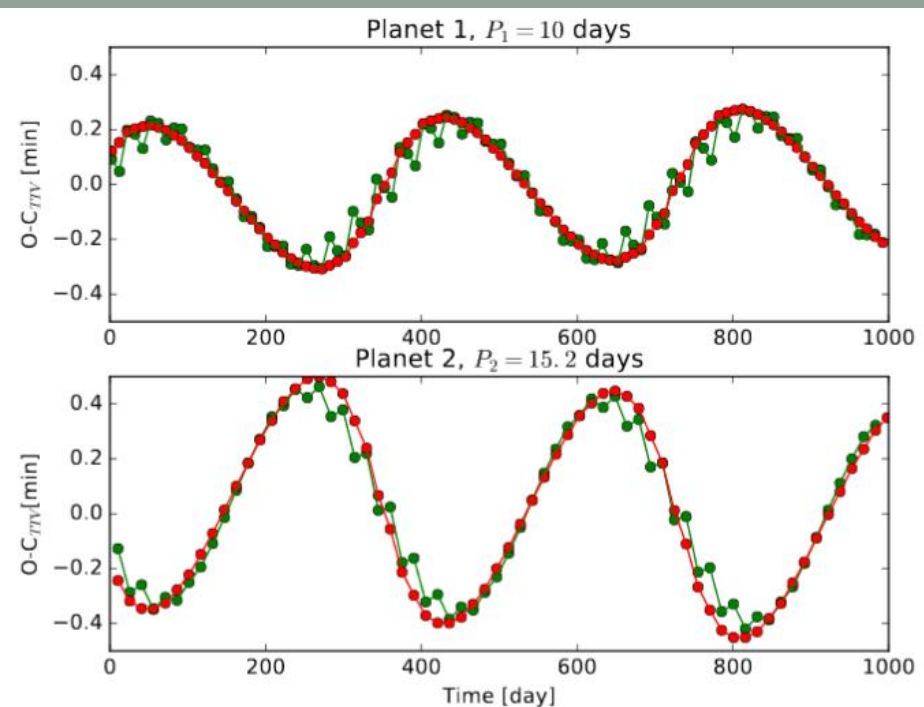
$$D = (R_p/R_\star)^2$$



Transit timing variations

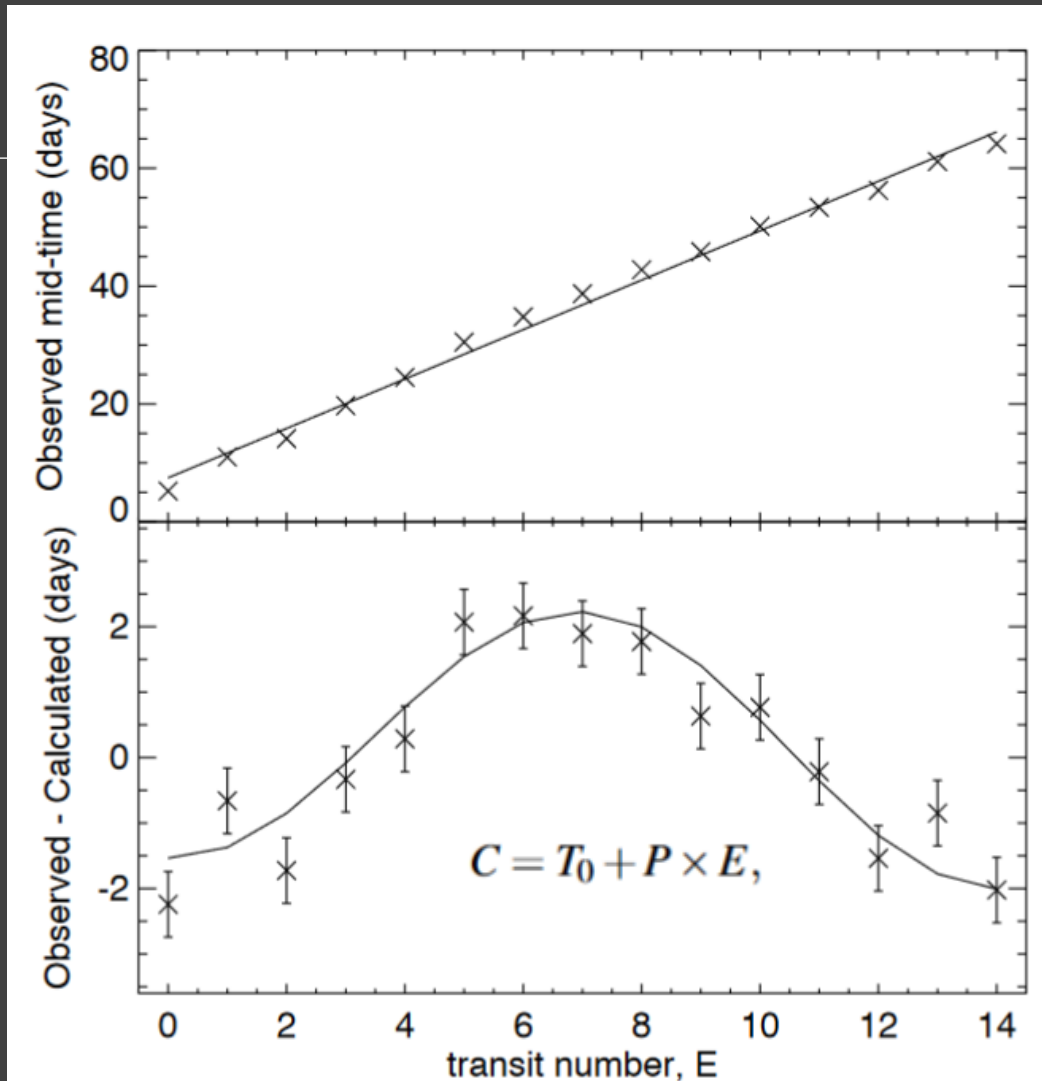
$$\delta t_1 = P_1 \frac{m_2}{m_0} f_{12}(\alpha_{12}, \theta_{12}), \quad \alpha_{ij} = \min(a_i/a_j, a_j/a_i)$$

$$\delta t_2 = P_2 \frac{m_1}{m_0} f_{21}(\alpha_{12}, \theta_{21}), \quad \theta_{ij} = (\lambda_i, e_i, \omega_i, I_i, \Omega_i, \lambda_j, e_j, \omega_j, I_j, \Omega_j)$$

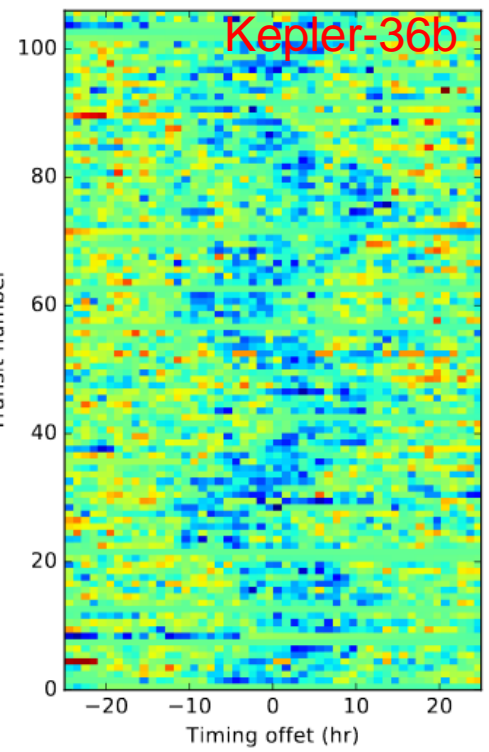


Transit-timing variations of two low-eccentricity planets with larger mass ratio (green) compared with two smaller mass planets with larger eccentricity $e_1=e_2=0.04$

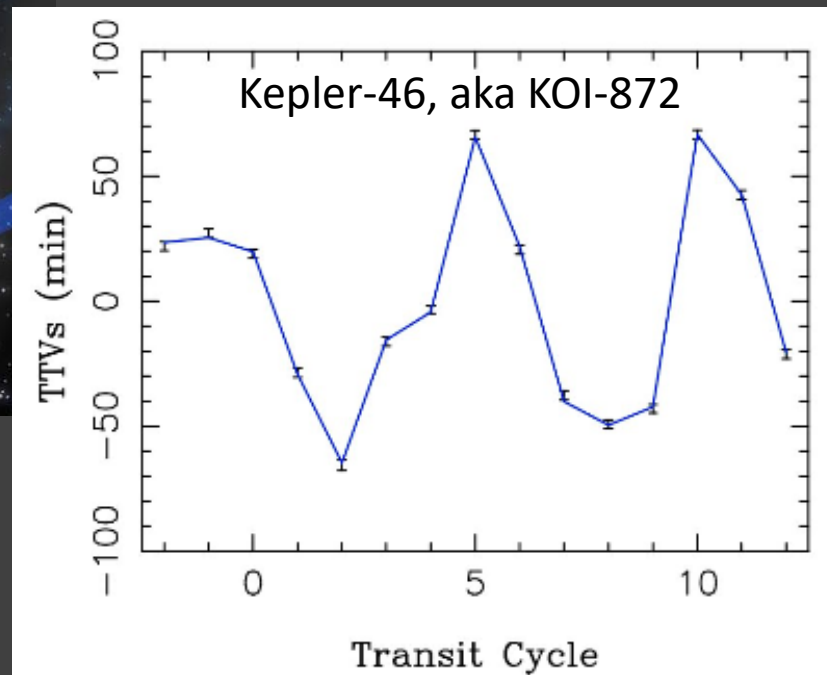
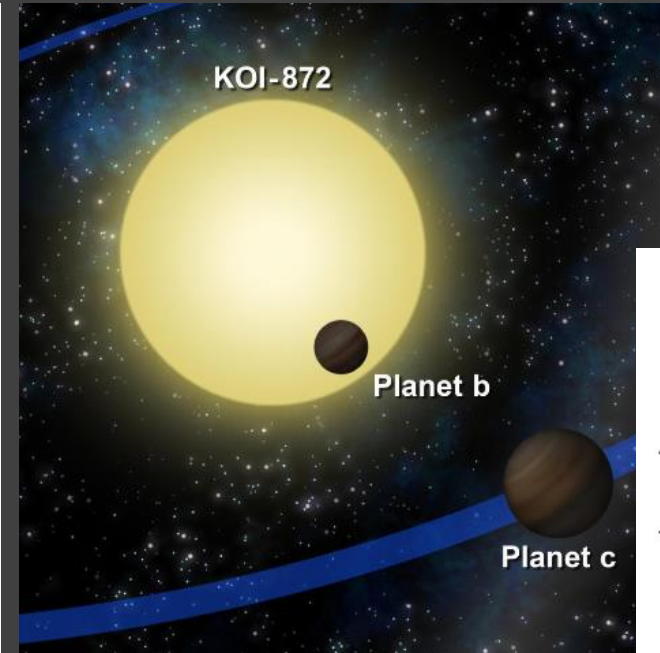
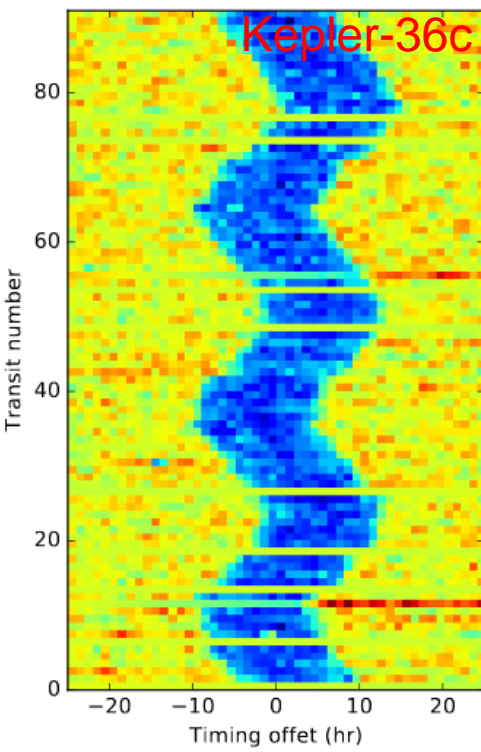
Planets are nearly in 3:2 resonance.



Transit timing variations (TTV)

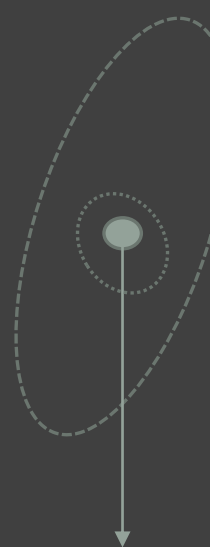
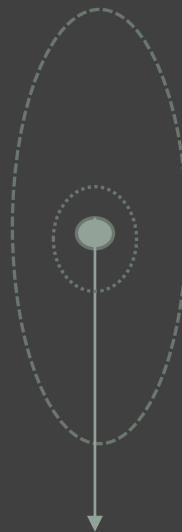
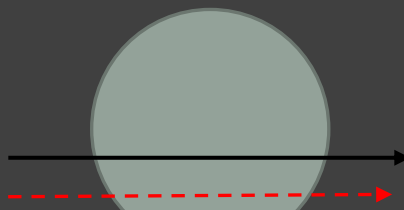
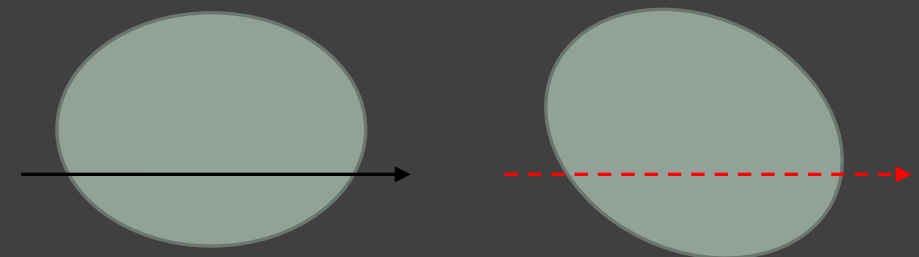


River plot



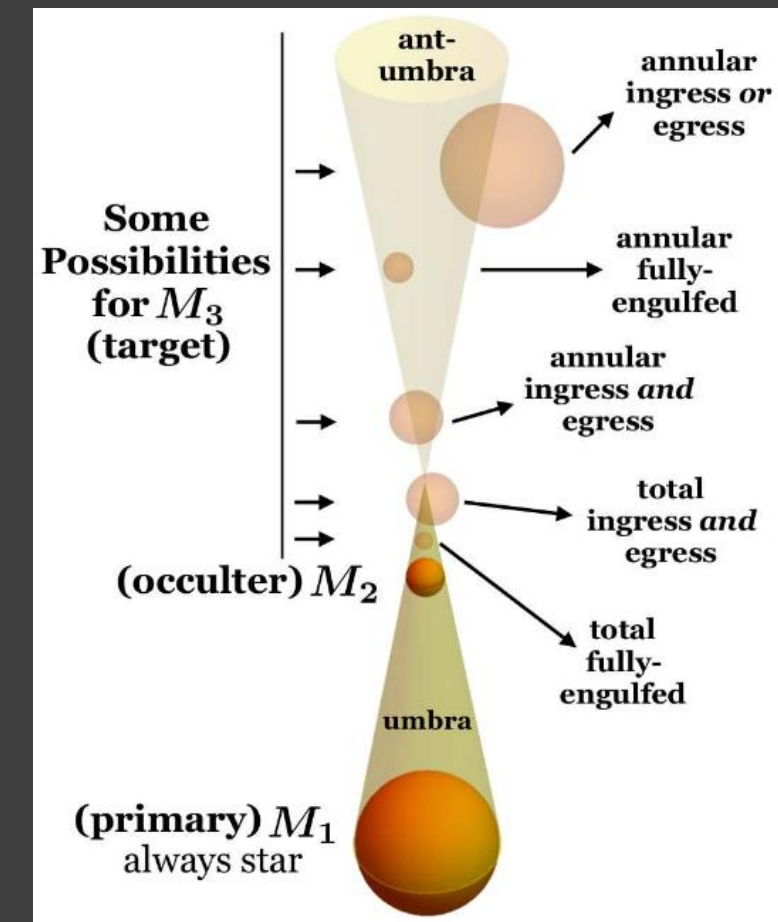
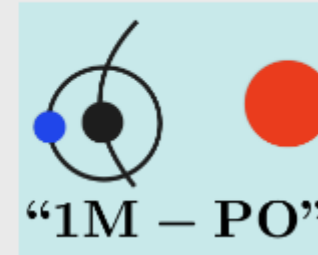
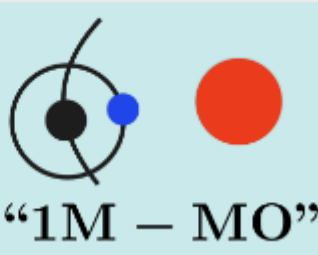
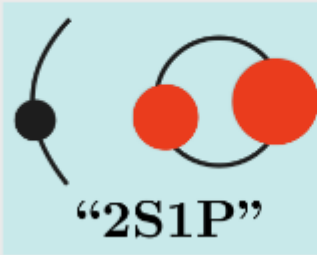
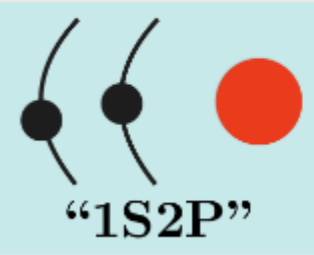
Transit duration variations (TDV)

- Torque due to the rotational oblateness of the star;
- Eccentricity variations due to a resonant interaction;
- Inclination changes due to secular precession of the orbital plane.

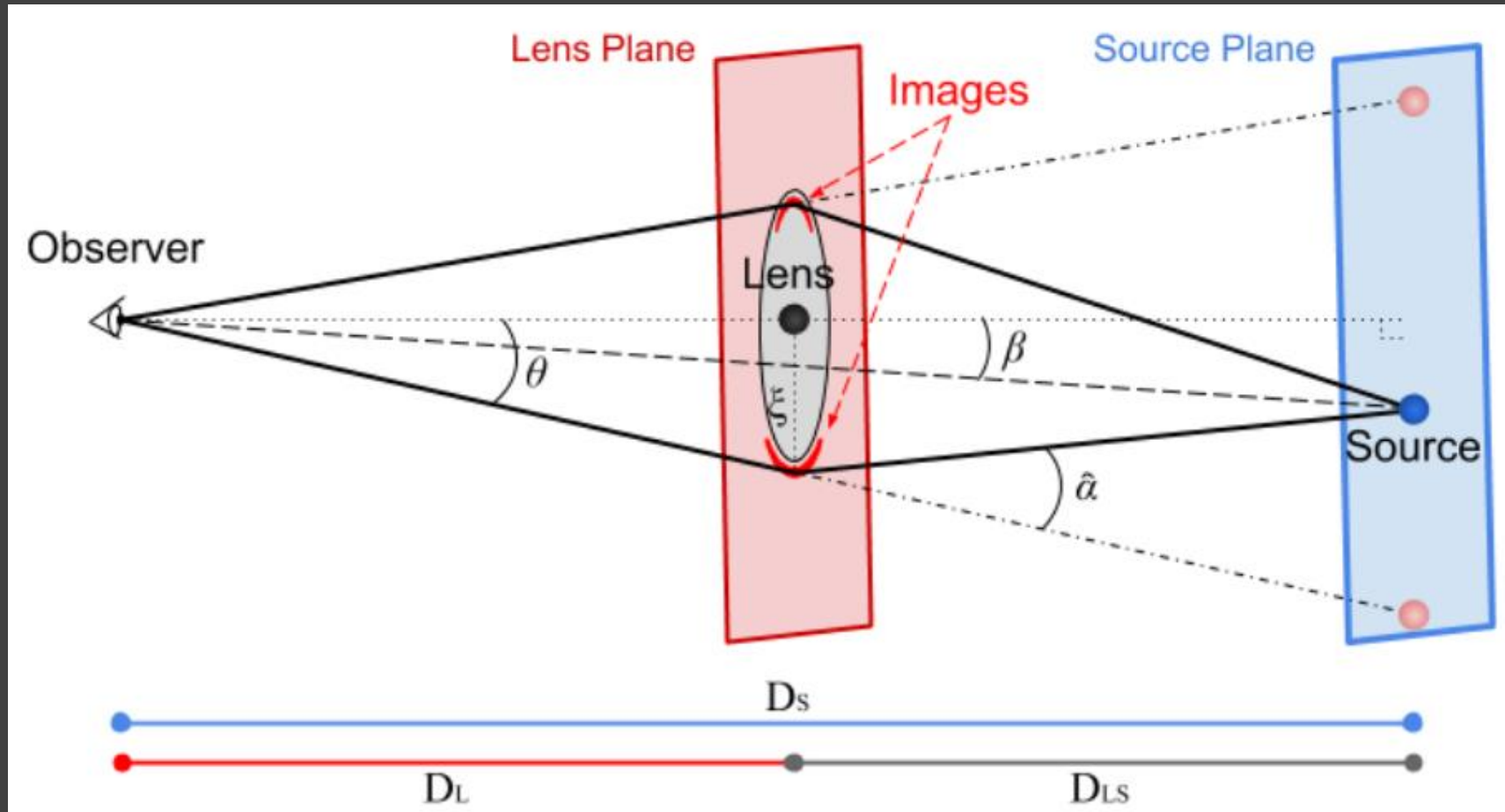


Calculations of transits in 3 body systems

$$\{a, e, i, \Omega, w, \Pi(t)\} \rightarrow \{x(t), y(t), z(t)\} \rightarrow \vec{r}(t)$$

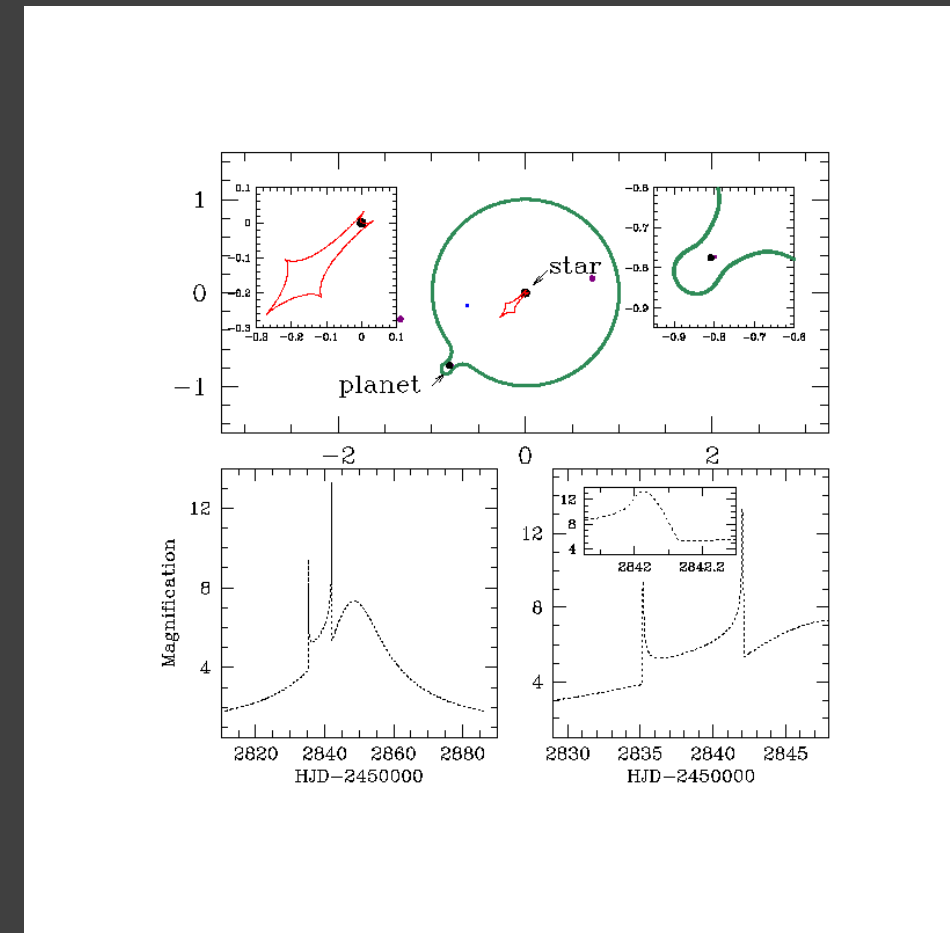
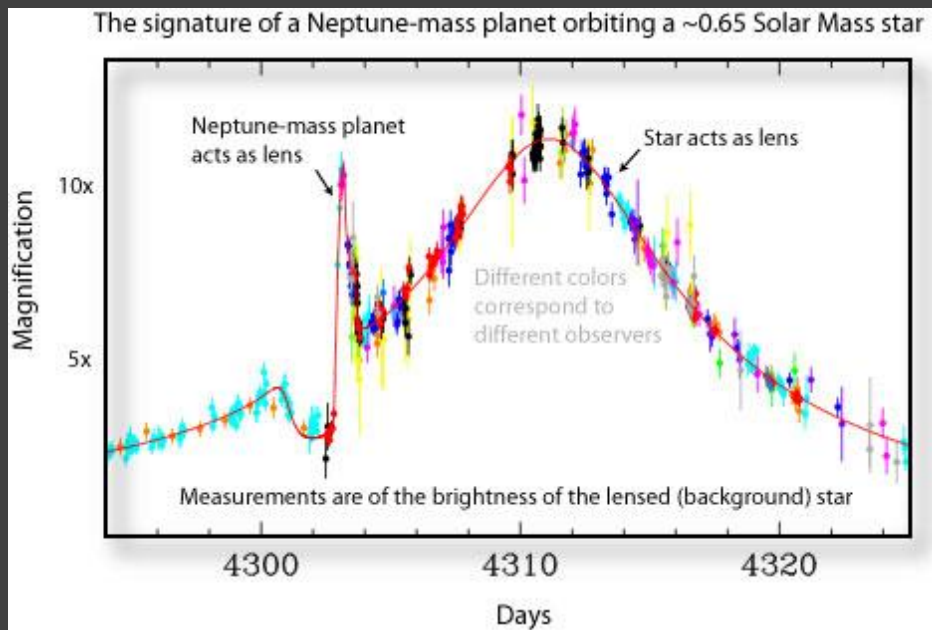


Microlensing



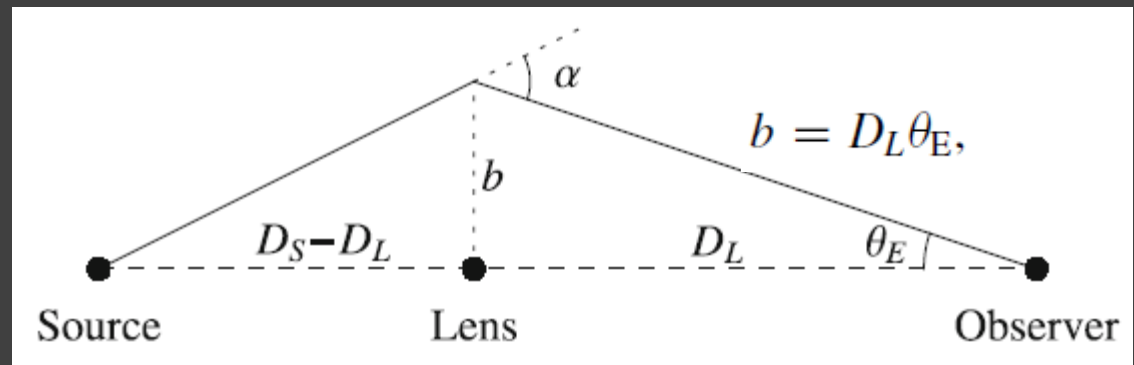
Exoplanet detection via microlensing

- Sensitive to low mass planets (down to $0.1 M_{\text{earth}}$)
- Sensitive to wide orbits (1-4 AU)
- Sensitive to free-floating planets



<https://www3.nd.edu/~bennett/moa53-ogle235/technical.gif>

Gravitational microlensing - 1



Probability of microlensing is small.
For stars it is $\sim 10^{-5} - 10^{-6}$ per year.
For planets it is lower, as $\theta_E \sim M^{1/2}$
and $M_{\text{planet}}/M_{\text{star}} \sim 10^{-4}$

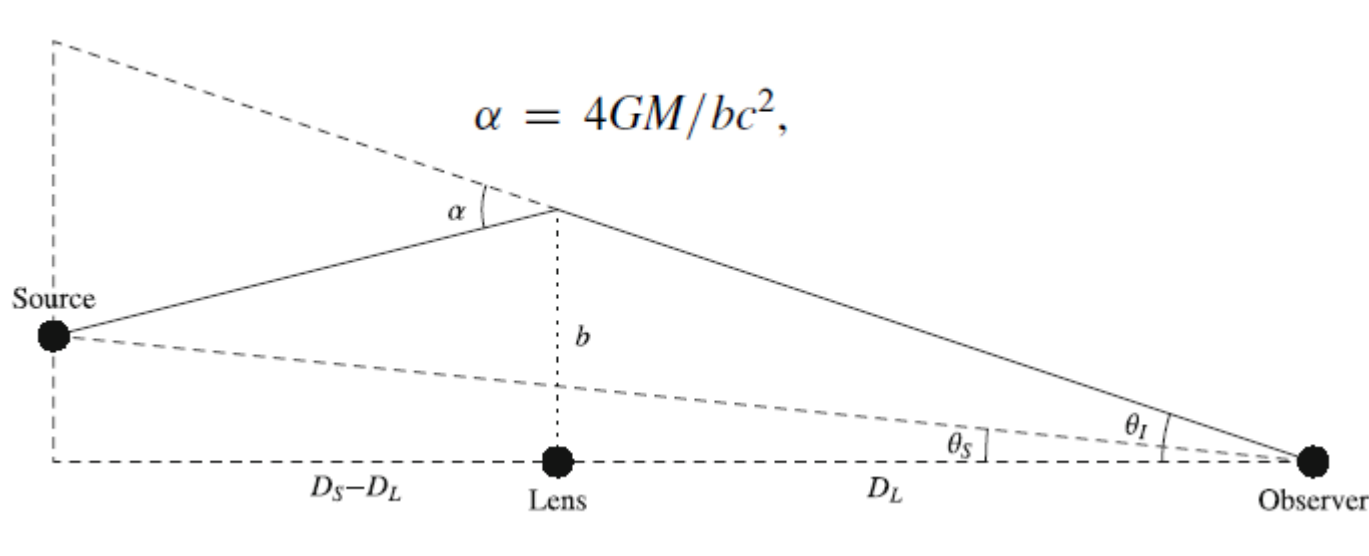
$$\alpha = b/D_L + b/(D_S - D_L).$$

$$\theta_E = \sqrt{\kappa M \pi_{\text{rel}}}; \quad \kappa \equiv \frac{4G}{c^2 \text{AU}} \simeq 8.14 \frac{\text{mas}}{M_\odot},$$

$$\pi_{\text{rel}} = \text{AU}(D_L^{-1} - D_S^{-1})$$

$$\tau = \int dD_L \pi (D_L \theta_E)^2 n(D_L) \sim \frac{4\pi G M n}{c^2} D^2 = \frac{4\pi G \rho}{c^2} D^2 \sim \frac{GM_{\text{tot}}}{D c^2} \sim \frac{v^2}{c^2}$$

Gravitational microlensing - 2



$$(\theta_I - \theta_S)D_S = \alpha(D_S - D_L)$$

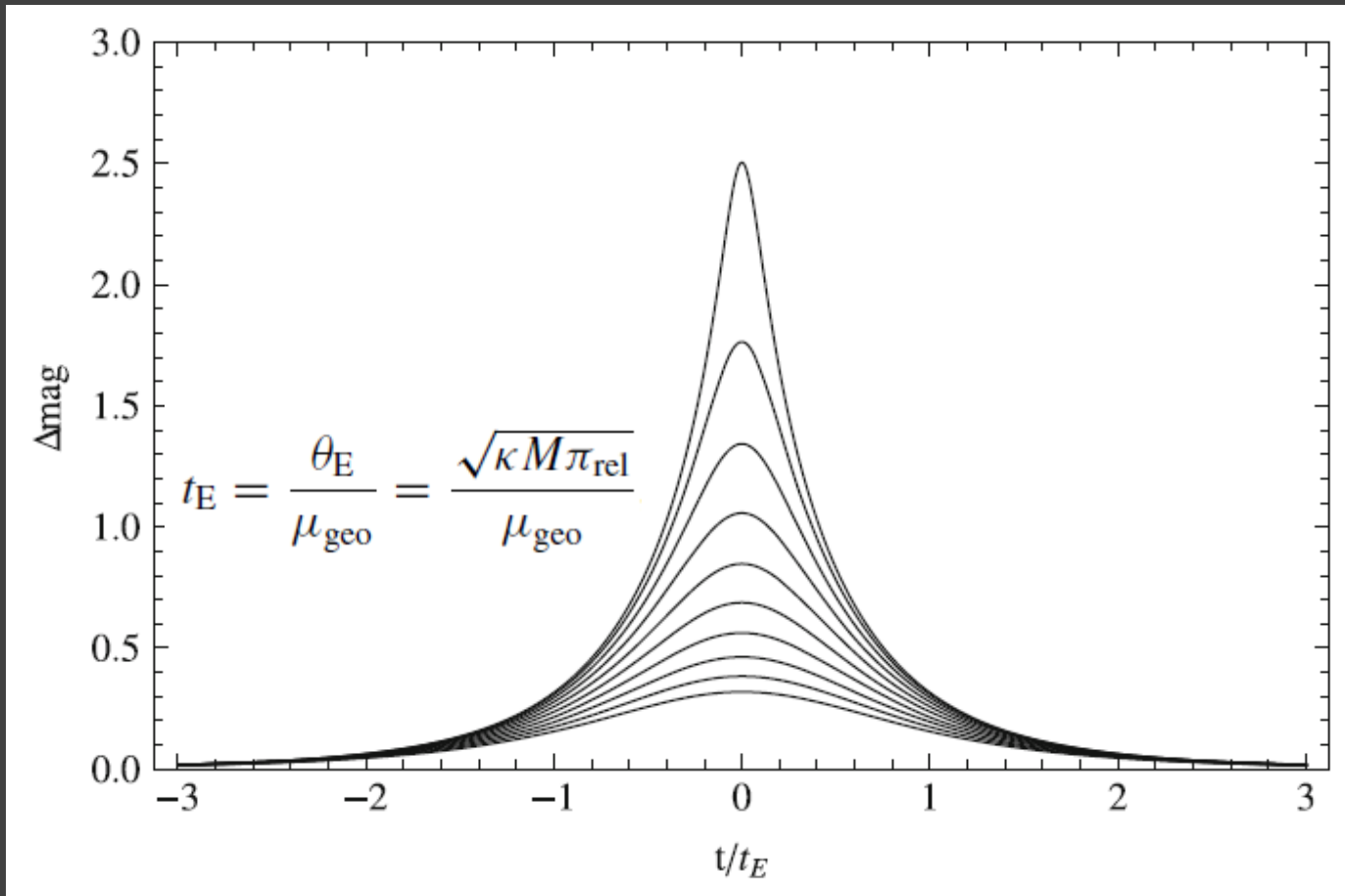
$$\theta_I(\theta_I - \theta_S) = \frac{4GM\pi_{\text{rel}}}{c^2 \text{AU}} \equiv \theta_E^2.$$

$$u_{\pm} = \frac{u \pm \sqrt{u^2 + 4}}{2}; \quad u \equiv \frac{\theta_S}{\theta_E} \quad u_{\pm} \equiv \frac{\theta_{I,\pm}}{\theta_E}.$$

$$A_{\pm} = \pm \frac{u_{\pm}}{u} \frac{\partial u_{\pm}}{\partial u} = \frac{A \pm 1}{2}$$

$$A = \frac{u^2 + 2}{u\sqrt{u^2 + 4}} = (1 - Q^{-2})^{-1/2}; \quad Q \equiv 1 + \frac{u^2}{2},$$

Light curves for point lenses



$$F(t) = f_s A(\mathbf{u}(t; t_0, u_0, t_E), \rho) + f_b;$$

$$\mathbf{u}(t; t_0, u_0, t_E) = (\tau(t), \beta) = \left(\frac{t - t_0}{t_E}, u_0 \right).$$

Finite size lens

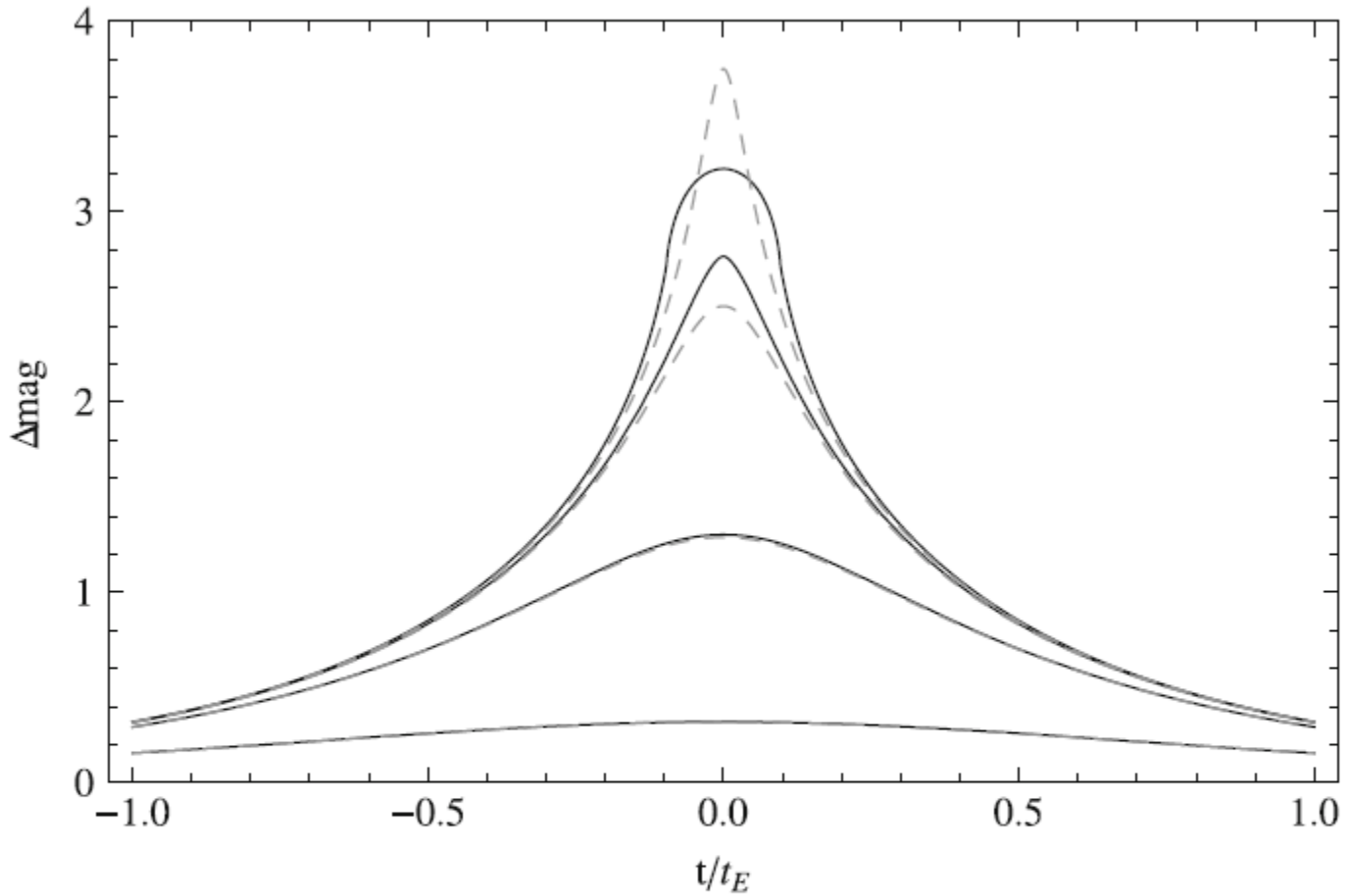
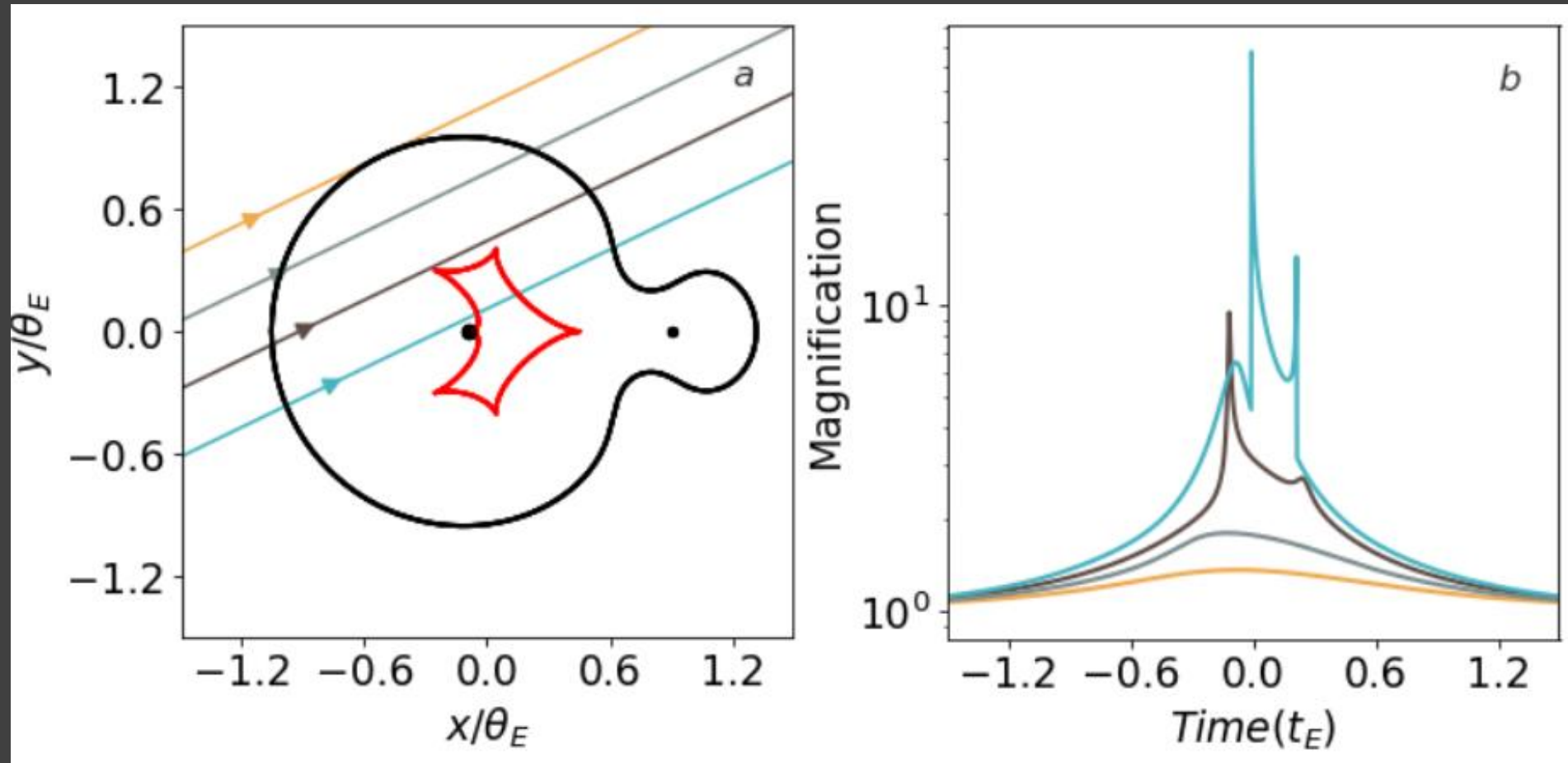


Fig. 3.4 Magnification as a function of time in microlensing events for an impact parameters $u_0 = 10^{-n}$ with $n \in \{-1.5, -1, -0.5, 0\}$. The angular source size is $0.1\theta_E$. Note that when the impact parameter is greater than the source radius, the magnification is higher than the corresponding Paczynski curve (dashed). When the impact parameter is smaller than the source radius (source passing right behind the lens), the magnification saturates

Light curves form different trajectories

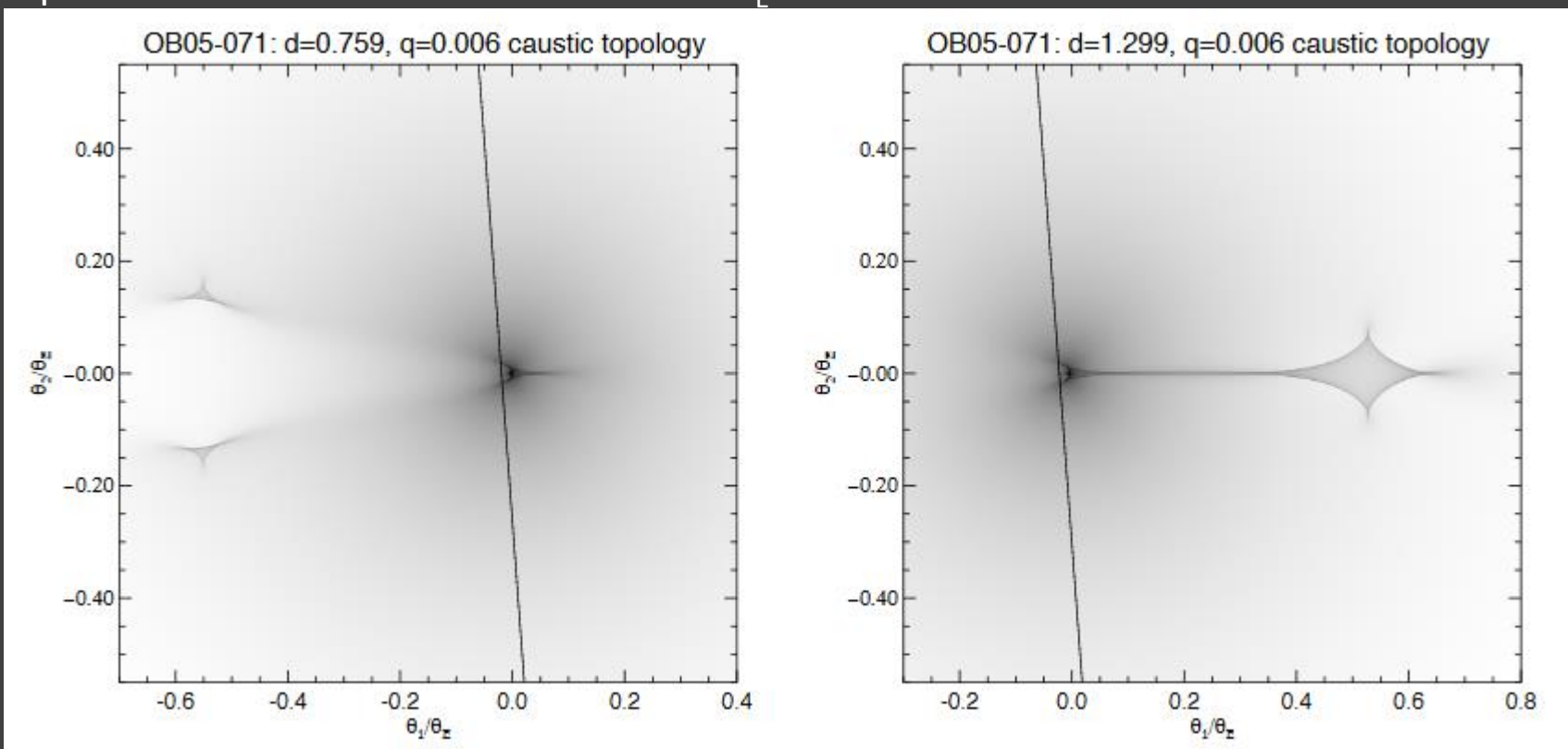


Binary lense

s – separation of components in units of the Einstein radius θ_E .

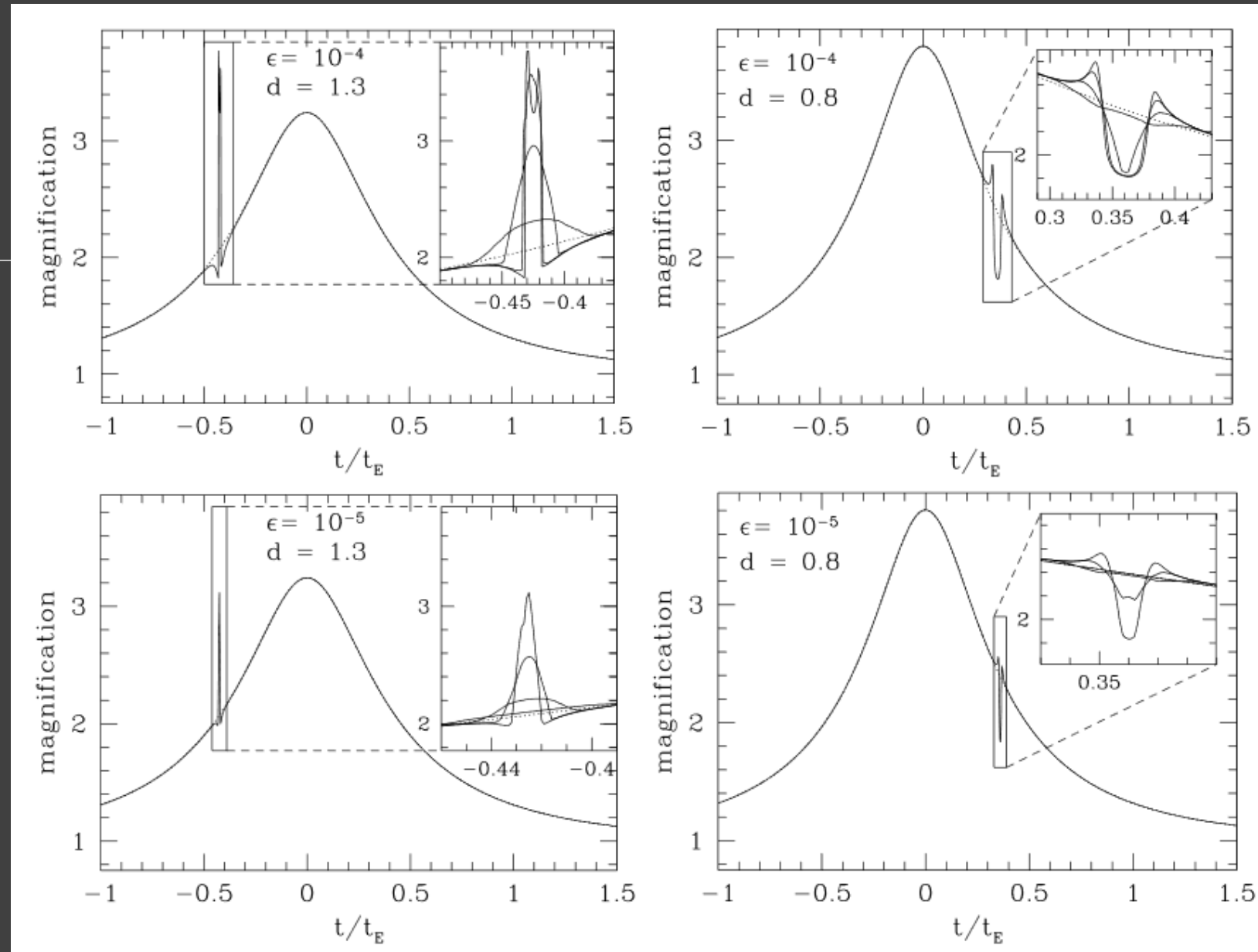
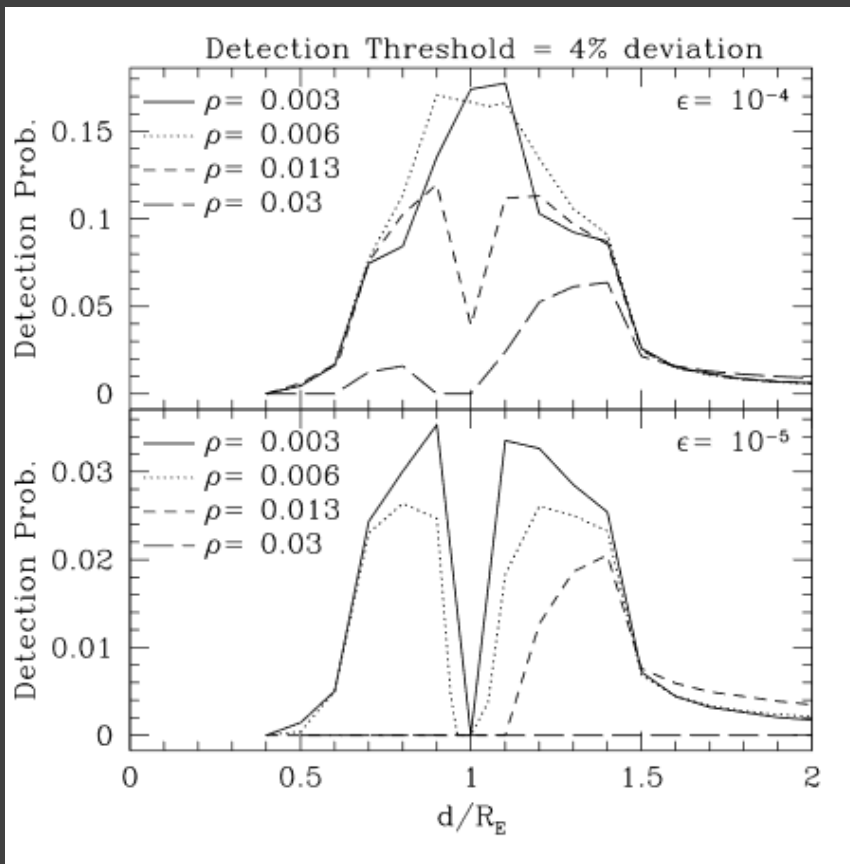
q - mass ratio.

$$r_{\perp} = s\theta_E D_L,$$

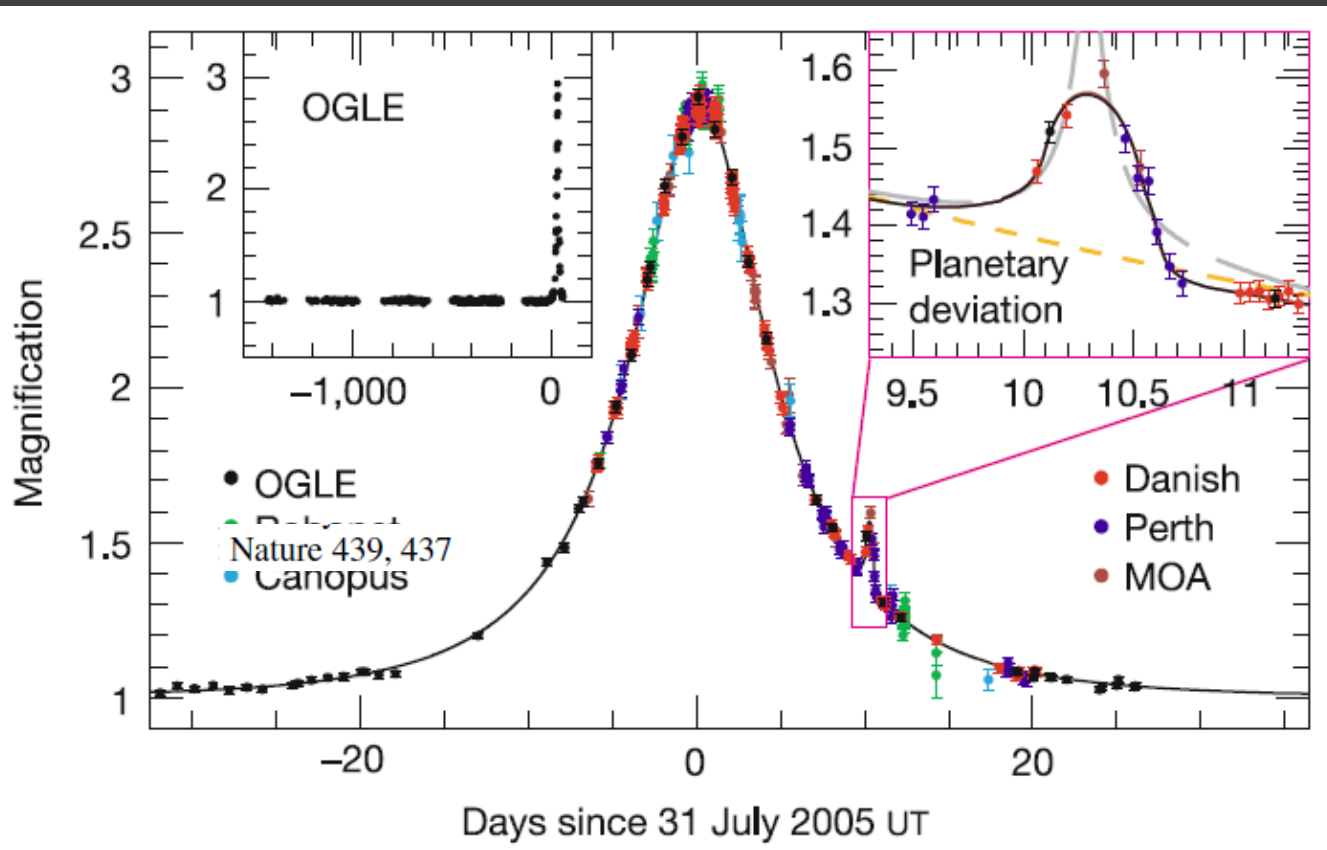


0902.1761

Light curves



Cold Neptune



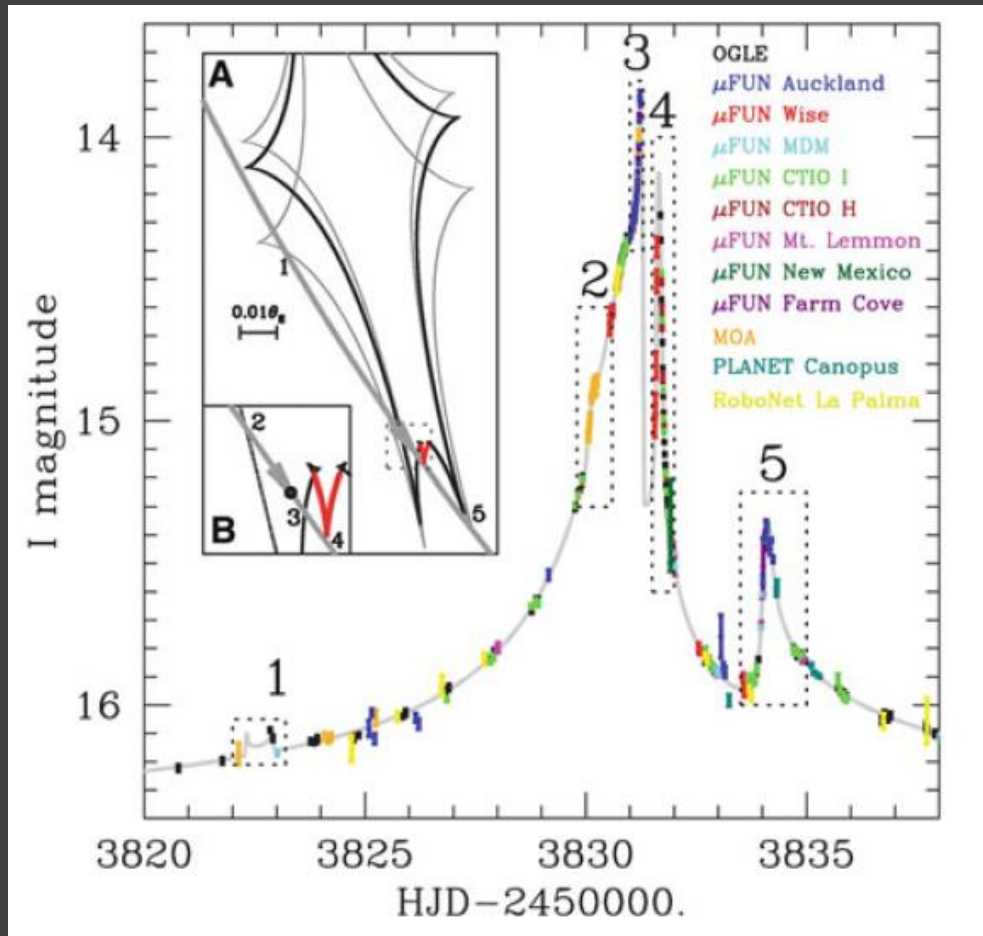
$$A_p = \frac{2}{\rho_p^2} = 2 \left(\frac{\theta_{E,p}}{\theta_*} \right)^2$$

$$\frac{t_p}{t_E} = \frac{\theta_*}{\theta_E}.$$

$$q = \frac{m_p}{M} = \frac{\theta_{E,p}^2}{\theta_E^2} = \frac{\theta_{E,p}^2}{\theta_*^2} \frac{\theta_*^2}{\theta_E^2} = \frac{A_p}{2} \frac{t_p^2}{t_E^2} \simeq 1.0 \times 10^{-4}.$$

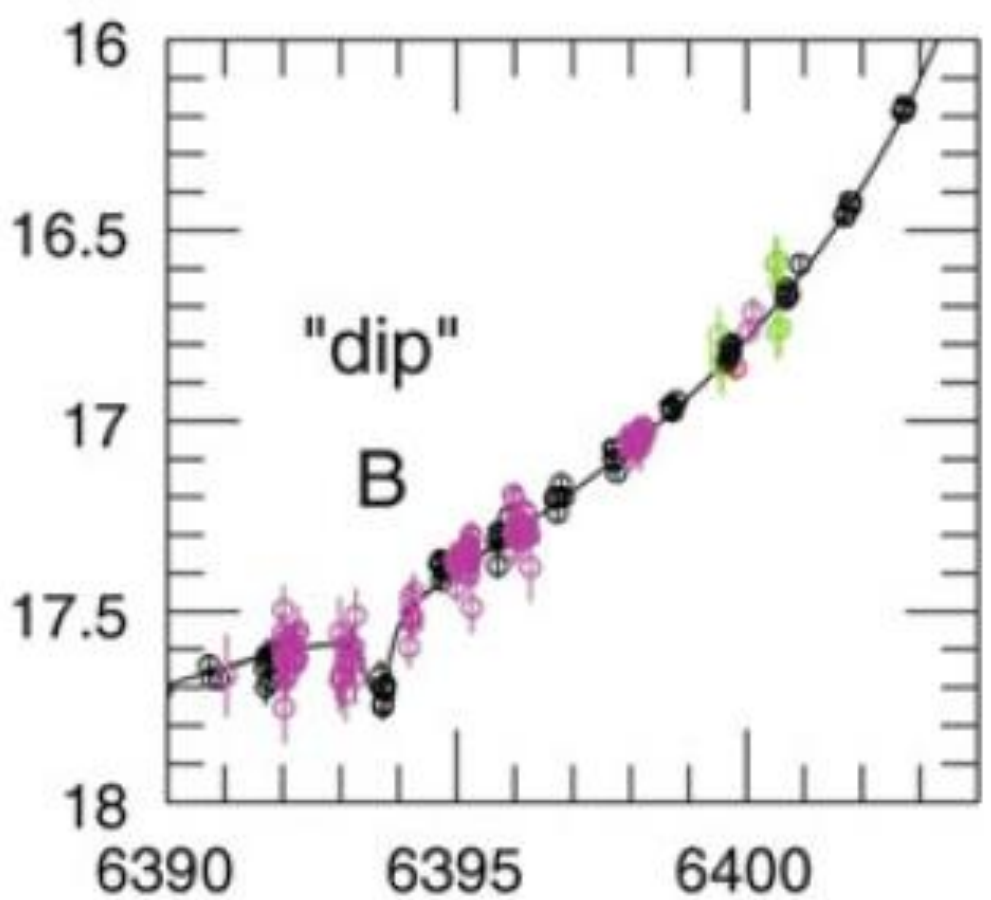
$$r_\perp = s\theta_E D_L = 2.2 \text{ AU} \frac{D_L}{8 \text{ kpc}}.$$

Solar system – like system

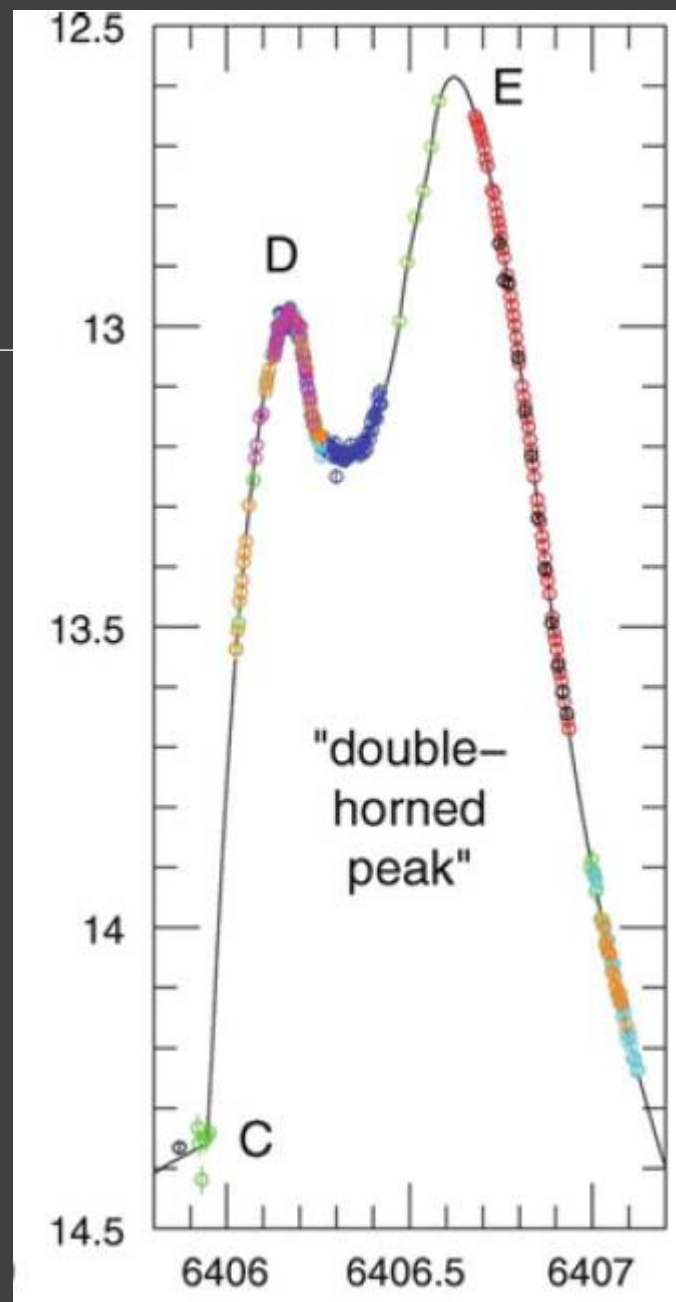


Jupiter and Saturn analogues.
Distances are slightly smaller
consistent with smaller mass
of the host star.

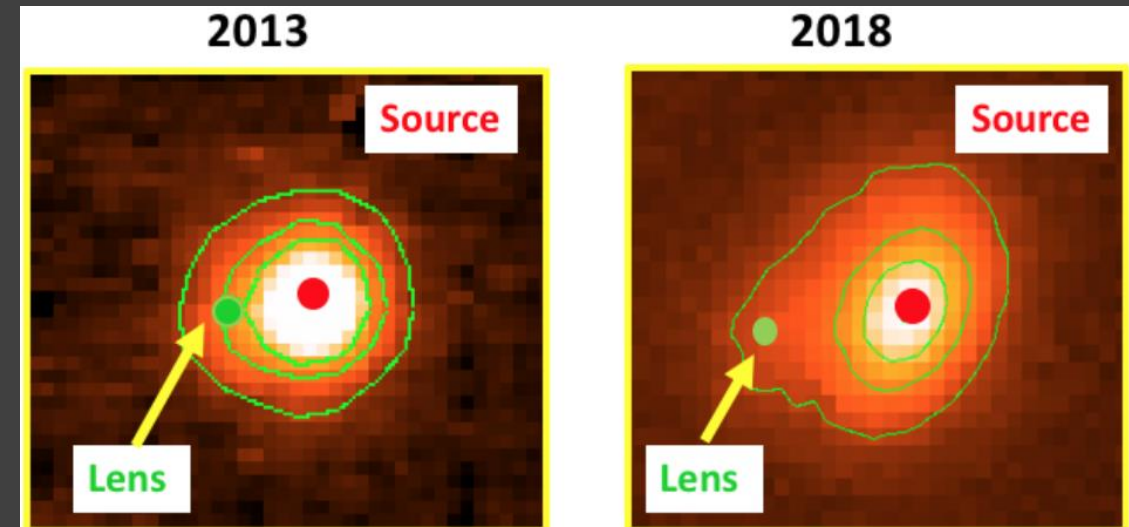
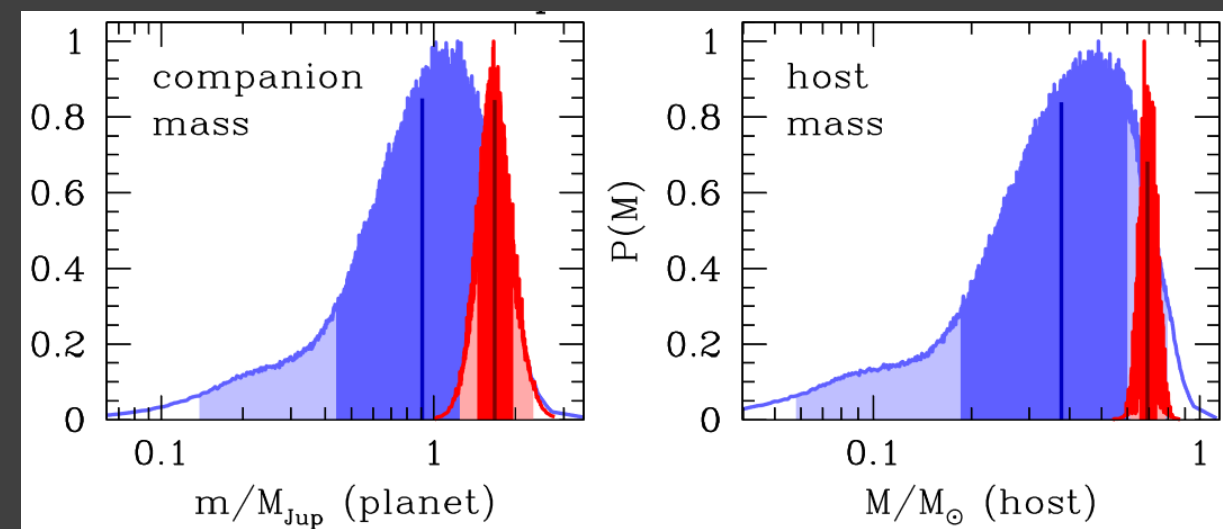
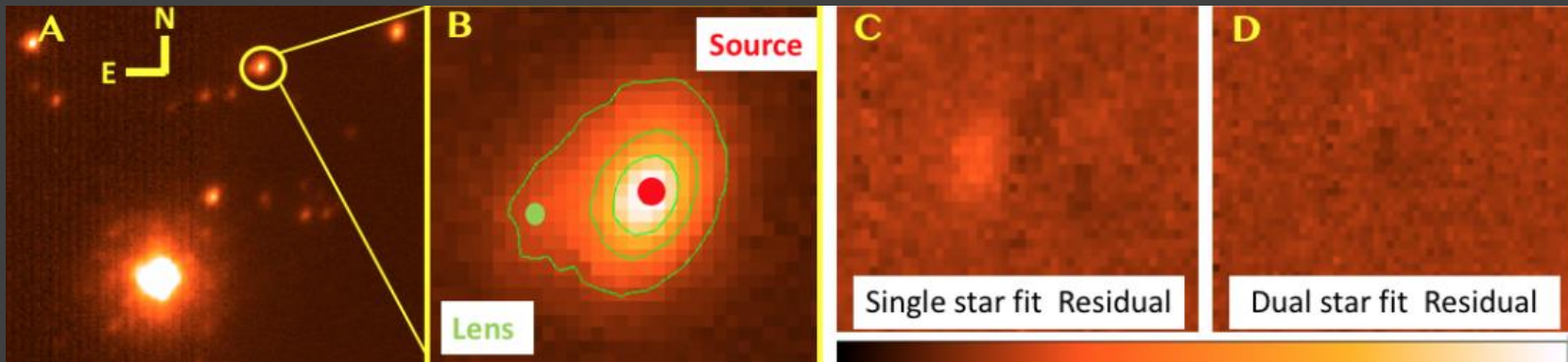
Dips due to planets



A terrestrial-mass planet in a binary.
The planet orbits a red dwarf (1 AU),
which orbits another star (15 AU)



Lensing star is visible!

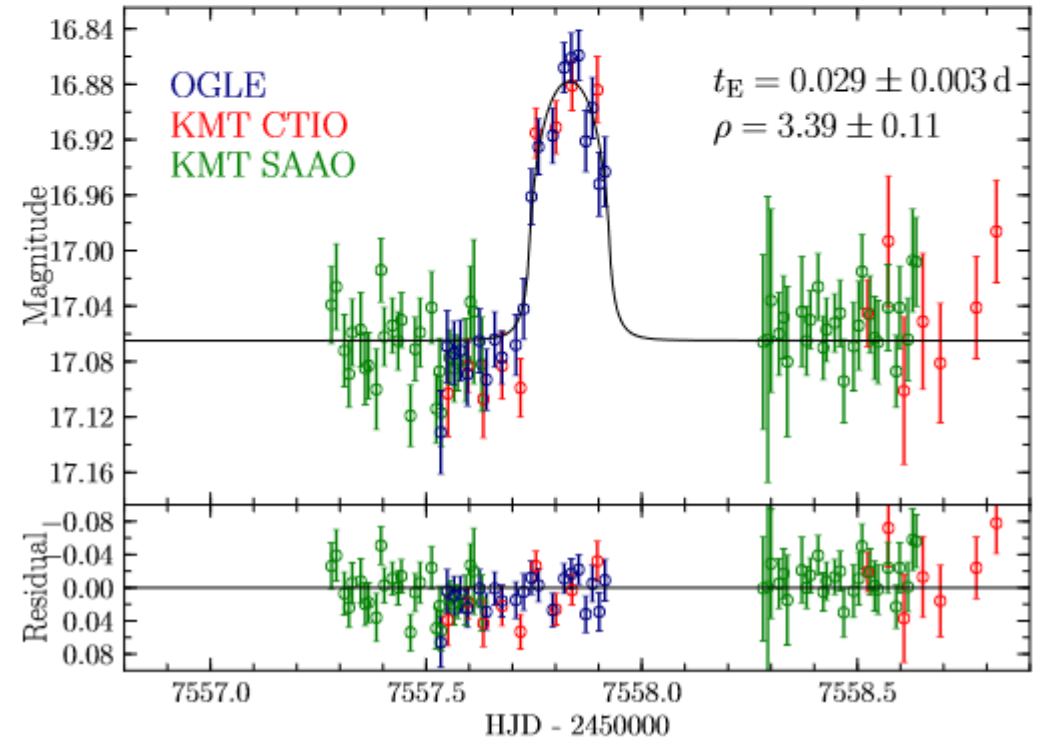
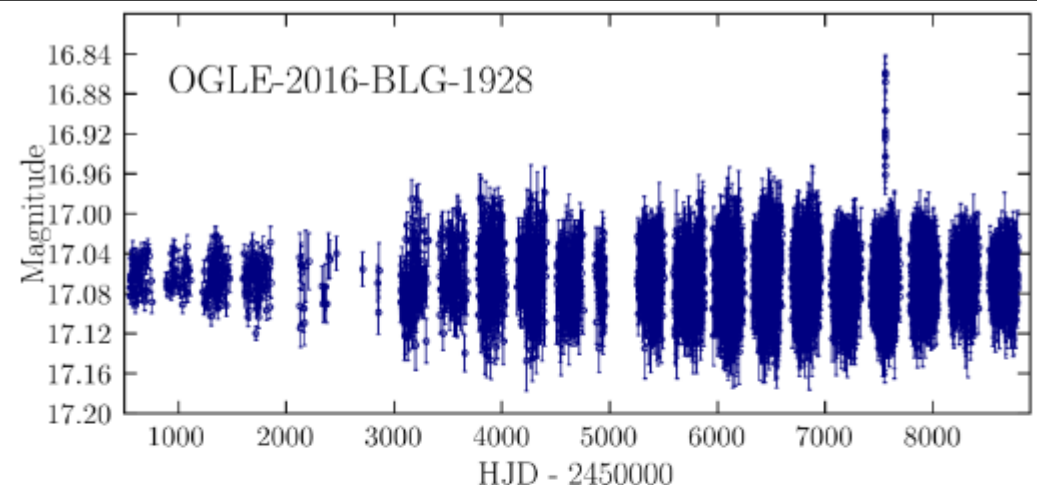


Rogue Earth-mass planet

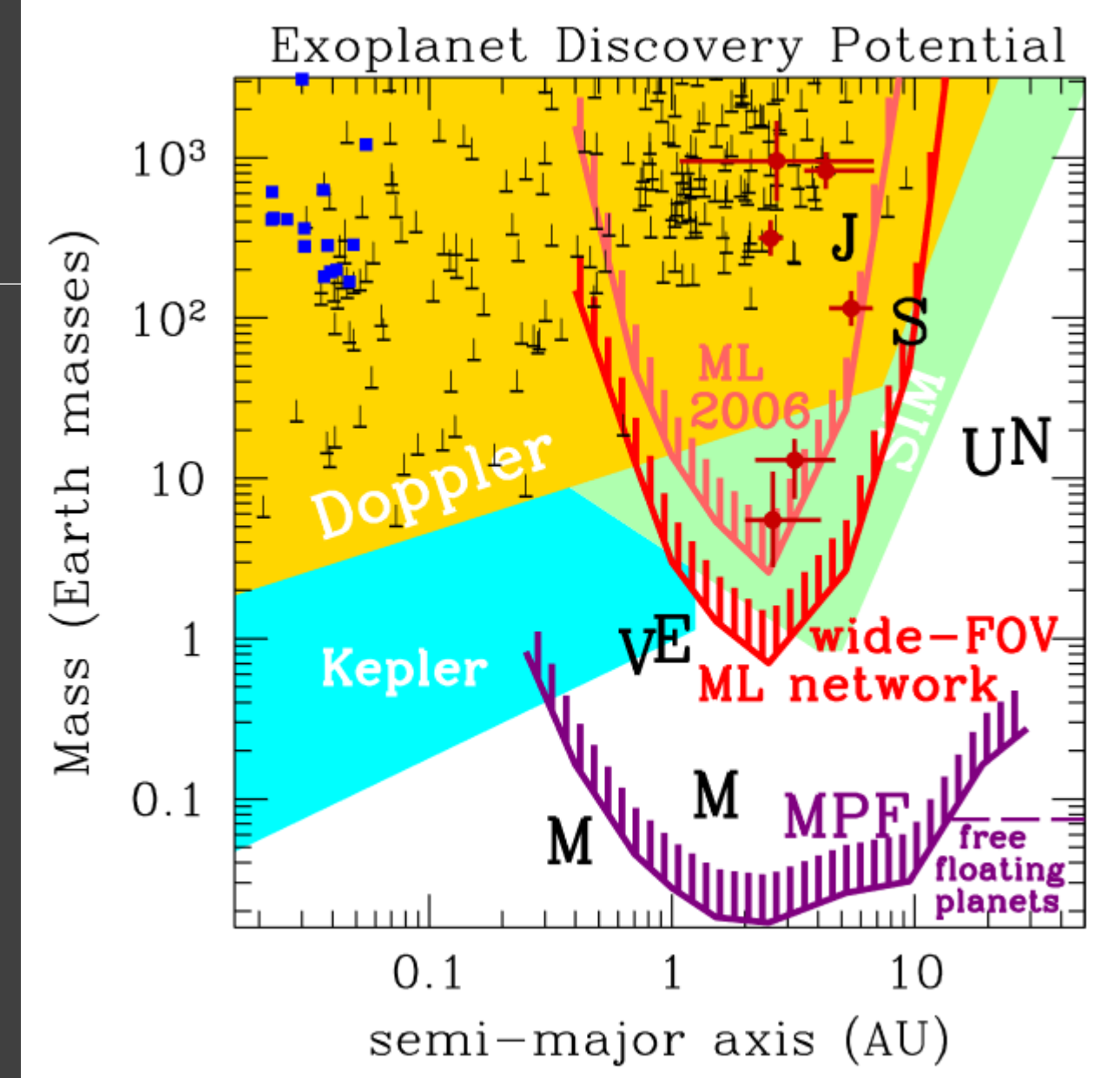
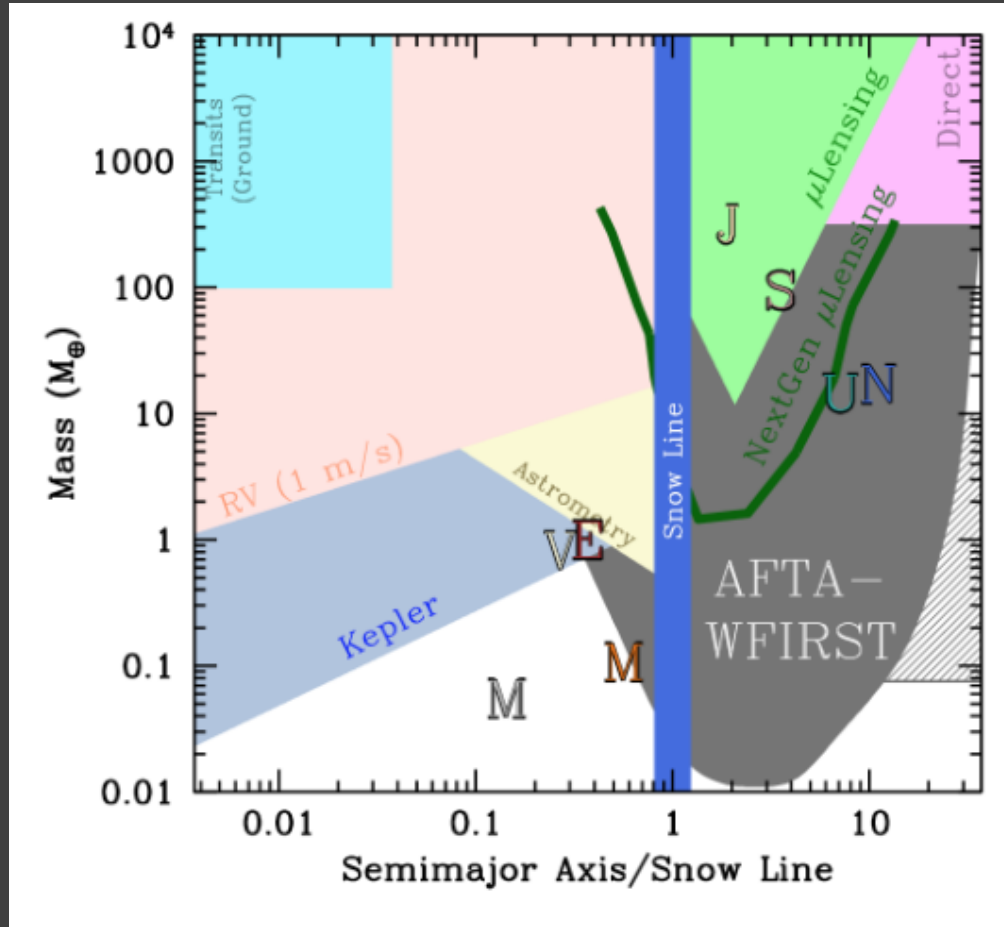
$$t_E = \frac{\theta_E}{\mu_{\text{rel}}} = 1.5 \text{ hr} \left(\frac{M}{0.3 M_\oplus} \right)^{1/2} \left(\frac{\pi_{\text{rel}}}{0.1 \text{ mas}} \right)^{1/2} \left(\frac{\mu_{\text{rel}}}{5 \text{ mas yr}^{-1}} \right)^{-1}$$

If the lens is in the Galactic disk, then the mass is $\sim 0/3$ Earth-mass.

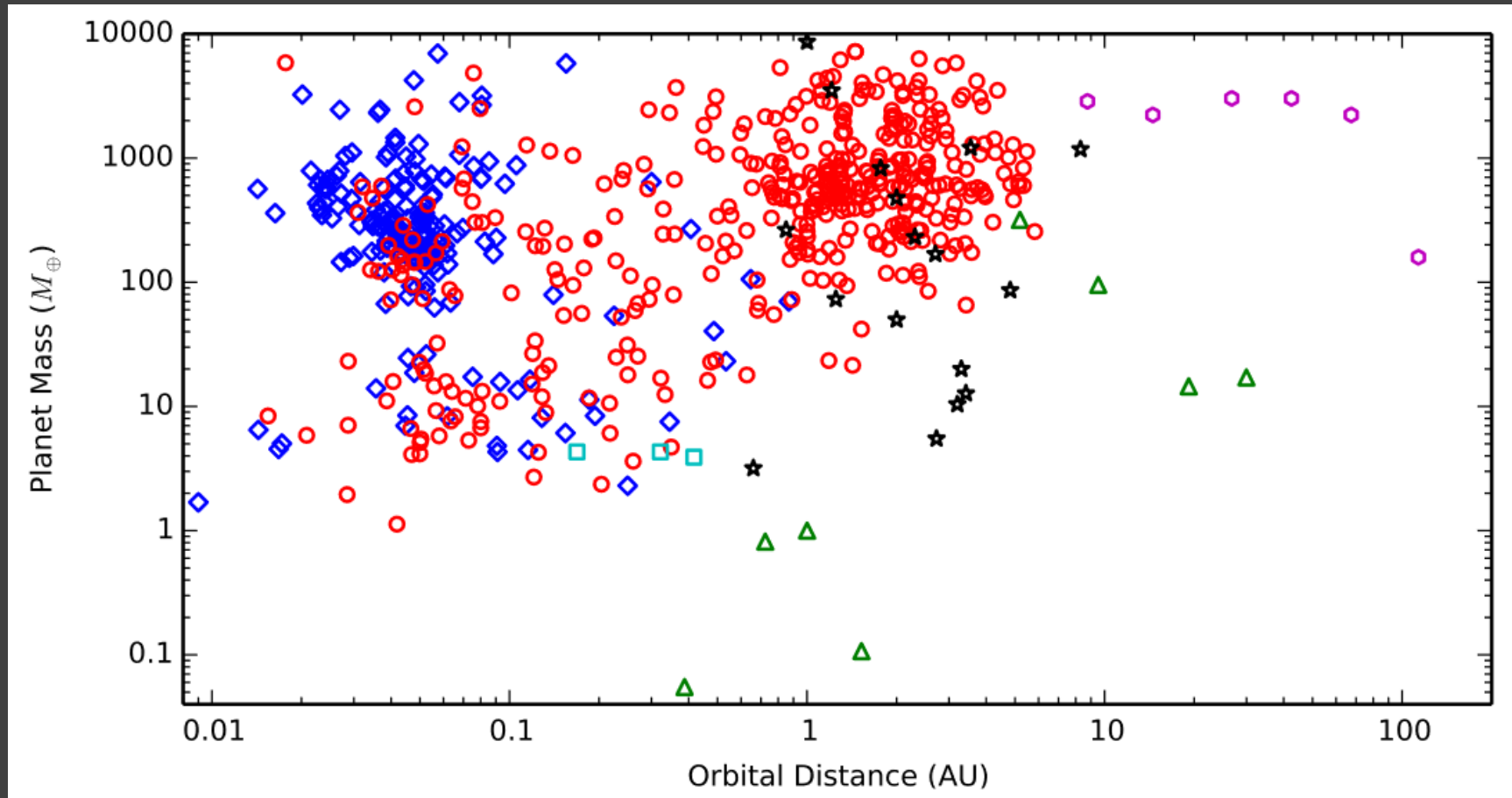
If it is in the bulge – then ~ 2 Earth masses.



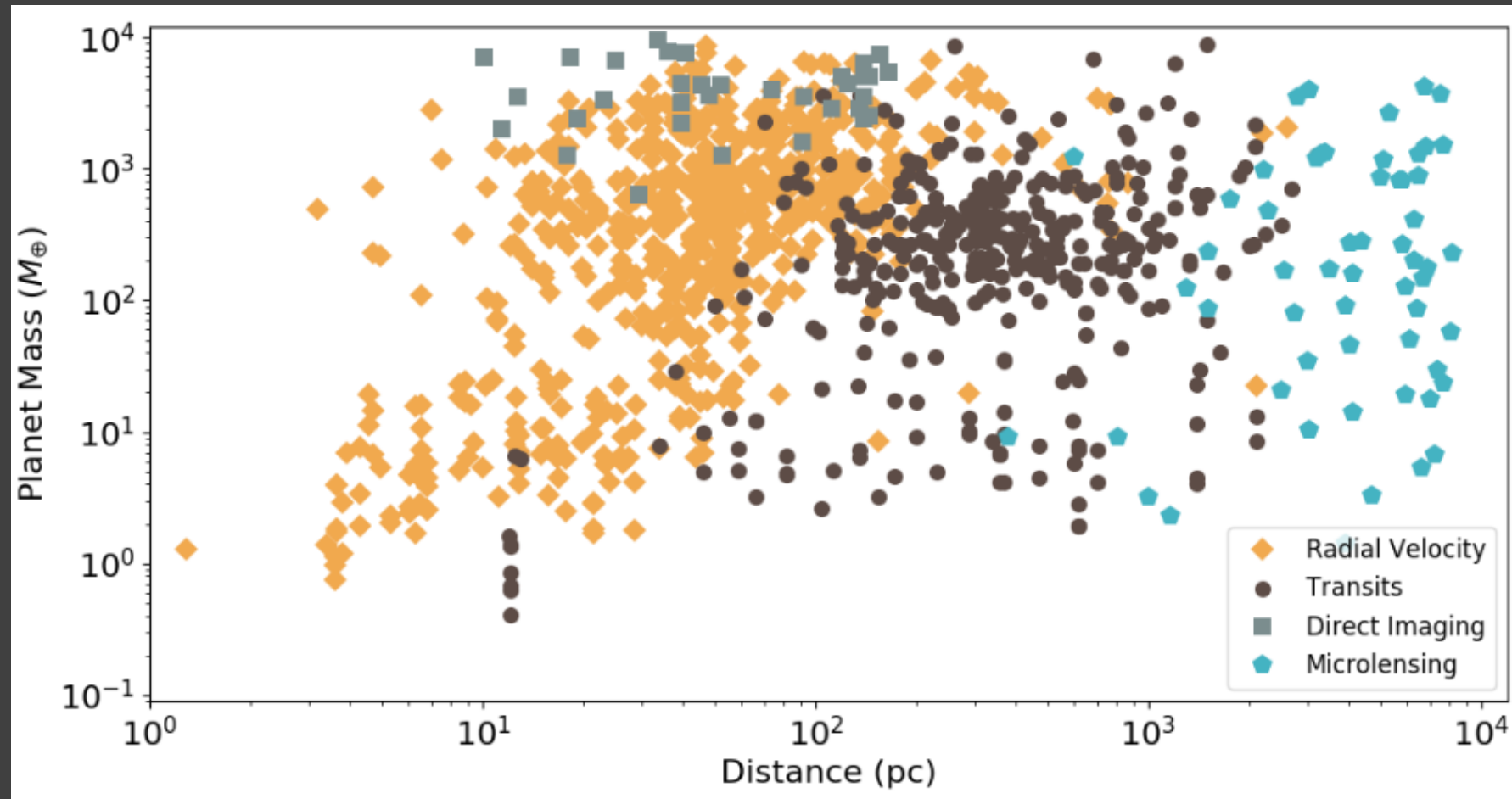
Comparison of three methods



Discoveries by different methods

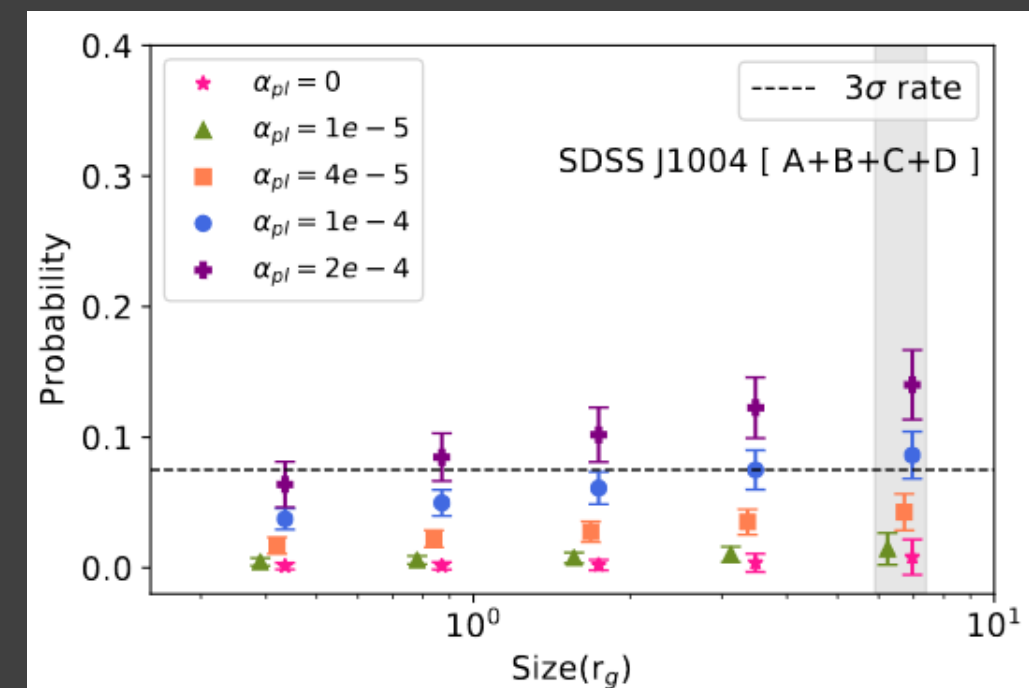
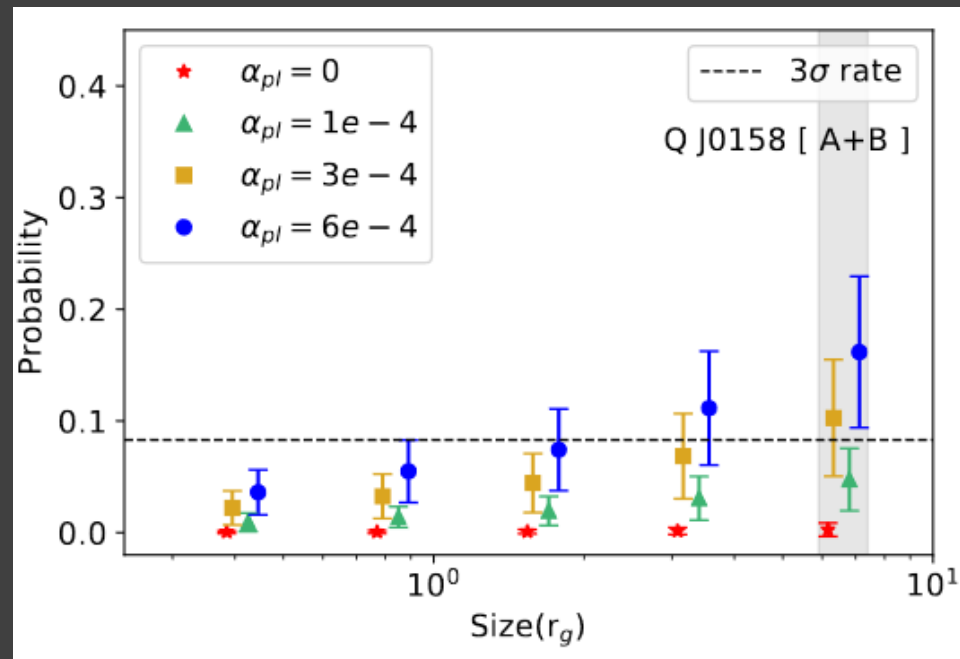


Microlensing wins in distance!



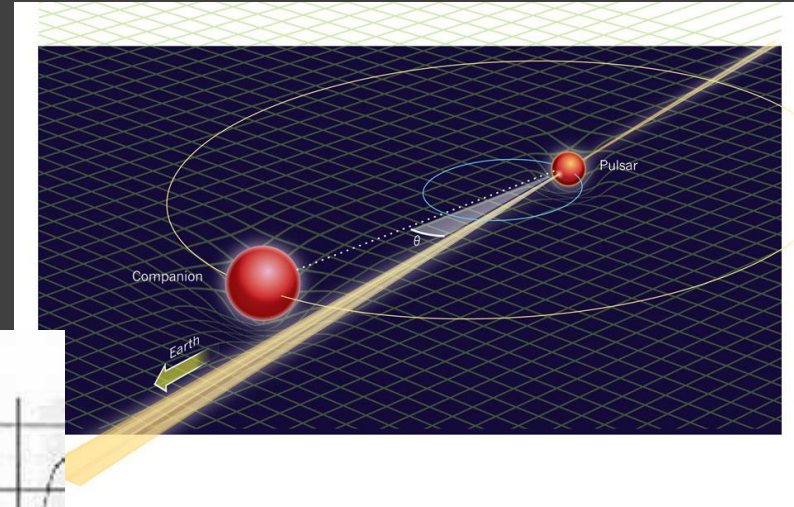
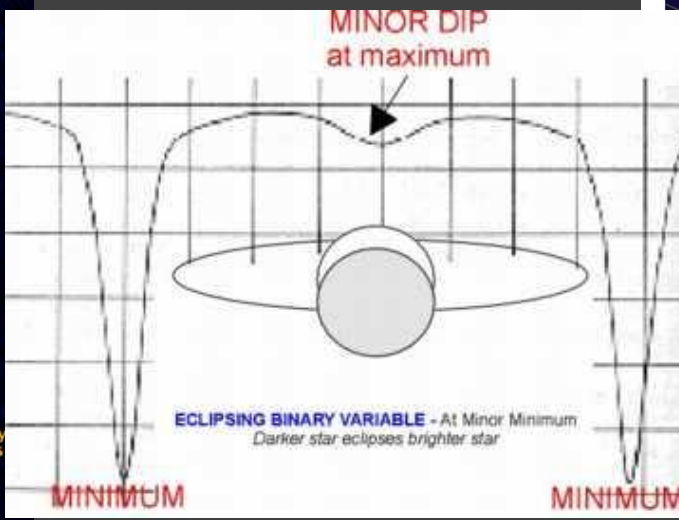
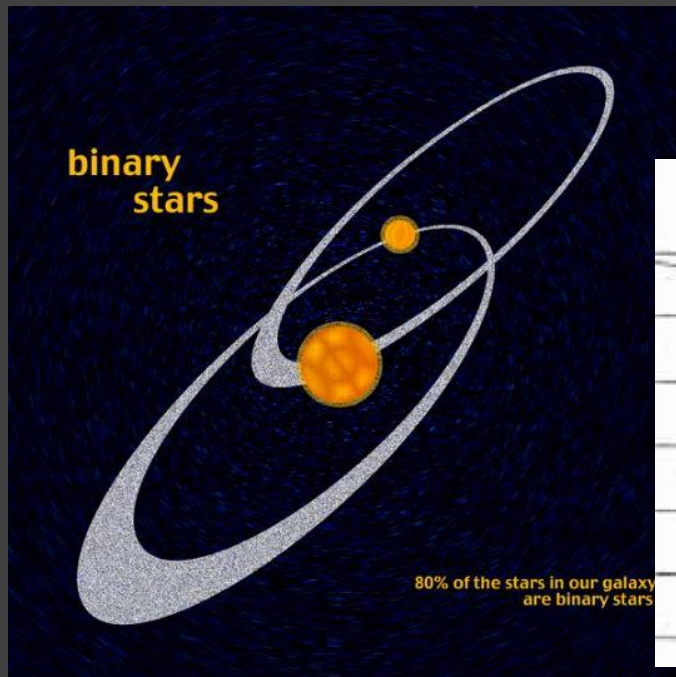
Extragalactic planets

Free-floating planets
detected due to
microlensing in X-rays:
observations of FeK α
from QSOs with Chandra.



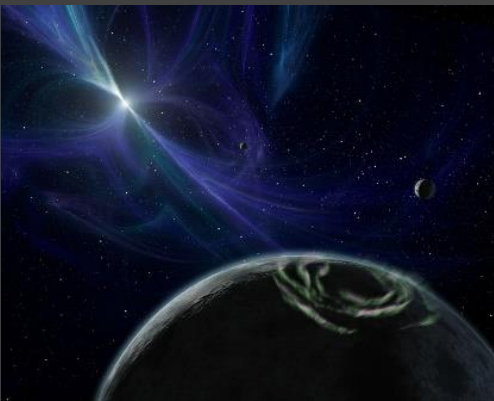
Timing

Observations of a periodic process
(radio pulsar, binary system, pulsating star)
allows to identify a perturber



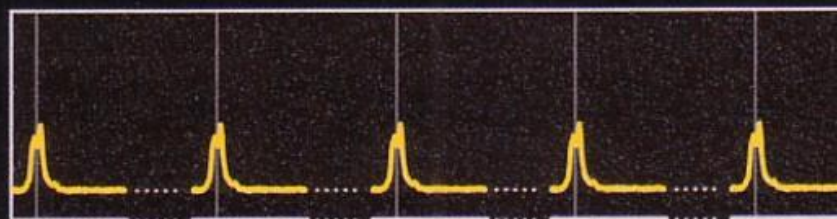
Planets around a radio pulsar

Wolszczan, Frail 1992



PSR B1257+12
Millisecond pulsar

Равномерный приход импульсов (нет планет)



Неравномерный приход импульсов (есть планеты)



Three light planets

Companion (in order from star)	Mass	Semimajor axis (AU)	Orbital period (days)
A (b)	$0.020 \pm 0.002 M_{\oplus}$	0.19	25.262 ± 0.003
B (c)	$4.3 \pm 0.2 M_{\oplus}$	0.36	66.5419 ± 0.0001
C (d)	$3.9 \pm 0.2 M_{\oplus}$	0.46	98.2114 ± 0.0002

Time delay

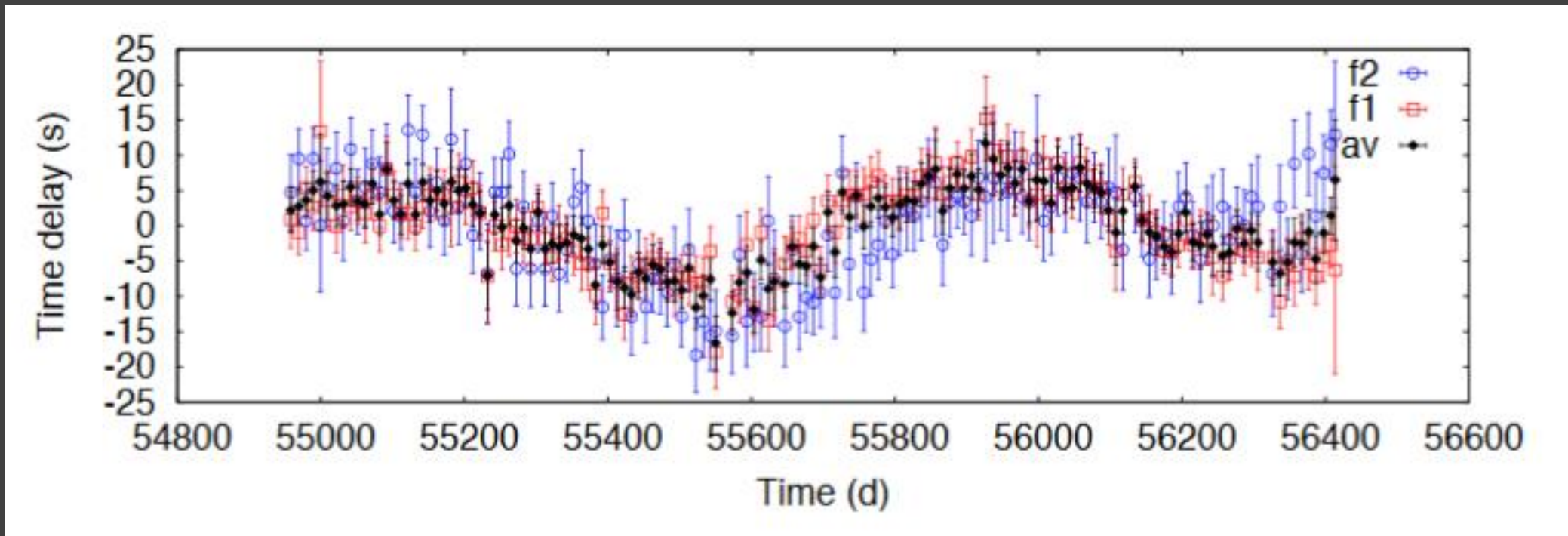
$$A \simeq \frac{a \sin i}{c} \frac{m_p}{M_{\star}},$$

$$\tau(t) = -\frac{1}{c} \int_0^t v_{\text{rad}}(t') dt'$$

$$v_{\text{rad}}(t) = -c \frac{d\tau}{dt}$$

See 1708.00896,
details in 1404.5649

Time delays for KIC 7917485



δ Scuti-type star

Planet: $M \sim 11 M_{Jup}$

$P_{orb} \sim 840$ days

Pulsations 1.18 and 1.56 hours.

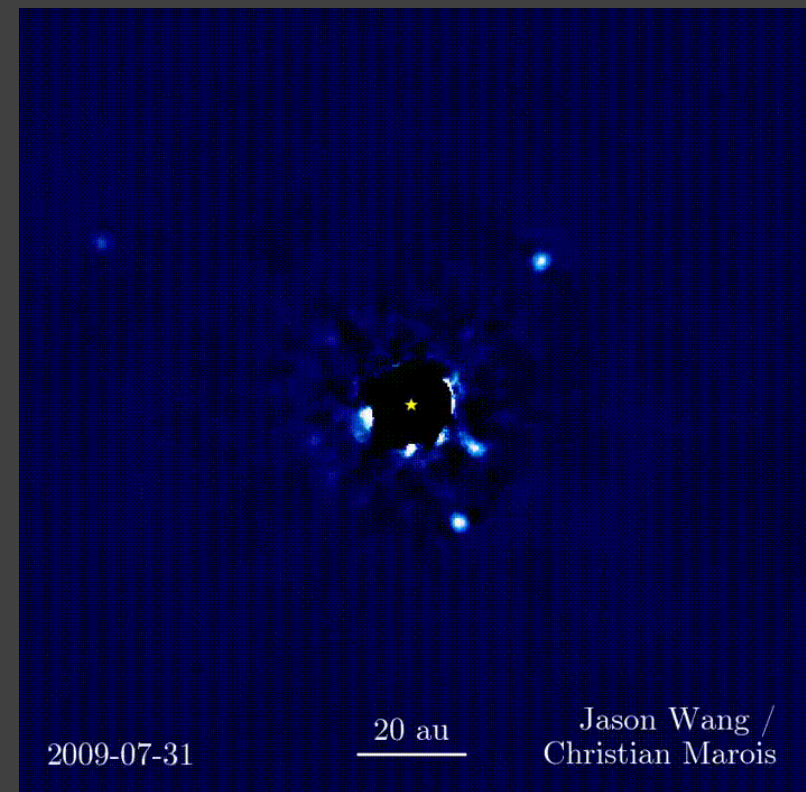
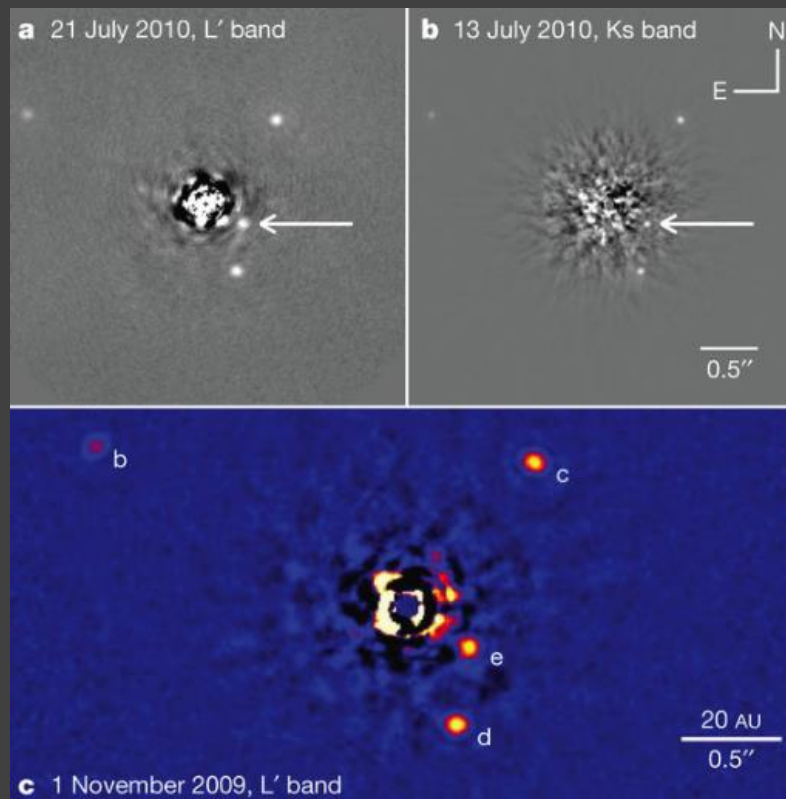
$\Delta t \sim 7$ sec

Habitable zone!

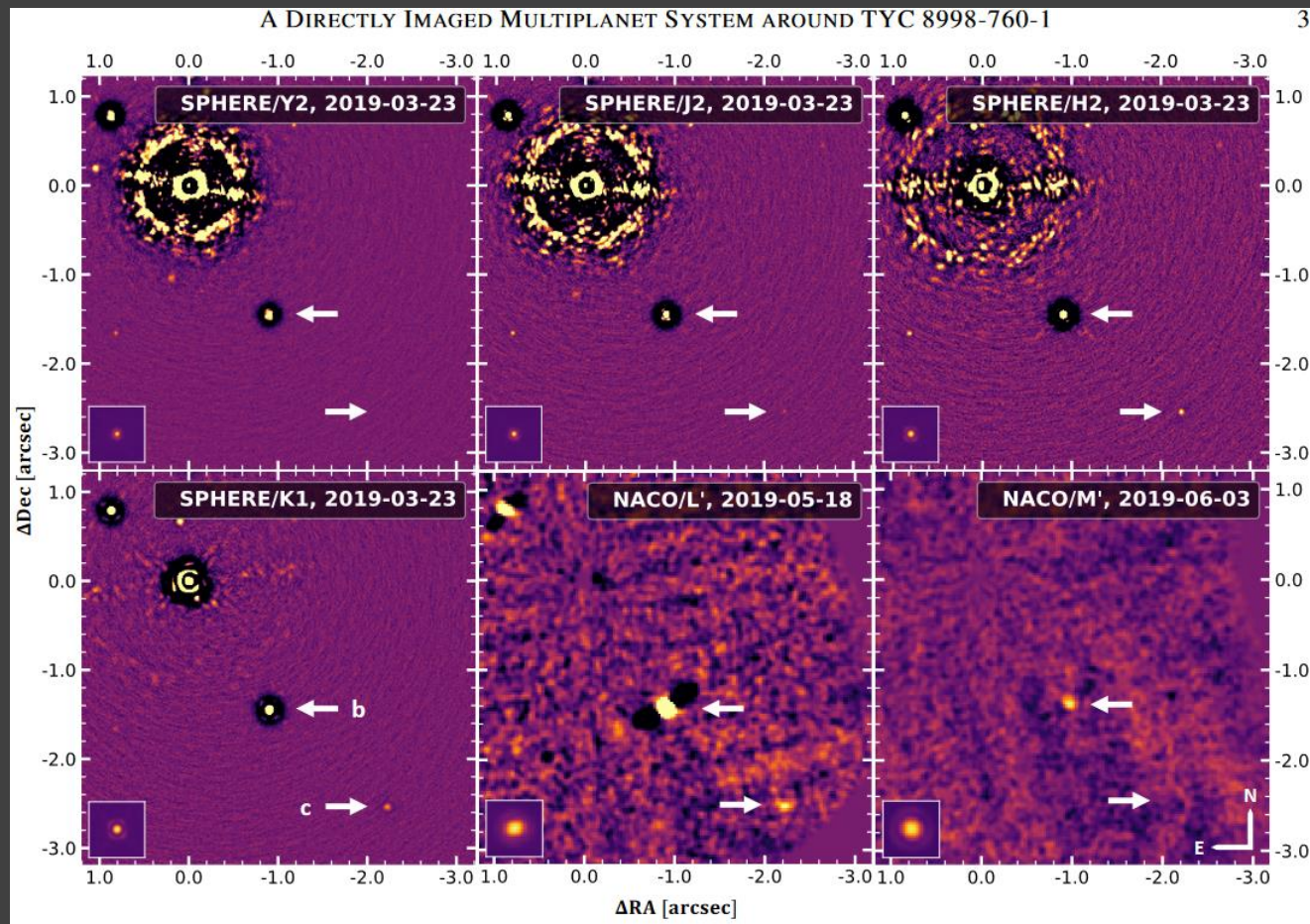
Direct imaging

Now it is possible to see self-luminous planets (10^{-5} in flux) at $>\sim 1$ arcsec.

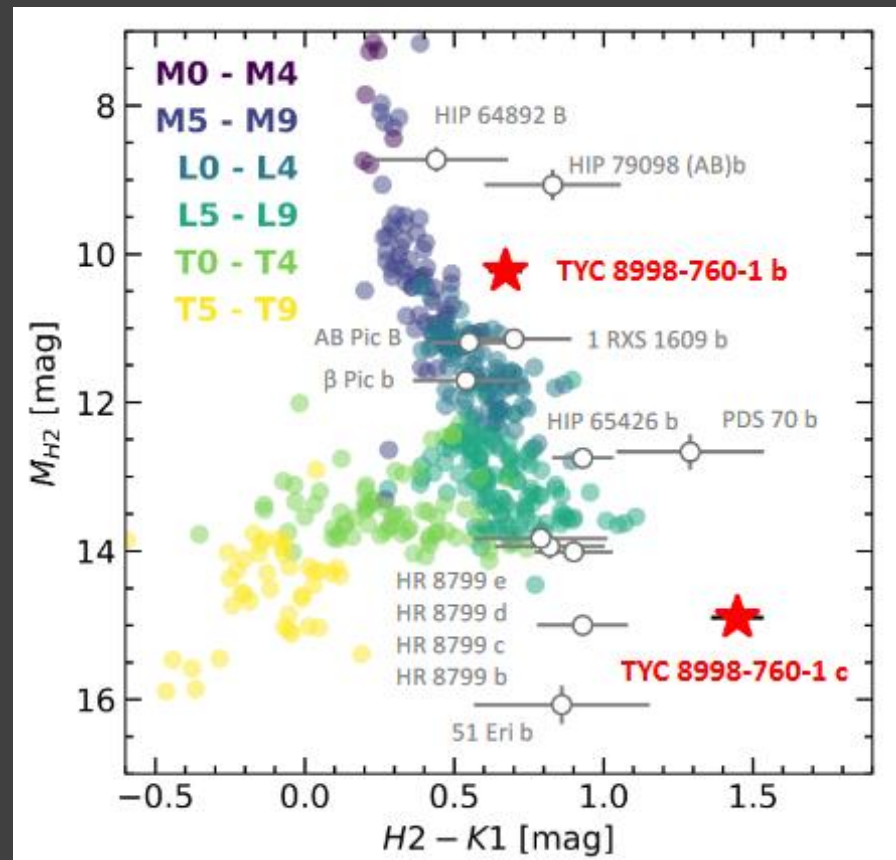
For comparison: Solar system analogue at 10 pc gives for Jupiter 10^{-9} in flux and 0.5 arcsec.



Distant planet



160 and 320 AU

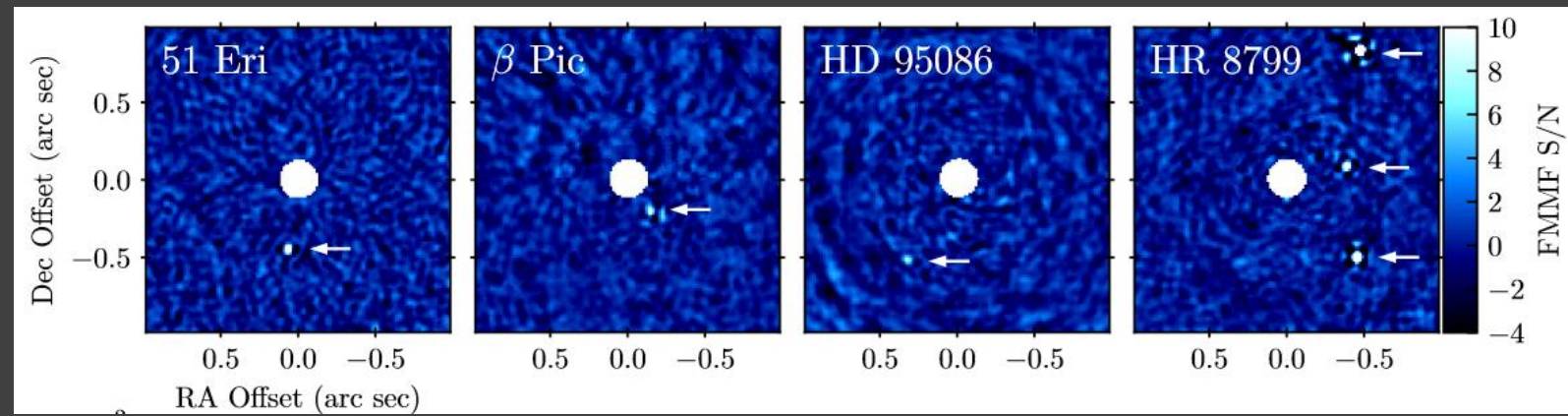
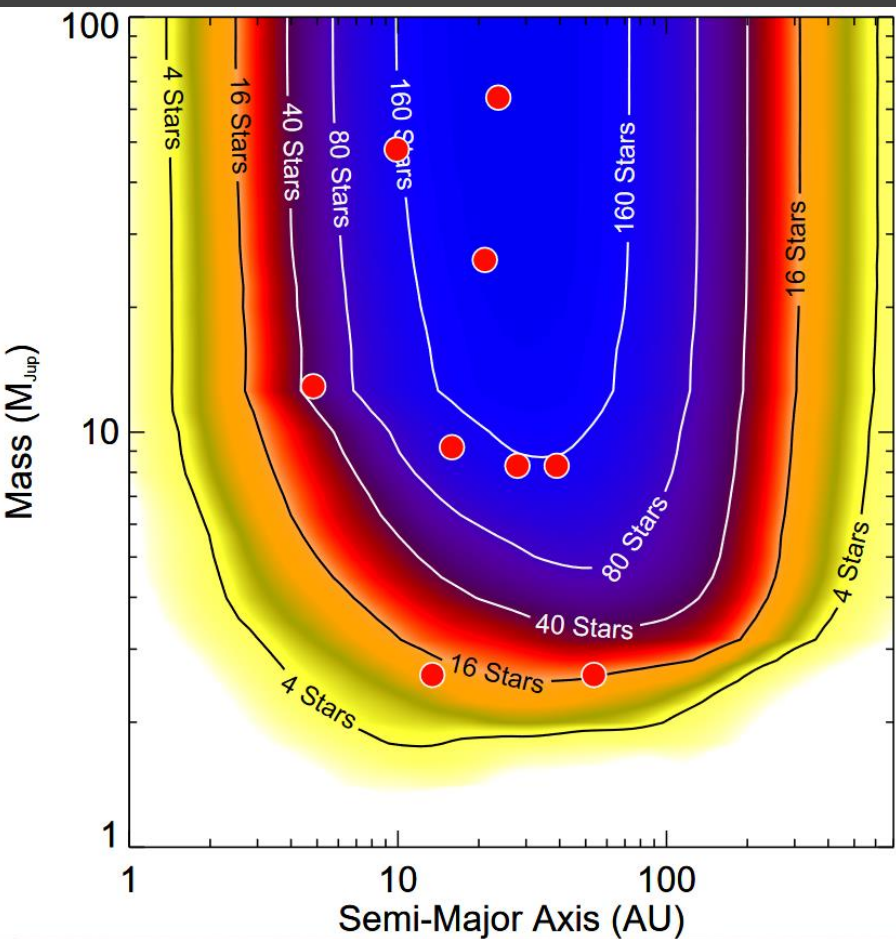


Telescope properties

Instrument	Telescope	Wavelength (μm)	Ang. resol. (mas)	Coronagraph
ACS	HST	0.2–1.1	20–100	Lyot
STIS	HST	0.2–0.8	20–60	Lyot
NAOS-CONICA	VLT	1.1–3.5	30–90	Lyot/FQPM
VISIR	VLT	8.5–20	200–500	—
SINFONI-SPIFFI	VLT	1.1–2.45	28–62	—
SPHERE	VLT	0.95–2.32	24–62	Lyot/APLC/FQPM
PUEO	CFHT	0.75–2.5	4–140	Lyot
CIAO	SUBARU	1.1–2.5	30–70	Lyot
OSIRIS	Keck I	1.0–2.4	20–100	—
AO-NIRC2	Keck II	0.9–5.0	20–100	Lyot
ALTAIR-NIRI	Gemini N.	1.1–2.5	30–70	Lyot
GPI	Gemini S.	0.9–2.4	24–62	Lyot/APLC
PALM-3000 PHARO	Hale 200''	1.1–2.5	60–140	Lyot/FQPM
PALM-3000 Project1640	Hale 200''	1.06–1.76	43–71	APLC
AO-IRCAL	Shane 120''	1.1–2.5	100–150	—

$$\Theta = (a/d)(1+e) = \\ = 1 \text{ arcsec} (a/\text{AU})(d/\text{pc})^{-1} (1+e)$$

GPIES survey (300 stars)

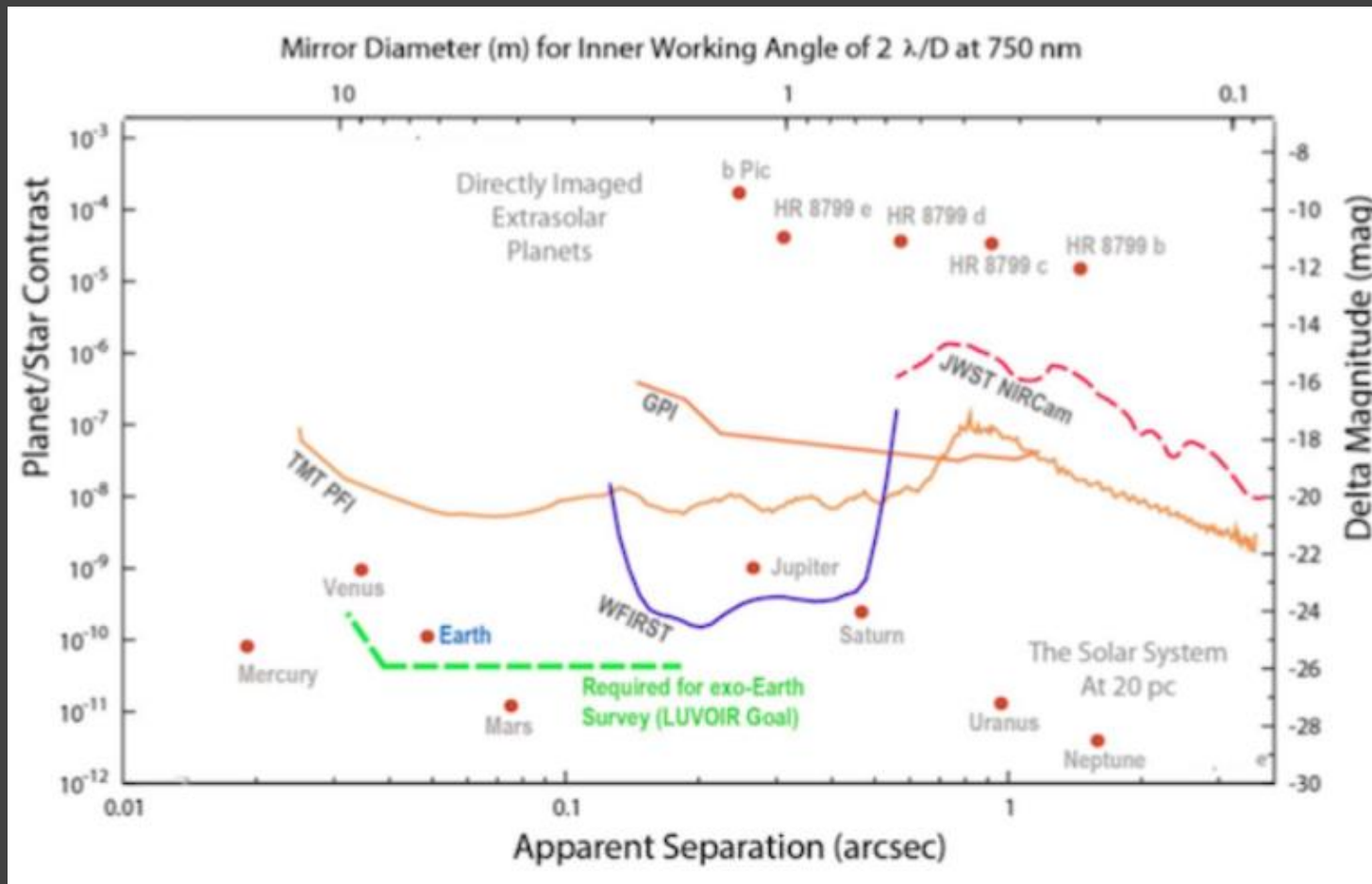


Gemini Planet Imager Exoplanet Survey

10-100 AU

6 planets + 3 brown dwarfs detected

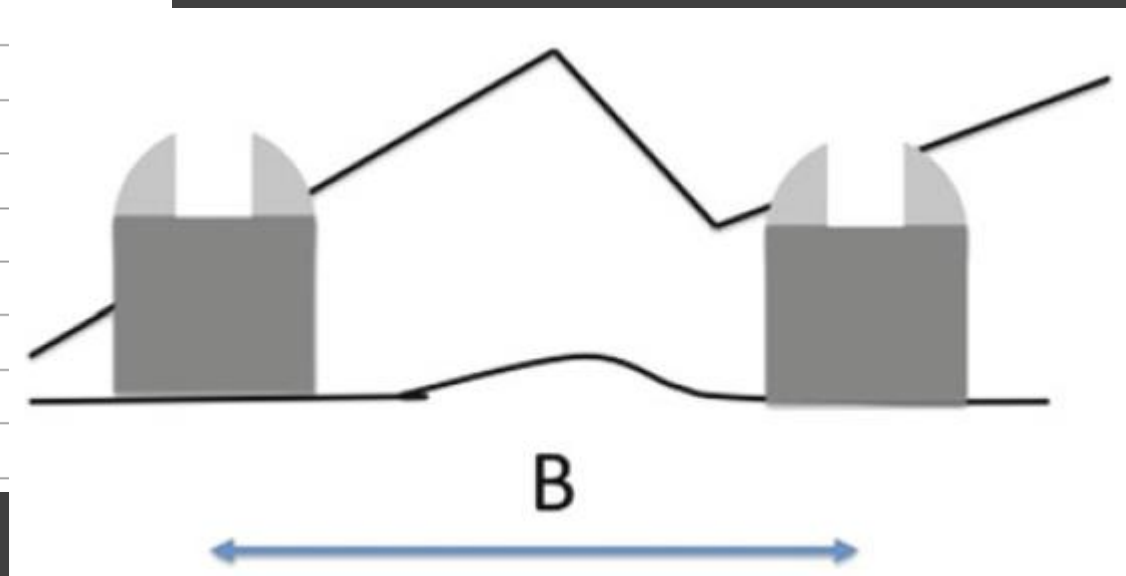
Direct imaging: present and future



Ground optical interferometers

Instrument	Interf.	Baseline (m)	Bands	Ang. res. (mas)	Spec. res.	Aperture
AMBER	VLTI	16–200	J,H,K	0.6–14	35–15,000	3
MIDI	VLTI	16–200	N	4–80	20–220	2
PIONIER	VLTI	16–200	H,K	1.5–45	15	4
V2	Keck I	85	H,K,L	2–5	25–1800	2
Nuller	Keck I	85	N	10–16	40	2
Mask	Keck	1–10	J to L	13–400	None	2
Classic	CHARA	34–330	H,K	0.5–7	None	2
FLUOR	CHARA	34–330	K	0.7–7	None	2
MIRC	CHARA	34–330	J,H	0.4–5	40–400	4
BLINC	MMT	4	N	250	None	2
LMIRCAM	LBTI	14–23	L,M	27–72	None	2
NOMIC	LBTI	14–23	N	72–200	None	2

Better resolution,
but smaller aperture



Coronagraphs

The diagram illustrates the optical path of a coronagraph. Light from the left passes through an Objective Lens, creating an Apodized Pupil. A Field Lens then focuses the light onto an Opaque Disk at the Focal Plane. This disk is positioned in front of a Lyot Stop, which is imaged onto the Imaging Plane. A Second Field Lens and a Focusing Lens are also shown. Below the diagram, a large image shows a star with a central occulting disk and a surrounding diffraction pattern. To the right, two smaller images labeled 'b' and 'c' show concentric rings, with 'b' having a scale bar of 2 μm and 'c' having a scale bar of 40 μm.

To obtain planet images different kinds of coronagraphs are used.

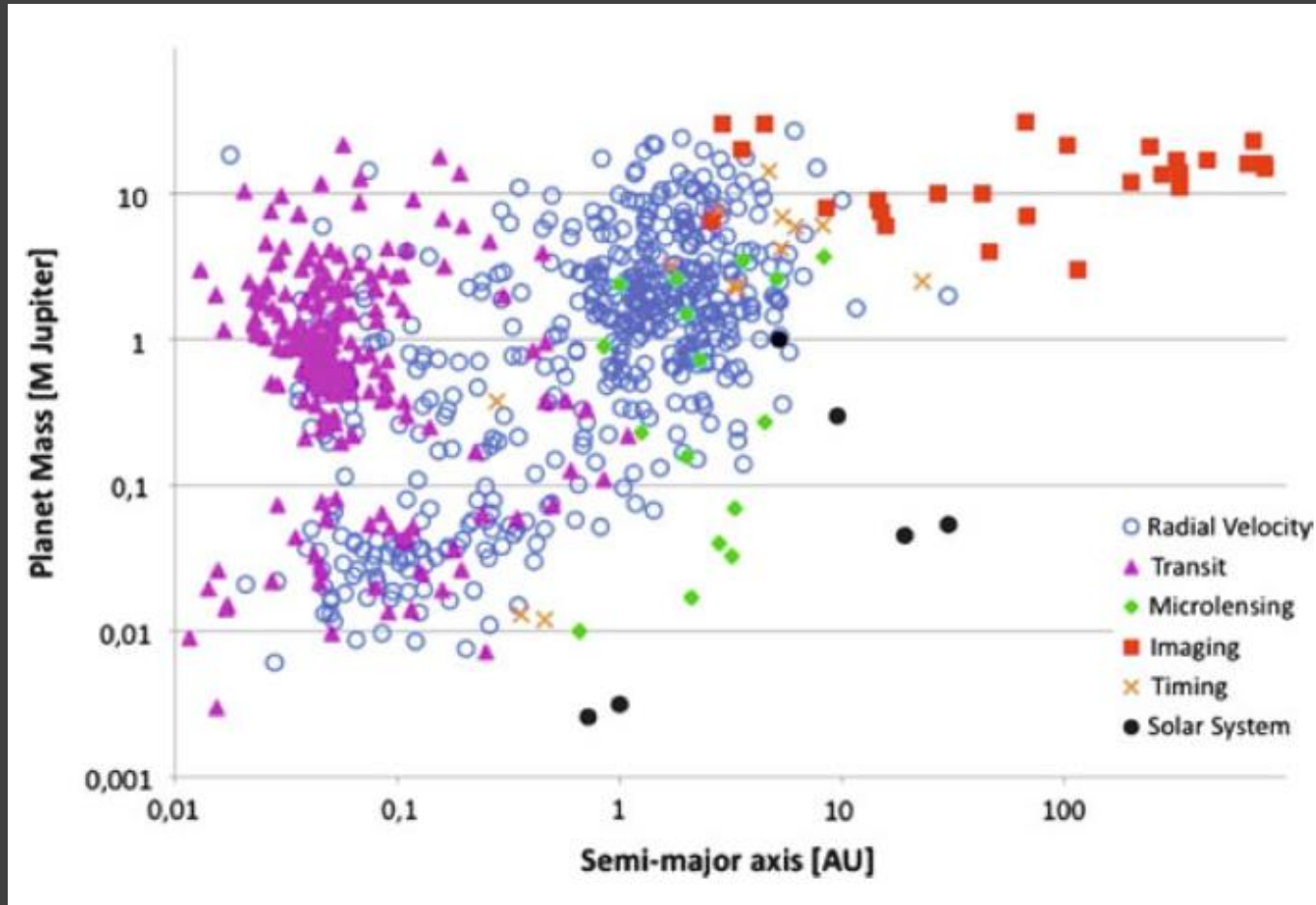
b $2 \mu\text{m}$

c $40 \mu\text{m}$

Riccardo Claudi (in Bozza et al. 2016)

May be a star shade will be used for WFIRST (Roman), see 2101.01272.

Imaging vs. other methods



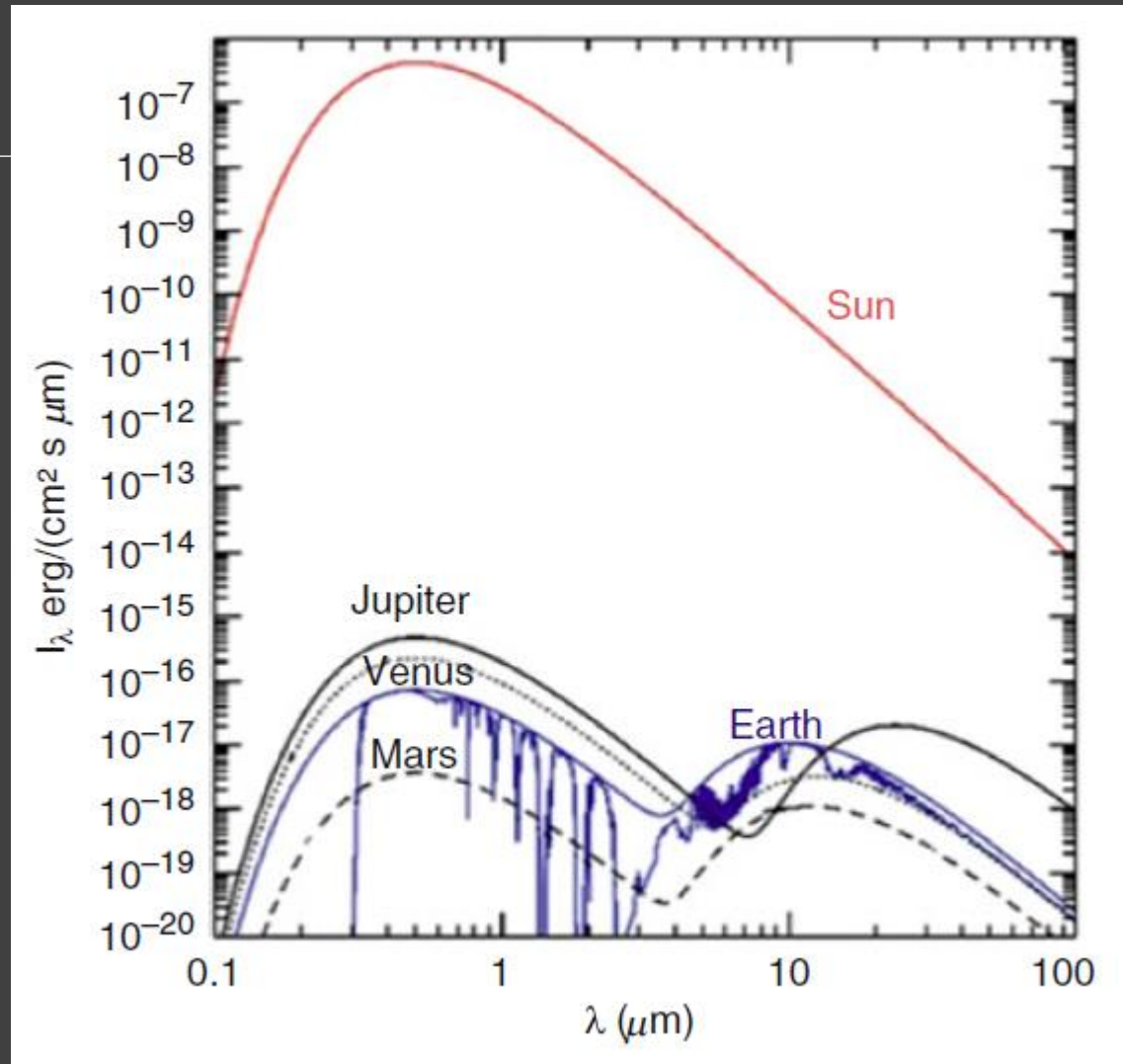
Solar system

Notice, how much better planets are visible in IR.
Especially Jupiter at 20-30 micrometers.

Reflected flux

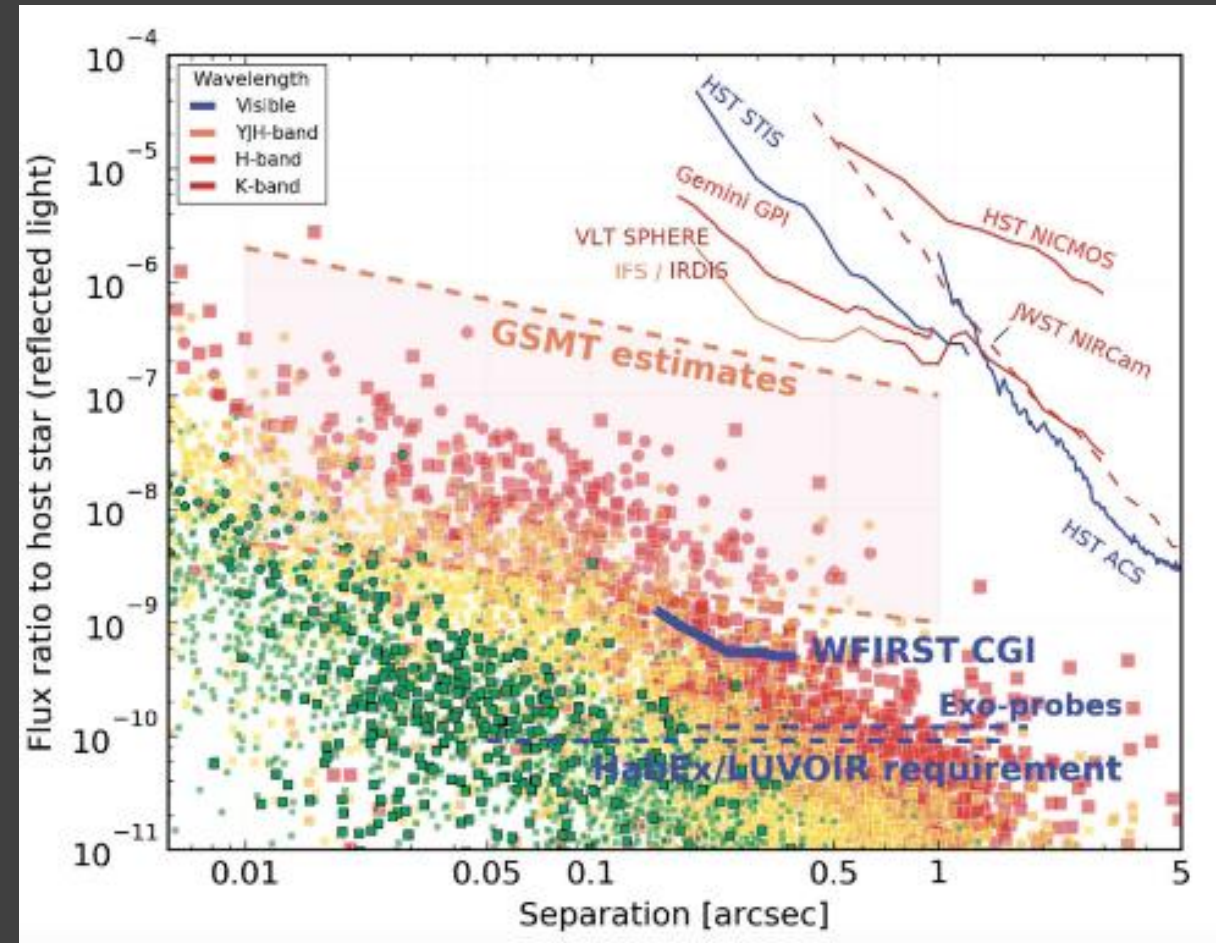
$$F_{\text{p,Vis}} = A(\lambda, t)\phi(t) \frac{R_p^2}{4a^2} B(\lambda, T_{\text{eff}}) R_{\star}^2,$$

(A – albedo, a – semimajor axis, ϕ - phase)

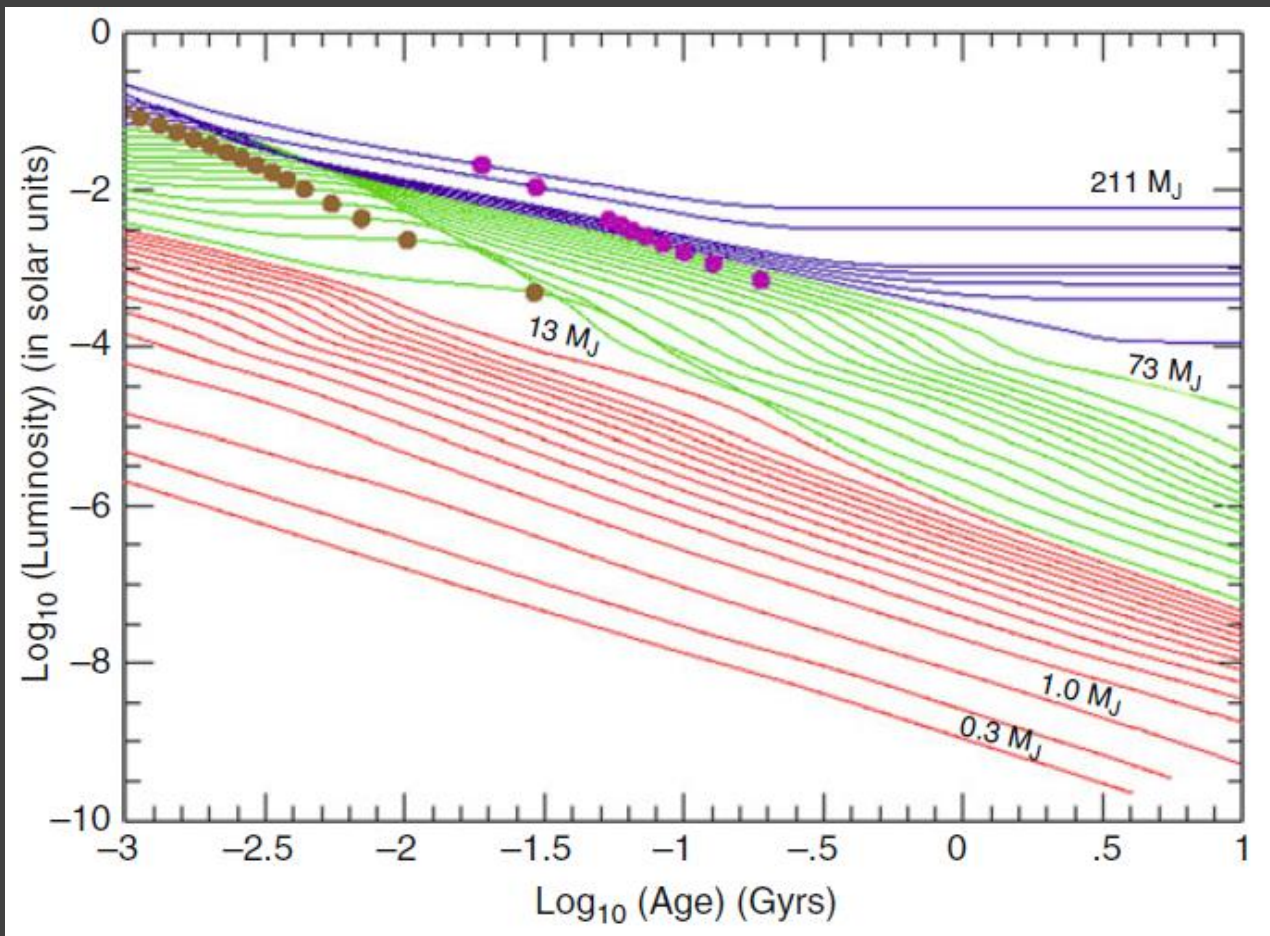


Future direct imaging in reflected light

Reflected light flux ratio versus
angular separation for current and future
direct imaging surveys

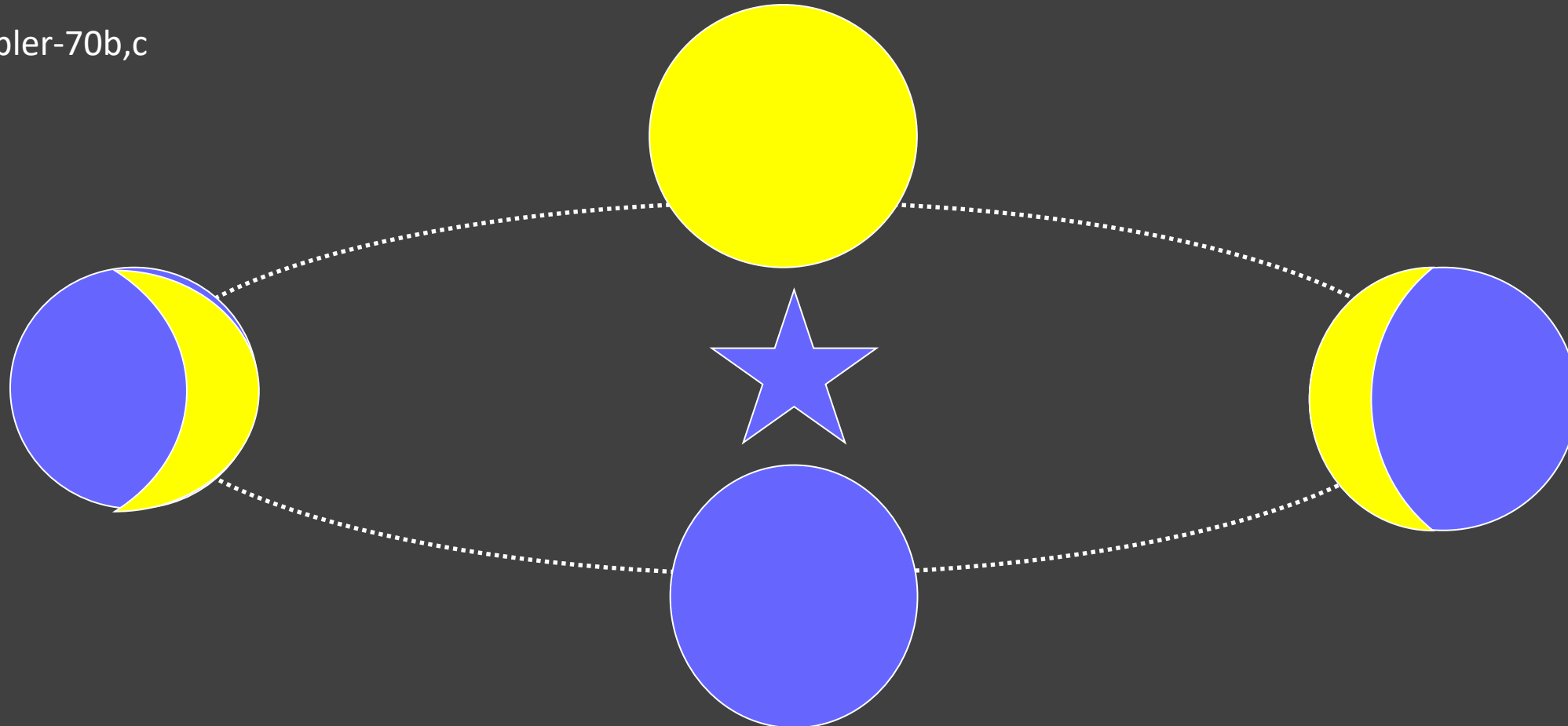


Young planets are hotter

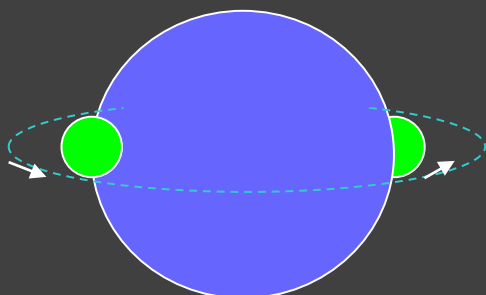


Planet light identification

Kepler-70b,c



IR light



55 Cnc e

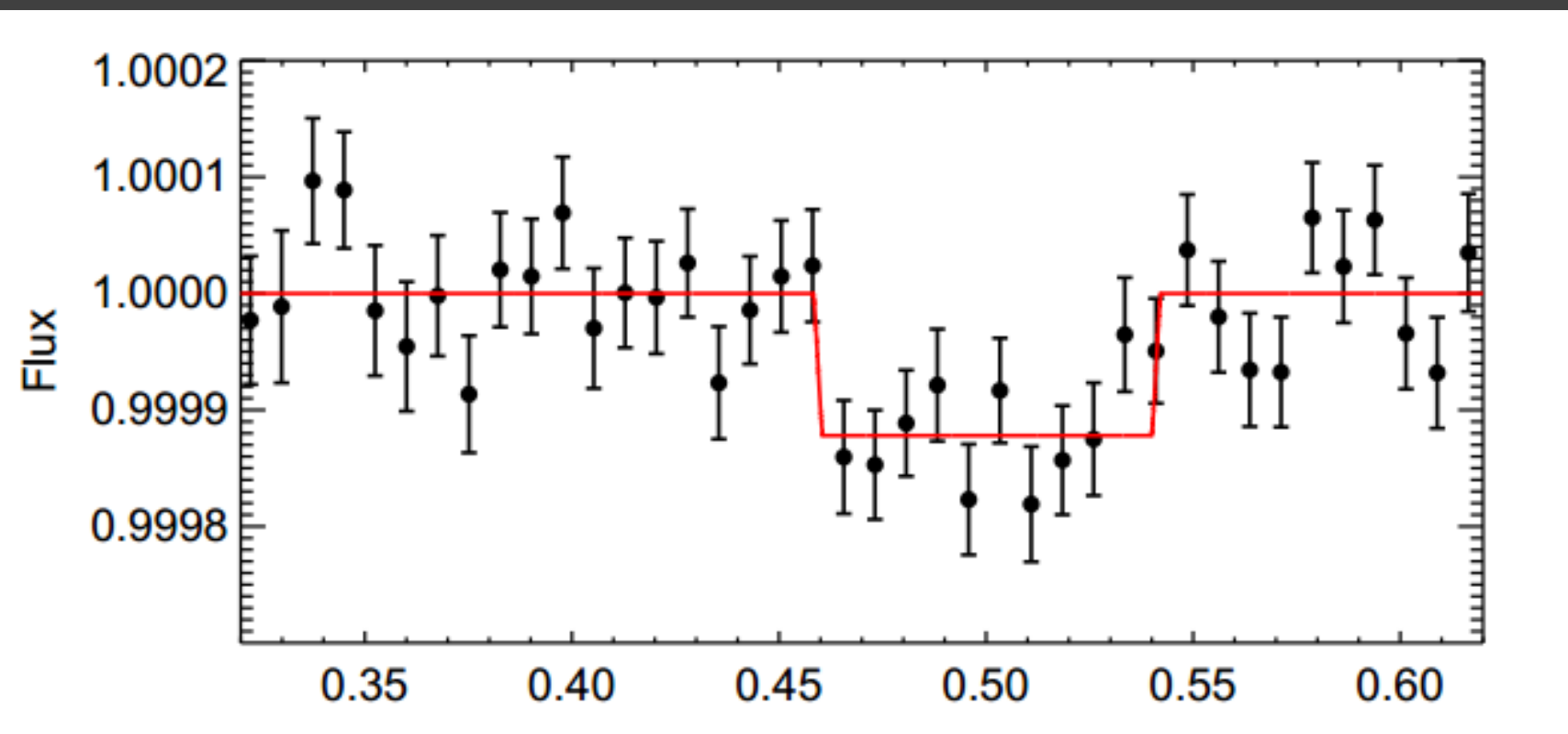
Mass: 7-8 Earth mass

Semi-major axis: 0.016 AU

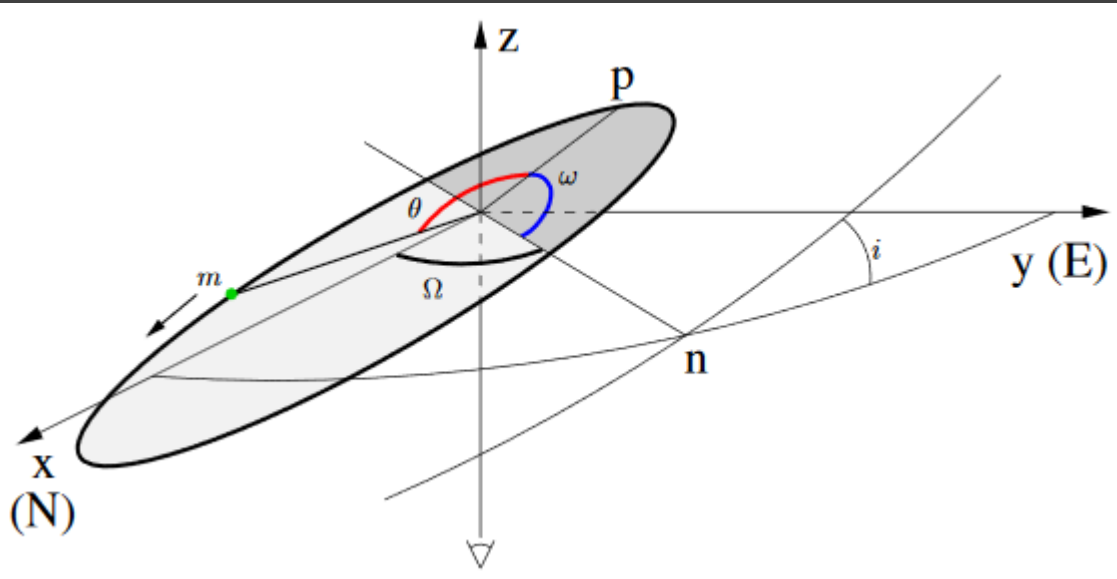
Orbital period: 0.74 days

Temperature 2000-2600K

Occultation light curve

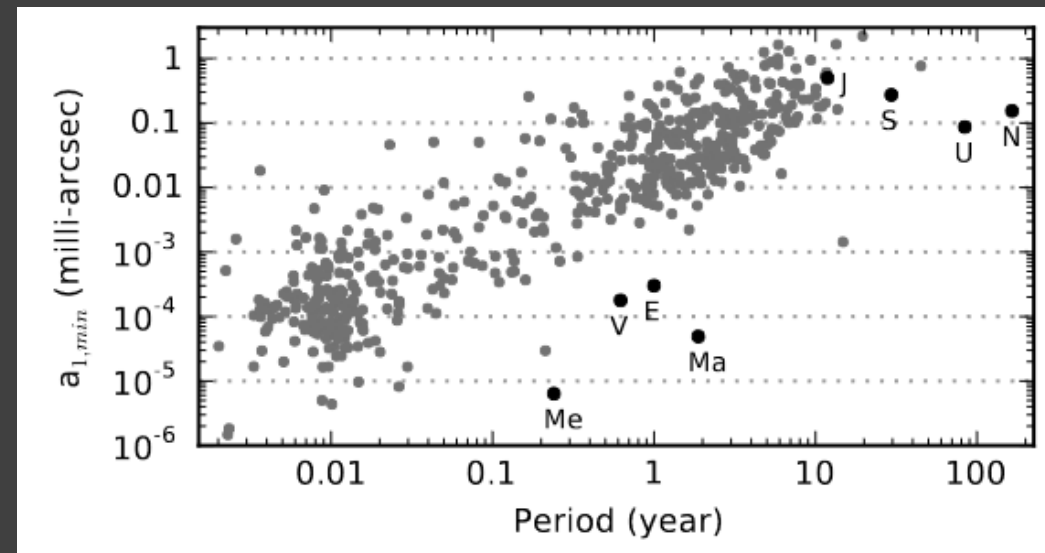


Astrometric detection



$$4\pi^2 \frac{\bar{a}_1^3}{P^2} = G \frac{M_P^3}{(M_* + M_P)^2},$$

Astrometry allows to determine $M_{\text{planet}}^3 / (M_{\star} + M_{\text{planet}})^2$



Data on 570 stars with planets are shown.
Solar system data is scaled for a star at 10 pc.

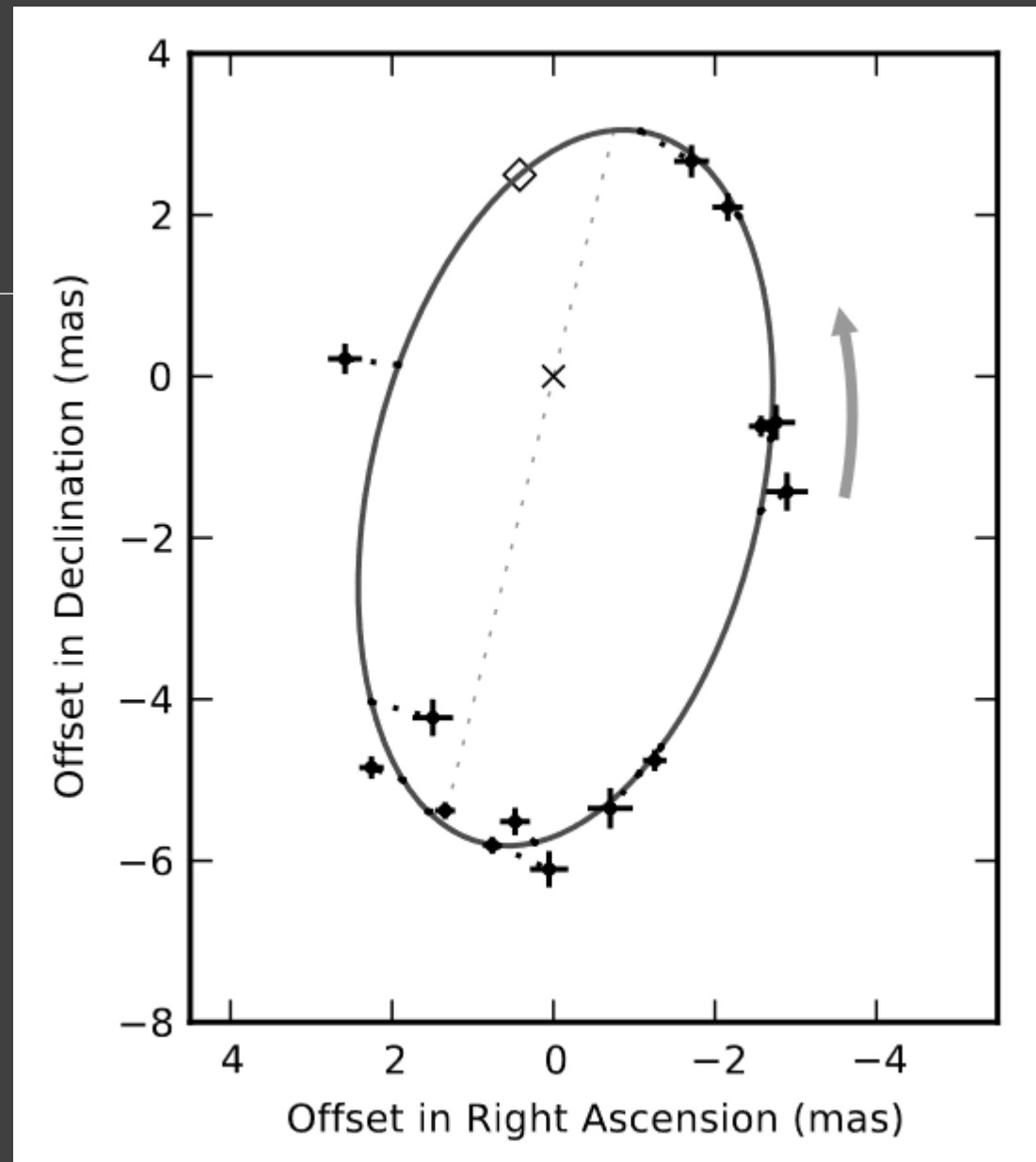
A former candidate

Came out to be a brown dwarf with $28 M_{\text{jup}}$.

Now waiting for Gaia data.

Fig. 15.— The barycentric orbit of the L1.5 dwarf DENIS-P J082303.1-491201 caused by a 28 Jupiter mass companion in a 246 day orbit discovered through ground-based astrometry with an optical camera on an 8 m telescope ([Sahlmann et al. \[2013a\]](#)).

Few other candidates have been mentioned by
Muterspaugh et al. (2010)



Fomalhaut B candidate

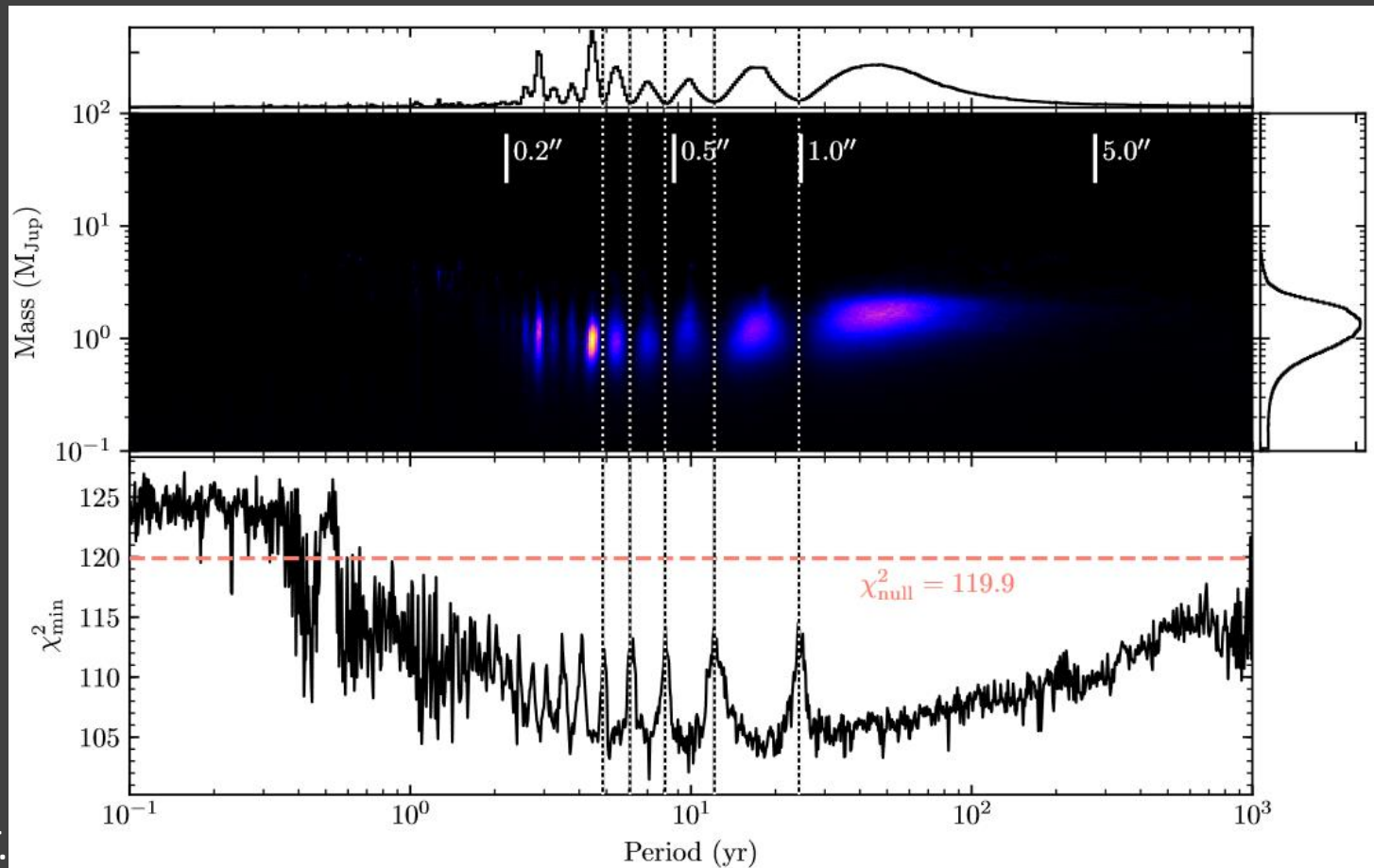
Fomalhaut is a binary system
(may be even triple).
Fomalhaut B (TW PsA)
is a red dwarf (K4Ve)
on a wide (light year) orbit.

Astrometry of Fomalhaut B
suggests a substellar component
due to measured acceleration.

Direct search puts a limit $M > 2 M_{\text{jup}}$.

But situation is still uncertain.

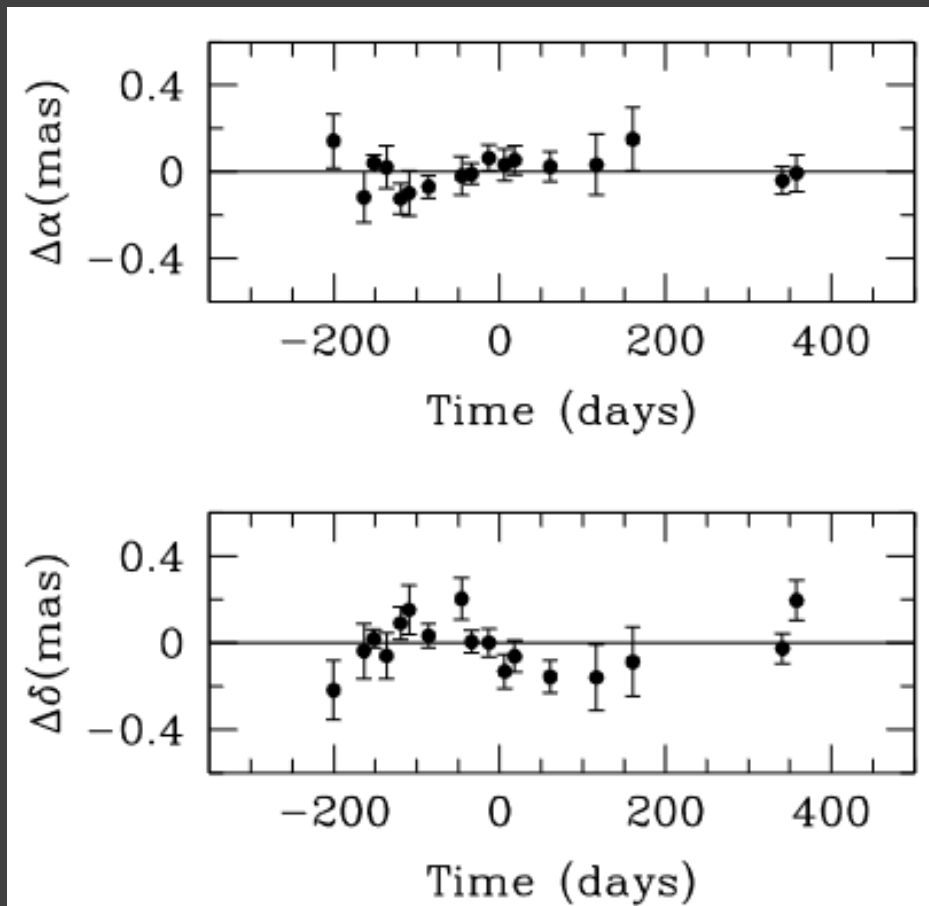
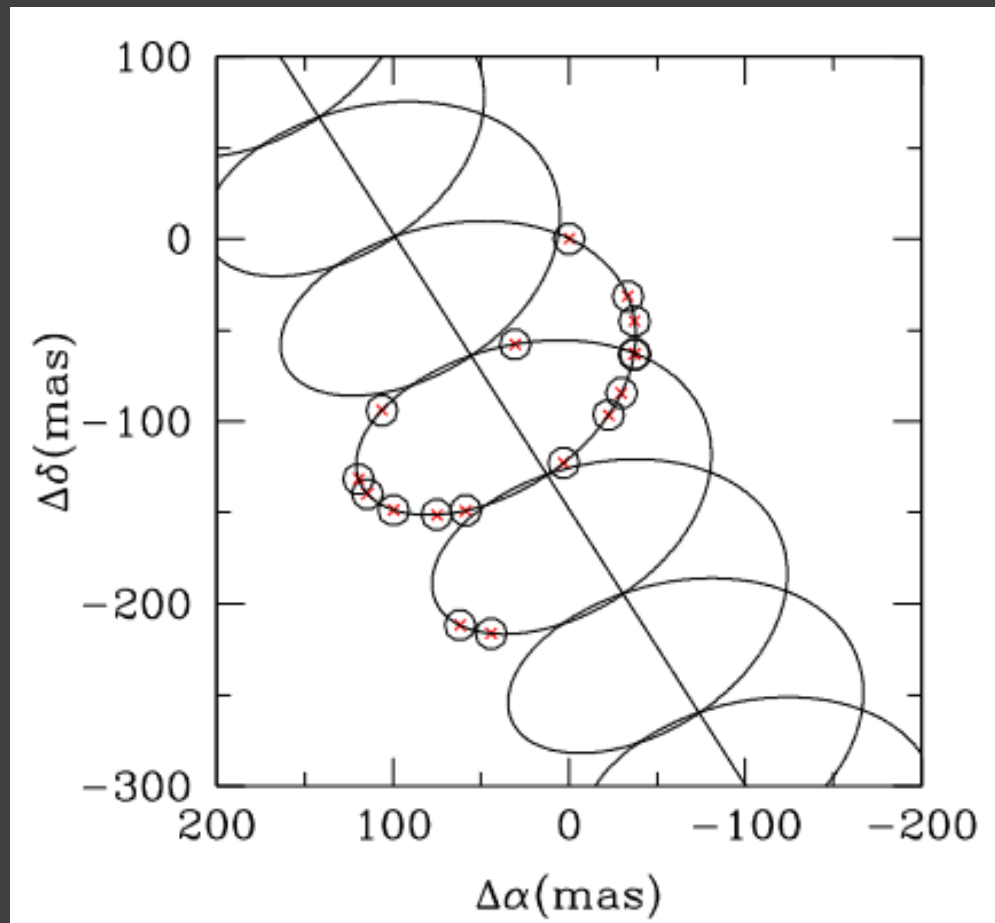
Can be searched for with JWST and WFIRST.



Astrometry in radio

Red dwarf
VLBA observations

Saturn mass planet
~220 days
Circular orbit ~0.3 a.u.



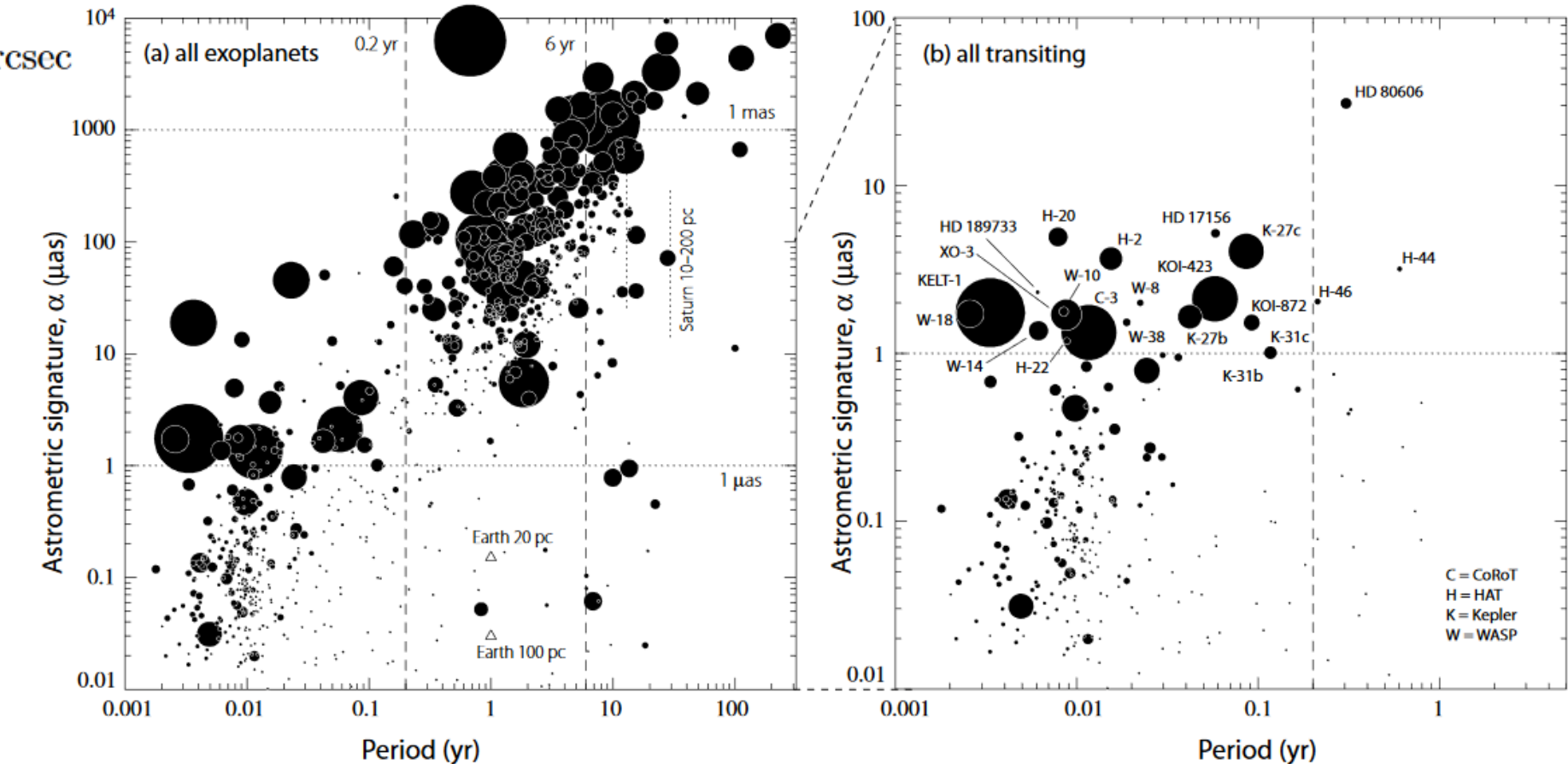
Gaia and astrometric microlensing

$$\alpha = \left(\frac{M_p}{M_\star} \right) \left(\frac{a_p}{1 \text{ AU}} \right) \left(\frac{d}{1 \text{ pc}} \right)^{-1} \text{ arcsec}$$

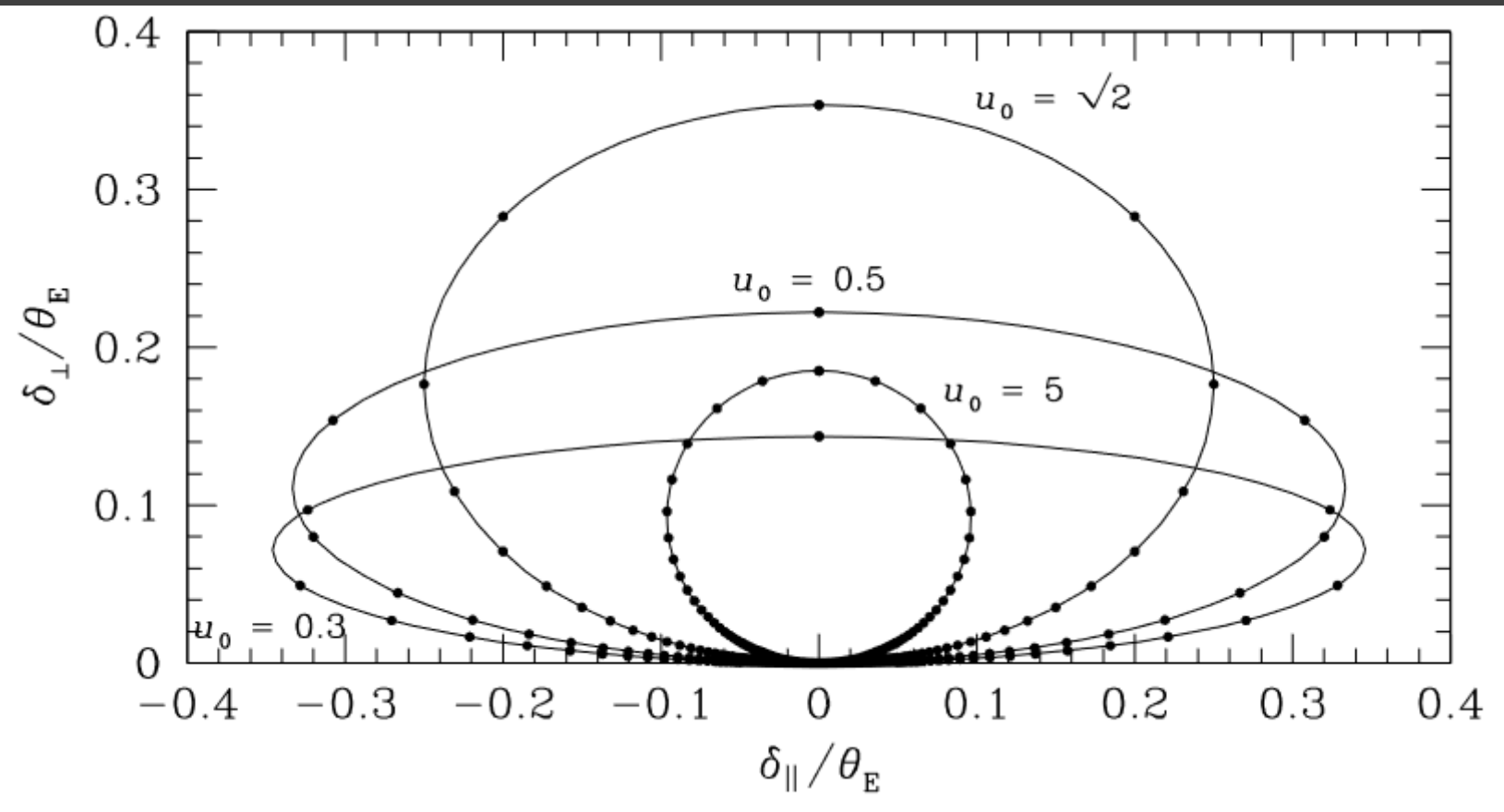
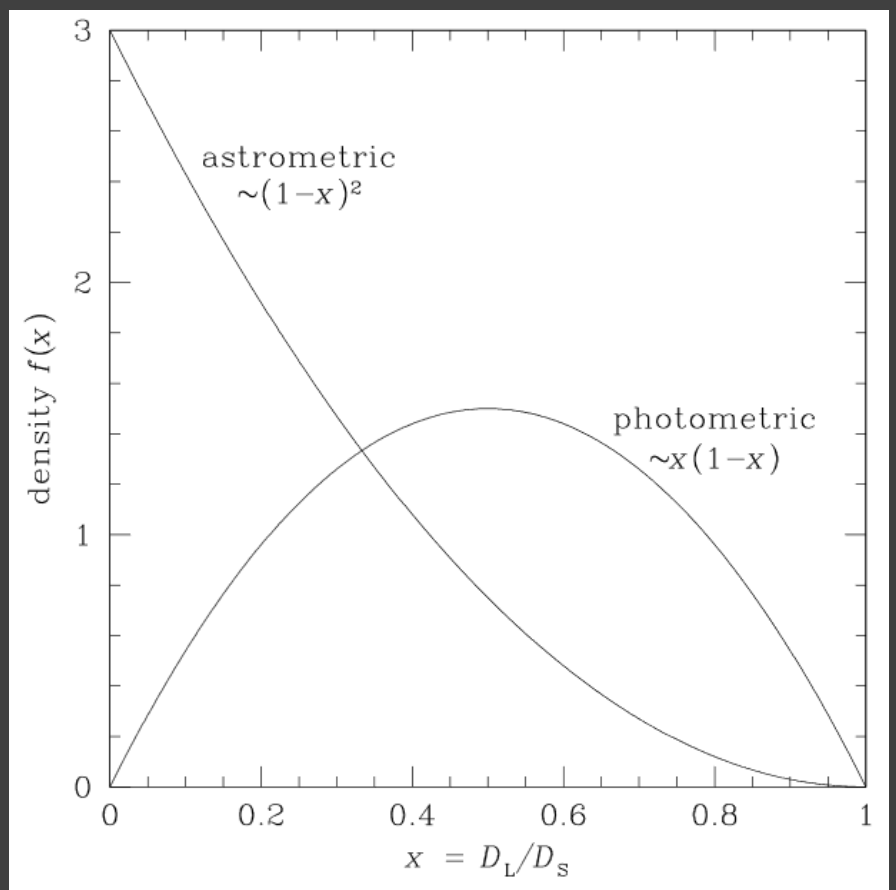
Precision of Gaia
is ~ 30 microarcsec
(see also 1704.02493).

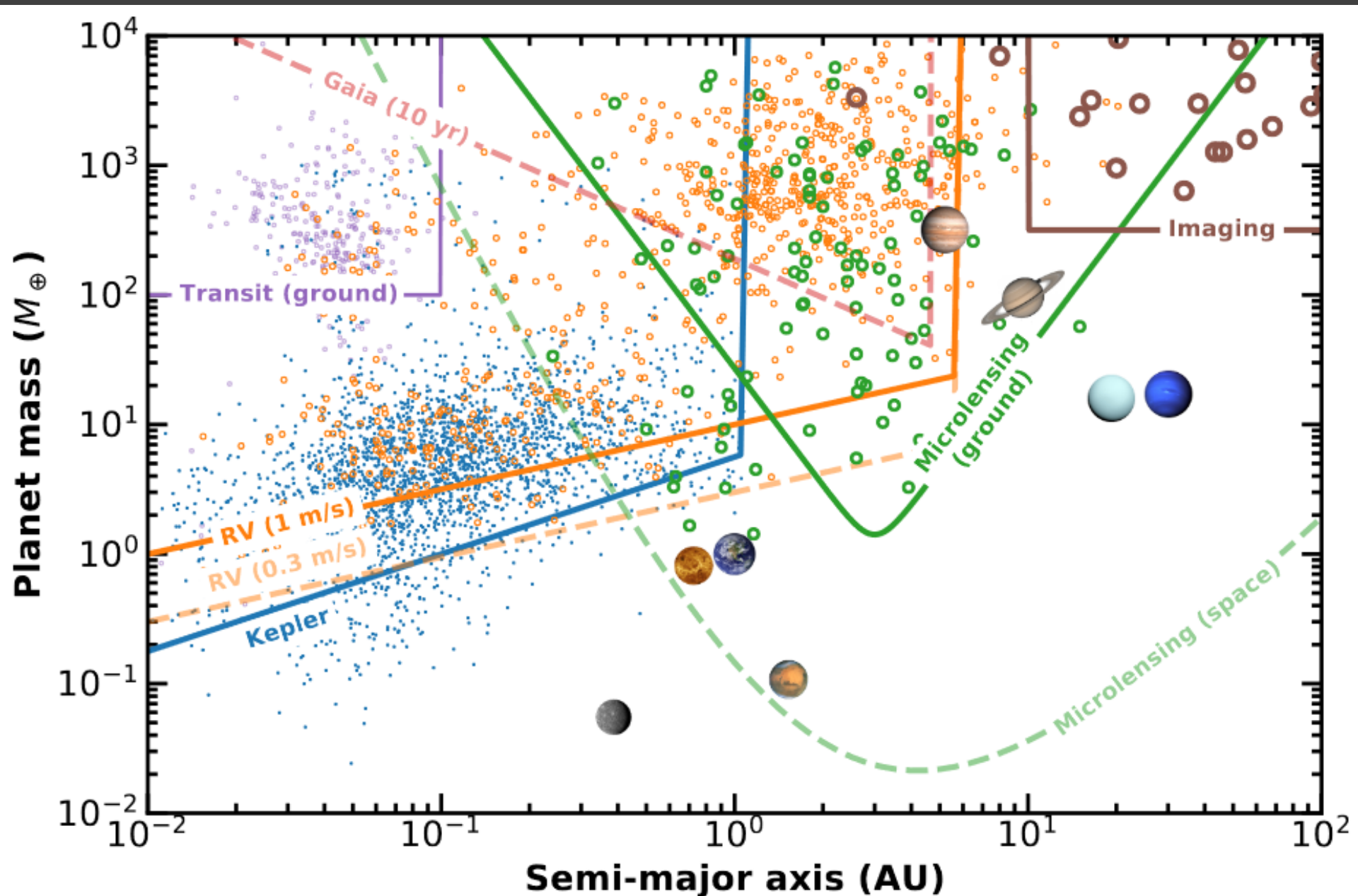
Optimistic estimates:
tens of thousand planets
($\sim 20000\text{-}30000$).

Mostly massive and
with long orbital periods
up to ~ 500 pc distance.

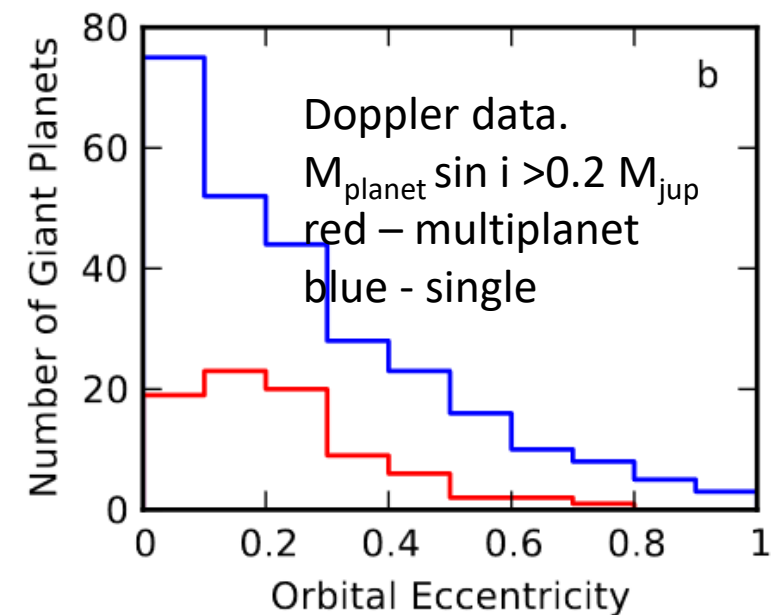
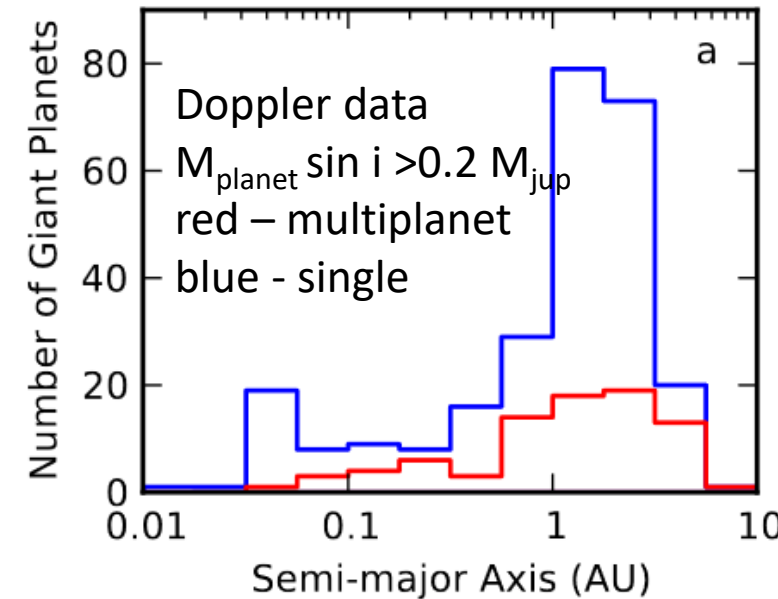
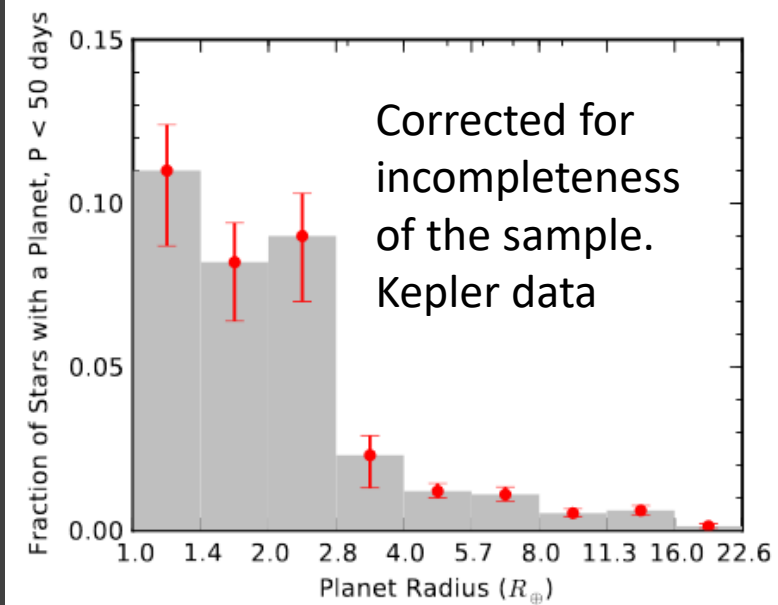
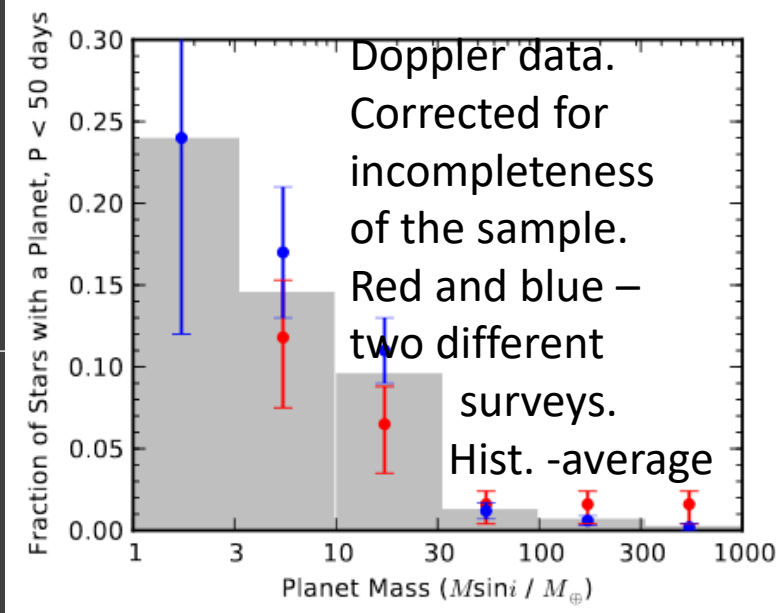


Astrometric microlensing





Planetary statistics



Literature

arxiv:1505.06869 Exoplanet Detection Techniques

arxiv:1504.04017 The Next Great Exoplanet Hunt

arxiv:1410.4199 The Occurrence and Architecture of Exoplanetary Systems

arXiv:1708.00896 Timing by Stellar Pulsations as an Exoplanet Discovery Method

arxiv:1706.09849 Transit Timing and Duration Variations for the Discovery and Characterization of Exoplanets

arxiv:1705.05791 Exoplanet Biosignatures: A Review of Remotely Detectable Signs of Life

arxiv:1704.07832 Mapping Exoplanets

arxiv:1701.05205 Characterizing Exoplanets for Habitability

arxiv:1411.1173 Astrometric exoplanet detection with Gaia

arxiv:1001.2010 Transits and Occultations

arxiv:0904.0965 Astrometric detection of earthlike planets

arXiv:0904.1100 Exoplanet search with astrometry

arxiv:0902.1761 Detection of extrasolar planets by gravitational microlensing

ApJ (2000) Dominik, Sahu Astrometric microlensing

arXiv:1810.02691 Microlensing searches for exoplanets